STUDIES OF
MARSSONINA AND *DREPANOPEZIZA*
SPECIES PATHOGENIC TO POPLARS

VOLUME IIA
FIGURES 1-86

ADRIAN SPIERS
1981

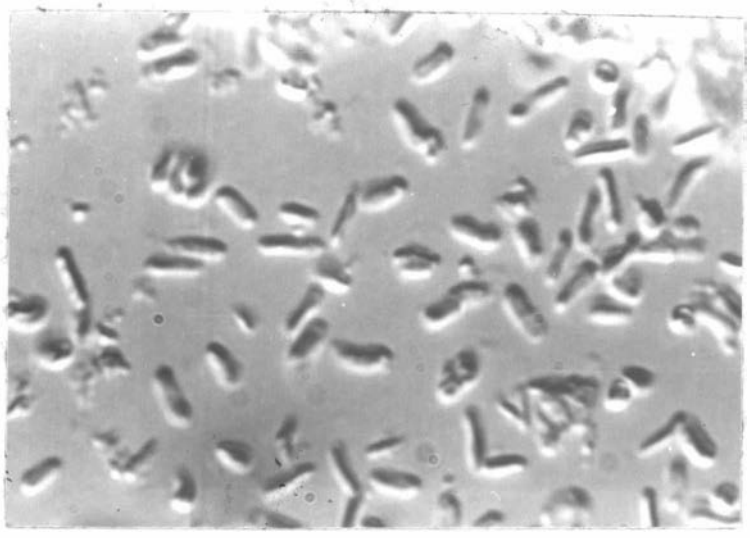

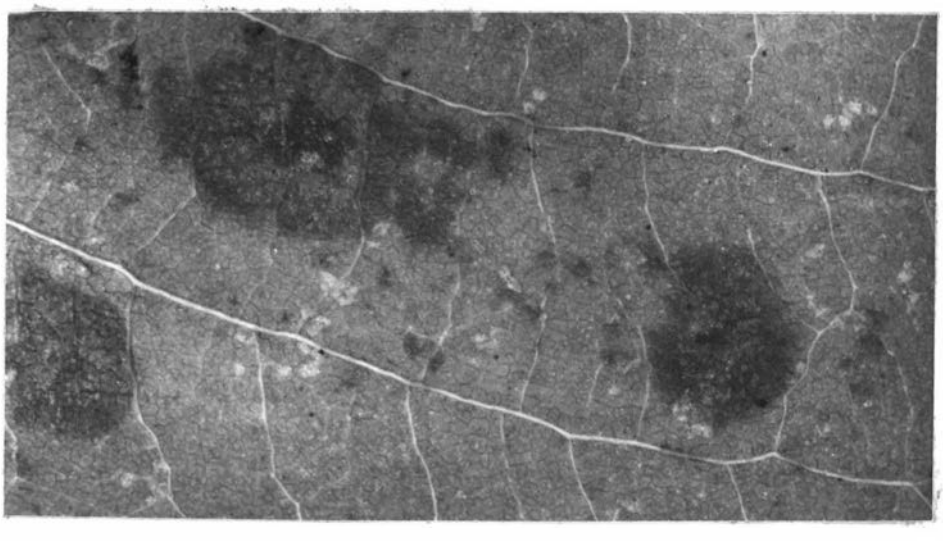

FIG. 1: Type material of *M. populi* (Lib.) Magn.

TOP: Symptoms exhibited by the adaxial leaf surface of *P. nigra* consisting of circular to irregular tan blotches.

CENTRE: Broadly obovoid to pyriform conidia divided unequally (27%) by a single septum. X 1,200.

BOTTOM: Unicellular, bacillate microconidia. X 1,200.

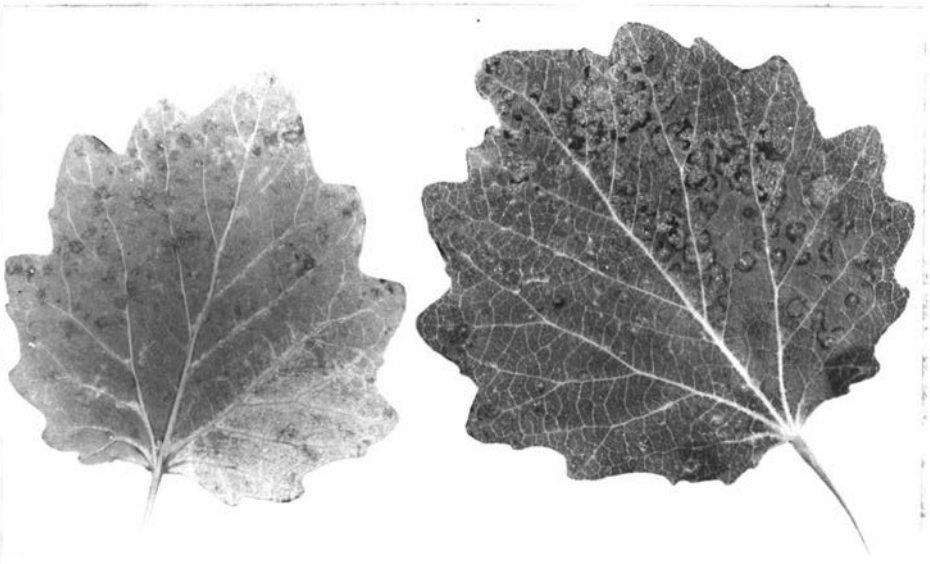

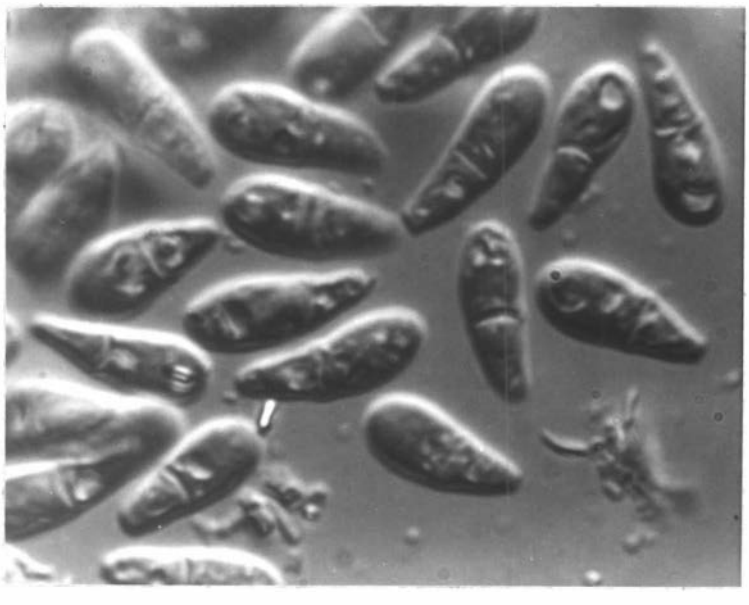

FIG. 2: Type material of *M. castagnei* (Desm. & Mont.) Magn.

TOP: Symptoms exhibited by *P. alba* consisting of circular lesions and irregular blotches on the adaxial leaf surface.

BOTTOM: Obovoid to broadly obovoid, straight to slightly curved conidia divided just below the middle (41%) by a single septum. X 1,200.

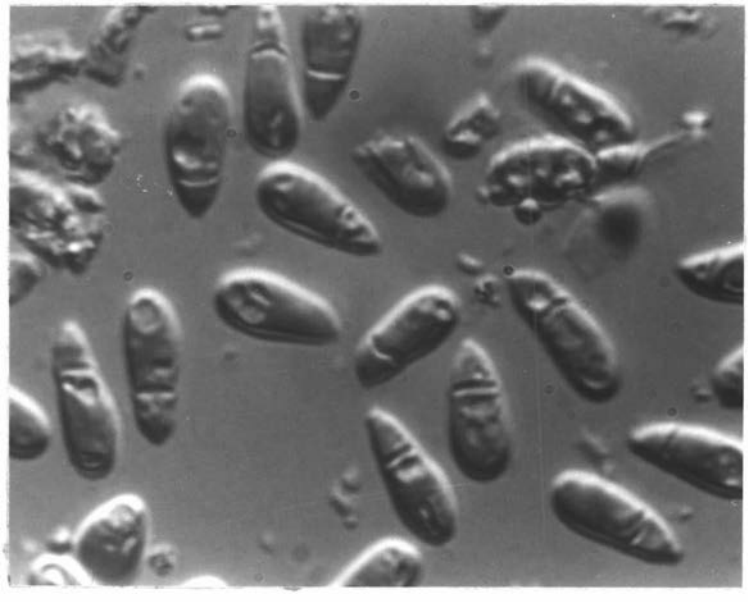

FIG. 3: Type material of *M. brunnea* (Ell. & Ev.) Magn.

TOP: Symptoms exhibited by *P. candicans* consisting of punctiform, black, circular to angular spots confluent in large areas, especially around the margin.

BOTTOM: Obovoid, straight to slightly curved conidia divided unequally by a single septum. X 1,200.

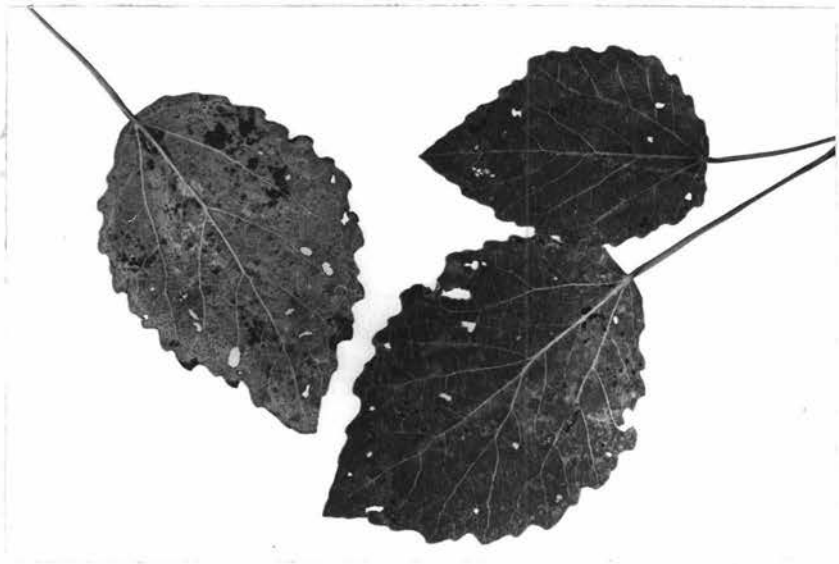

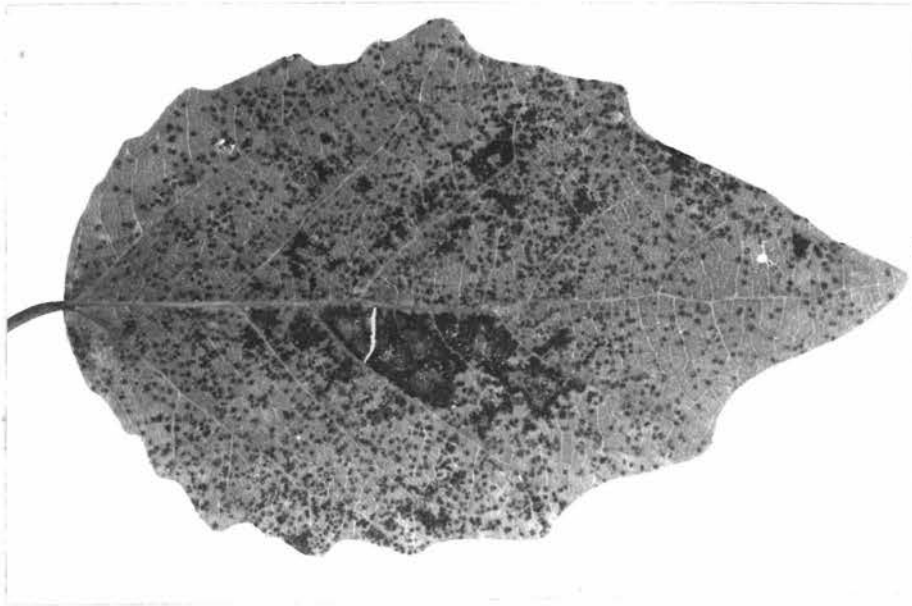

FIG. 4: Lectotype material of *M. tremulae* Kleb.

TOP: Symptoms exhibited by *P. tremula* consisting of discrete punctiform lesions and irregular blotches formed by coalescence of lesions.

CENTRE: Symptoms exhibited by the abaxial leaf surface of *P. tremula* consisting of discrete punctiform lesions and blotches often covered with amber spore masses.

BOTTOM: Obovoid, straight to slightly curved conidia divided unequally by a single septum. X 1,200.

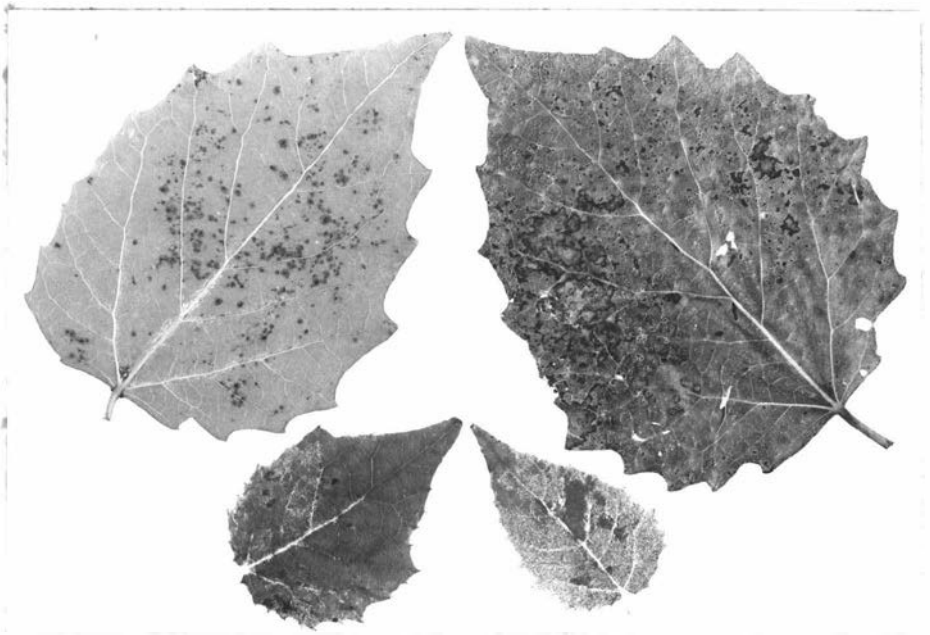

FIG. 5: Field material of *M. tremuloidis* Kleb. on *P. grandidentata* (Nr. 18; Klebahn, 1918).

TOP: Symptoms exhibited by the adaxial leaf surface of *P. grandidentata* consisting of discrete black punctiform circular to angular lesions and irregular necrotic patches.

CENTRE: Symptoms exhibited by the abaxial leaf surface of *P. grandidentata* consisting of circular black lesions covered with amber spore masses.

BOTTOM: Narrowly obovoid, straight to slightly curved conidia divided unequally (32%) by a single septum. X 1,200.

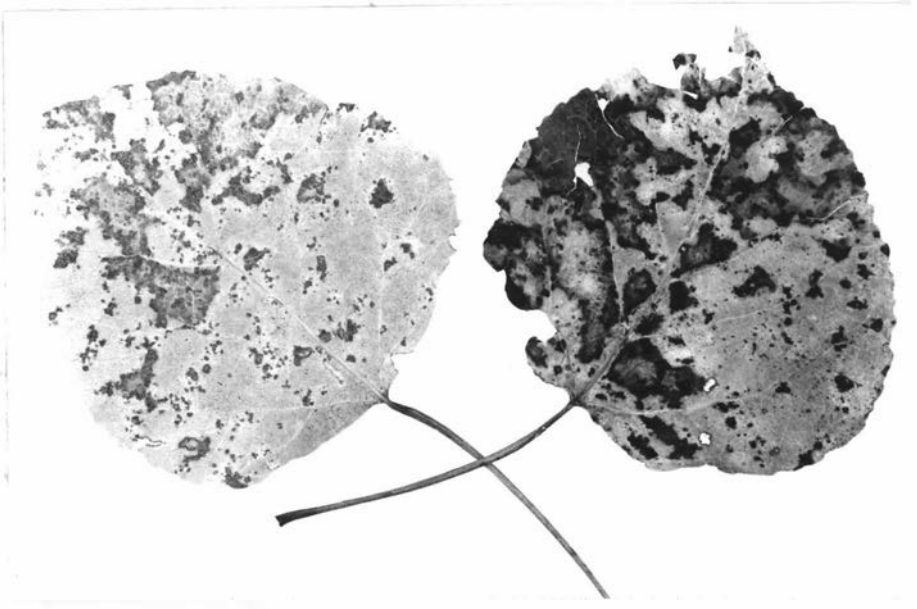

FIG. 6: Herbarium material of *M. tremuloidis* Kleb.

TOP: Symptoms exhibited by *P. tremuloides*. Adaxially and abaxially, discrete punctiform lesions and irregular necrotic blotches. Lesions on the adaxial surface are covered with amber spore masses.

BOTTOM: Narrowly obovoid, straight to slightly curved conidia divided unequally (31%) by a single septum. X 1,200.

FIG. 8: Conidia of *M. populi* from herbarium material. X 1,200.

TOP: Ex *P. marilandica*, Hannovers Munden Germany, collected by Butin, 20.8.1955.

CENTRE: Ex *P. nigra* cv. Italica, Herrmannsberg Germany, collected by Zycha, 16.8.1965.

BOTTOM: Ex *P. nigra* cv. Italica, Stockholm Sweden, collected by Eriksson, 5.8.1884.

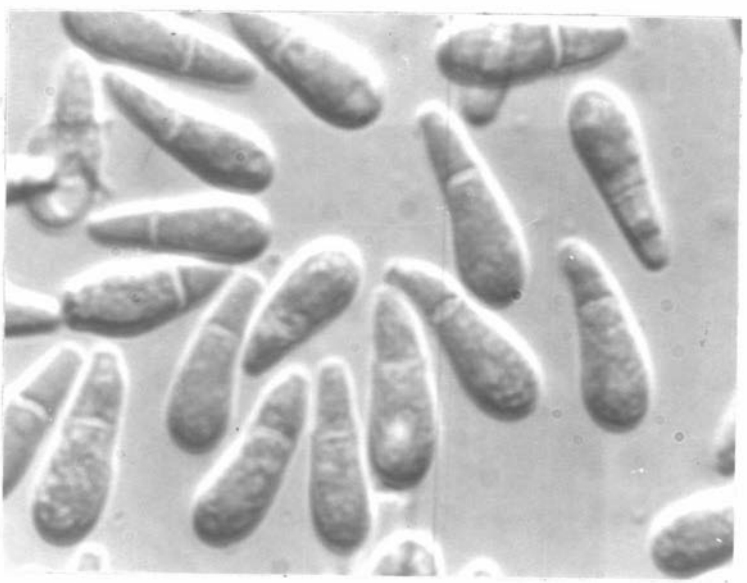

FIG. 9: Conidia of *M. castagnei* from herbarium material. X 1,200.

TOP: Ex *P. alba*, Ontario Canada, collected by Savile, 29.7.1945.

CENTRE: Ex *P. alba*, Kansas USA, collected by Bartholomew, 10.10.1930.

BOTTOM: Ex *P. alba*, Dublin Ireland, collected by O'Riordain 31.10.1979.

FIG. 10: Conidia of *M. brunnea* from herbarium material. X1,200.

TOP: Ex *P. tremula*, Hansiried Switzerland, collected by Rimpau, 22.10.1960.

CENTRE: Ex *P. canadensis*, Wisconsin USA, collected by Davis, 24.8.1926.

BOTTOM: Ex *P. tremuloides*, Fallen leaf lake, California USA, collected by Darker, 7.9.1929.

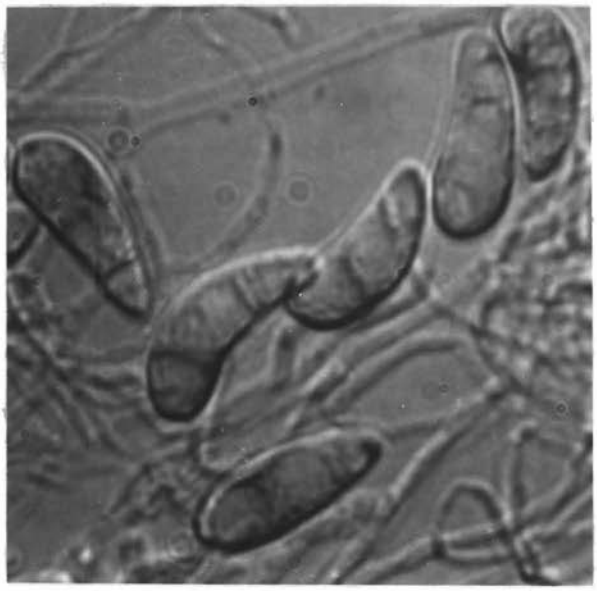

FIG. 13: Influence of growth media on conidium morphology of *M. populi* (Po 1) following 10 days incubation at 20°C under a 12 h white light photoperiod. X 1,200.

TOP LEFT: Potato dextrose agar (PDA).

TOP RIGHT: Cornmeal dextrose agar (CDA).
Note the comparable morphology of conidia from PDA and CDA and the presence of pseudosepta in conidia.

CENTRE: 15%V8 juice agar (15%V8). Note guttules.

BOTTOM LEFT: Potato carrot agar plus 10%V8 juice (PC-10).
Note guttules.

BOTTOM RIGHT: Potato carrot agar (PCA).
Note the comparable morphology of conidia from 15%V8, PC-10 and PCA.

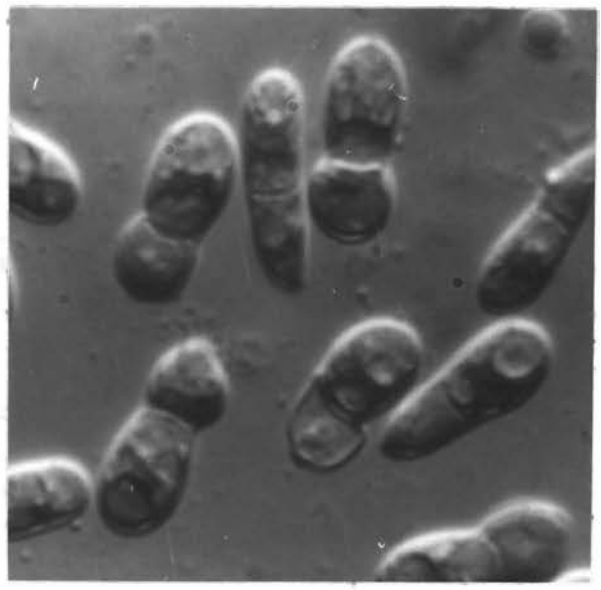

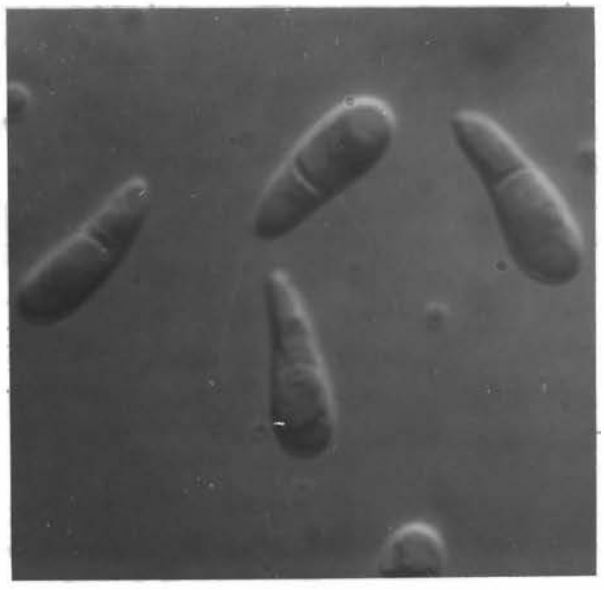

FIG. 14: Influence of growth media on conidium morphology of *M. castagnei* (Cs 2) following 10 days incubation at 20°C under a 12 h white light photoperiod. X 1,200.

TOP LEFT: Potato dextrose agar (PDA).

TOP RIGHT: Cornmeal dextrose agar (CDA).
Note the comparable morphology of conidia from PDA and CDA.

CENTRE: 15%V8 juice agar (15%V8).

BOTTOM LEFT: Porato carrot agar plus 10%V8 juice (PC-10).

BOTTOM RIGHT: Potato carrot agar (PCA).
Note the comparable morphology of conidia from 15%V8, PC-10 and PCA.

FIG. 15: Influence of growth media on conidium morphology of *M. brunnea* following 10 days incubation at 20°C under a 12 h white light photoperiod. X 1,200.

TOP LEFT: Potato dextrose agar (PDA).

TOP RIGHT: Cornmeal dextrose agar (CDA).
Note the comparable morphology of conidia from PDA and CDA and the presence of pseudosepta.

CENTRE: 15%V8 juice agar (15%V8).

BOTTOM LEFT: Potato carrot agar plus 10%V8 juice (PC-10).

BOTTOM RIGHT: Potato carrot agar (PCA).
Note the comparable morphology of conidia from 15%V8, PC-10 and PCA.

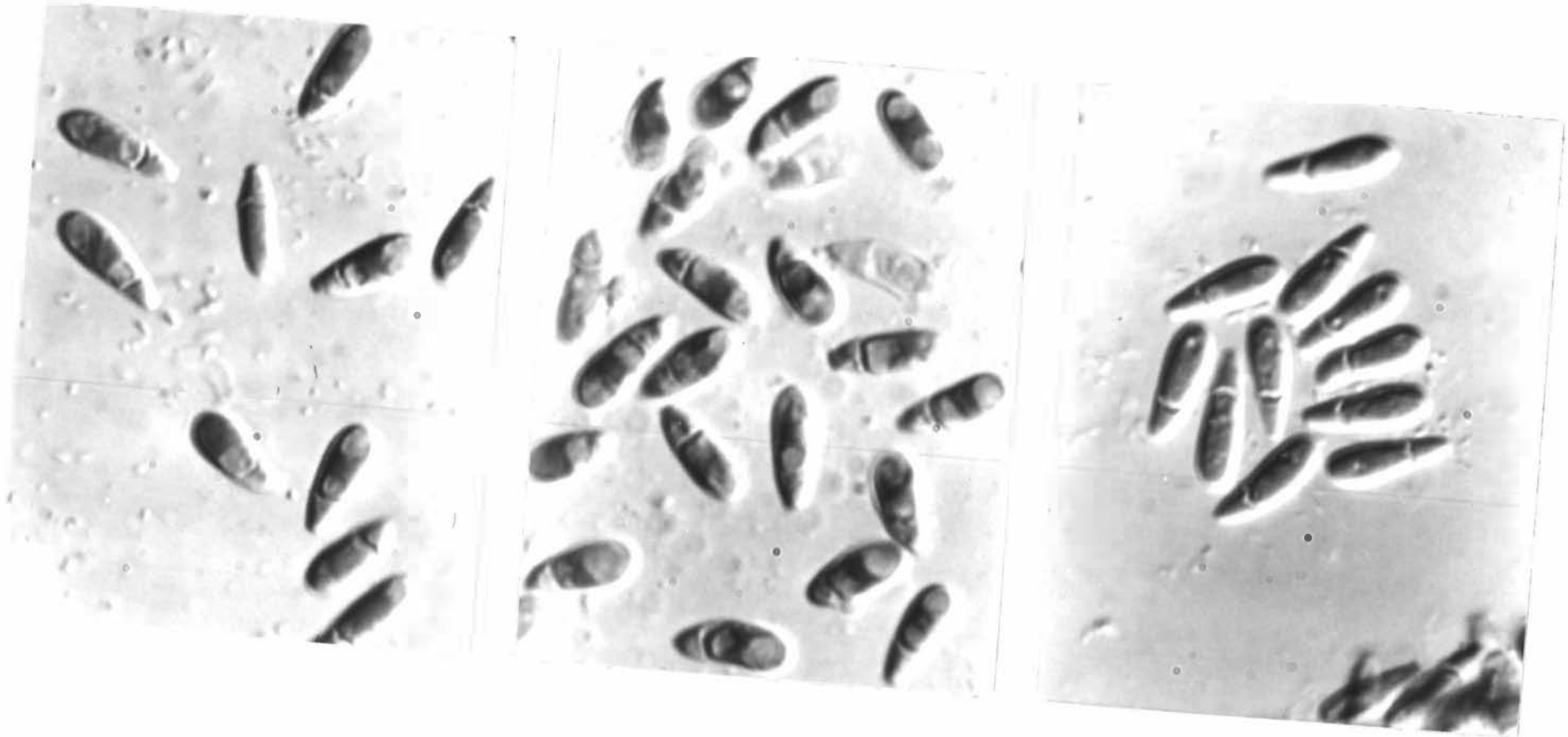

FIG. 16: Influence of host resistance on conidium morphology of *M. brunnea* (Br 5) following 12 days incubation at 20°C under a 12 h white light photoperiod. X 1,200.

TOP: Ex *P. deltoides* cv. ANU 60/129.

CENTRE: Ex *P. alba* var. pyramidalis.

BOTTOM: Ex *P.* x *euramericana* cv. Marilandica Greatford

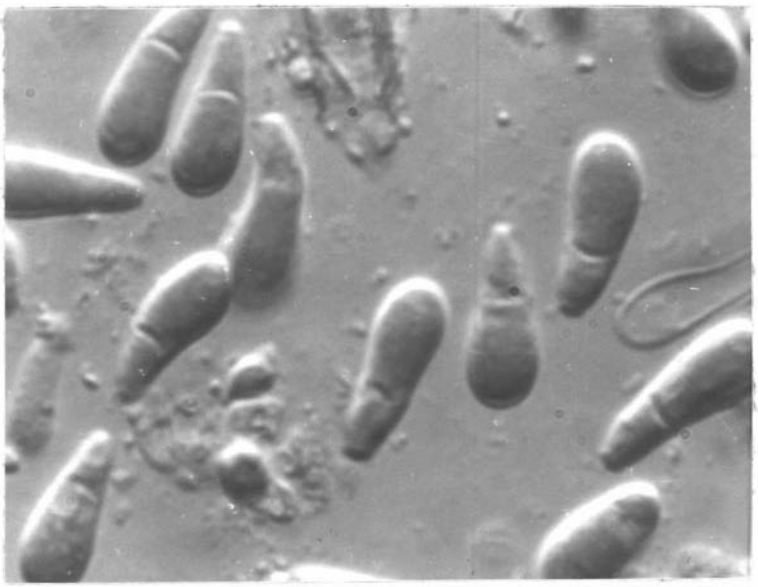

FIG. 17: Influence of host resistance on conidium morphology of *M. castagnei* (Cs 2) following 12 days incubation at 20°C under a 12 h white light photoperiod. X 1,200.

TOP: Ex *P. fremontii* x *P. nigra* Sempervirens cv. ANU66/9.

CENTRE: Ex *P. alba* cv. B02.

BOTTOM: Ex *P. deltoides* x *P. alba* cv. Delmak 26.

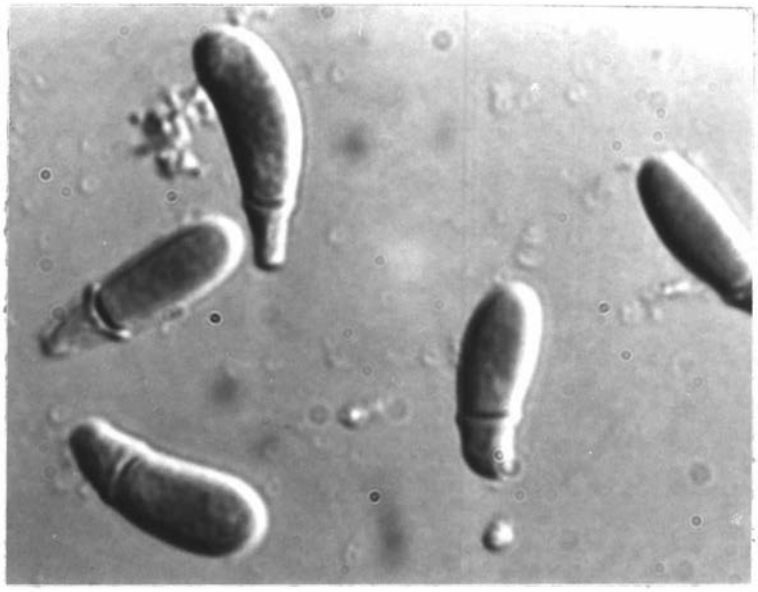

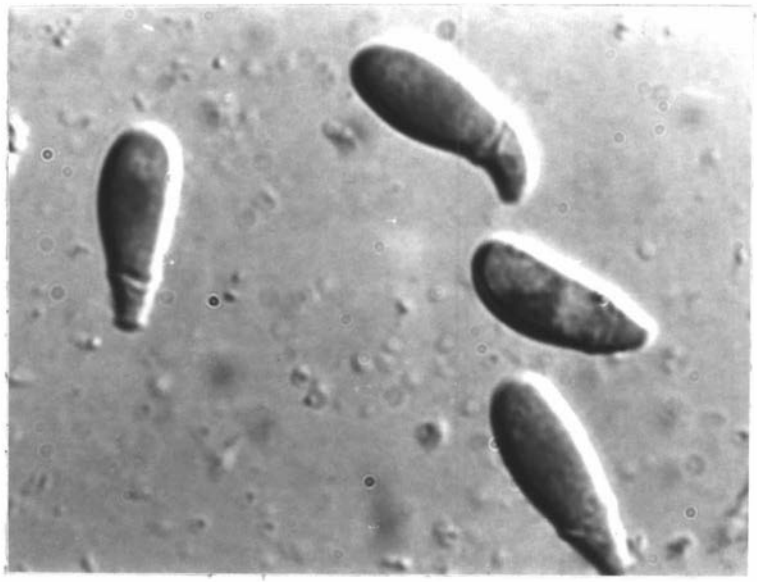

FIG. 18: Influence of host resistance on conidium morphology of *M. populi* (Po 6) following 12 days incubation at 20°C under a white light photoperiod. X 1,200.

TOP: Ex *P. nigra* cv. Italica.

CENTRE: Ex *P.* x *euramericana* cv. 'Marilandica F'.

BOTTOM: Ex *P. deltoides* x *P. maximowiczii* cv. I83/58.

FIG. 19: Conidium morphology of *M. brunnea* (Br 5, Br 5L1) on *P. nigra* cv. Italica 'Aurea' and 15%V8 following 10 days incubation at 20°C under a 12 h white light photoperiod. X 1,200.

TOP LEFT: Conidia (Br 5) ex *P. nigra* cv. Italica 'Aurea'.

BOTTOM LEFT: Conidia ('Large conidium variant' Br 5L1) ex *P. nigra* cv. Italica 'Aurea'.

TOP RIGHT: Conidia (Br 5) ex 15%V8.

BOTTOM RIGHT: Conidia ('Large conidium variant' Br 5L1) ex 15%V8.

Note 1: The large difference in dimensions between conidia of Br 5 and Br 5L1.

Note 2: Within both forms the comparable conidium morphology expressed on host tissue and agar.

FIG. 20: Conidium morphology of *M. castagnei* (Cs 2) on *P. nigra* cv. Italica 'Aurea' and 15%V8 following 10 days incubation at 20°C under a 12 h white light photoperiod. X 1,200.

TOP: Conidia ex *P. nigra* cv. Italica 'Aurea'.

CENTRE: Conidia ex 15%V8 agar.

BOTTOM: Conidia of the normal form and a 'large conidium variant' on 15%V8.
Note that apart from dimensions, the two forms of conidia are morphologically similar.

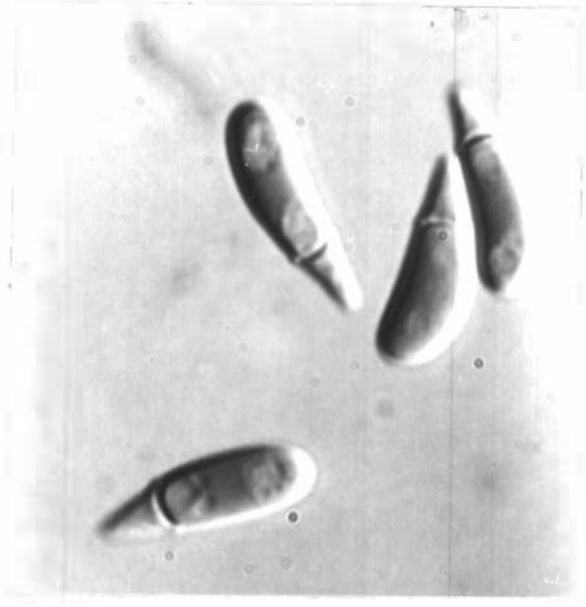

FIG. 21: Conidium morphology of *M. populi* (Po 6, Po 6L) on *P. nigra* cv. Italica 'Aurea' and 15%V8 agar following 10 days incubation at 20°C under a 12 h white light photoperiod. X 1,200.

TOP LEFT: Conidia (Po 6) ex *P. nigra* cv. Italica 'Aurea'.

BOTTOM LEFT: Conidia (Po 6L) ex *P. nigra* cv. Italica 'Aurea'.

TOP RIGHT: Conidia (Po 6) ex 15%V8.

BOTTOM RIGHT: Conidia (Po 6L) ex 15%V8.

Note 1: The large difference in dimensions between conidia of Po 6 and Po 6L.

Note 2: Within both forms the comparable conidium morphology expressed on host tissue and agar.

FIG. 24: Morphology of microconidiophores from host tissue.

TOP LEFT: *M. populi* ex *P. nigra* cv. Italica, Dublin, Ireland. X 1,200.

TOP RIGHT: *M. populi* ex *P. nigra* cv. Italica, Dublin, Ireland with delimited secondary microconidium initial. X 12,000.

BOTTOM LEFT: *M. castagnei* ex *P. alba* cv. Dublin, Ireland with expanding secondary microconidium initial. X 10,500.

BOTTOM RIGHT: *M. brunnea* ex *P.* x *euramericana* cv. NL 2194, Palmerston North, New Zealand. Branched microconidiophore with expanding secondary microconidium initial. X6,400.

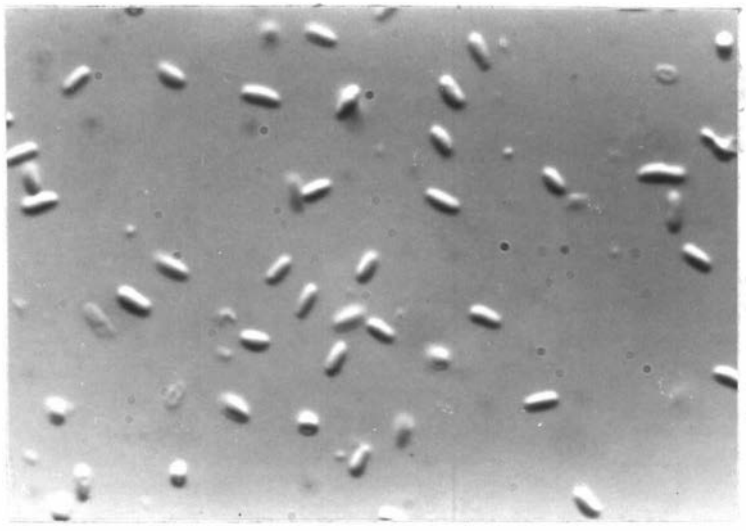

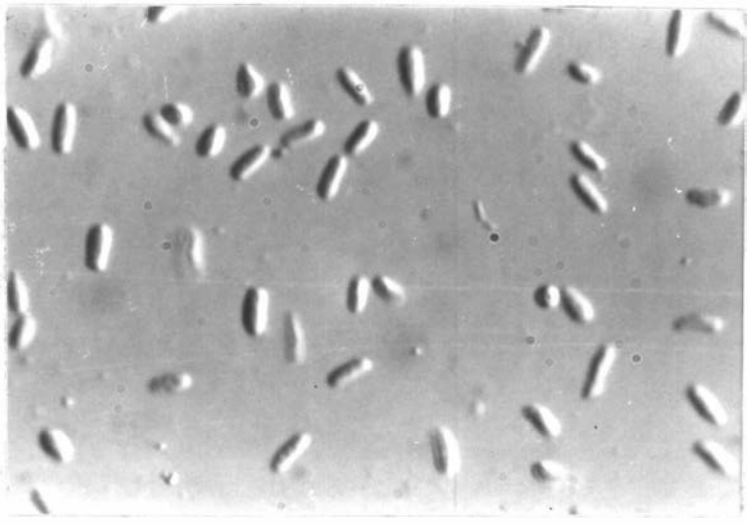

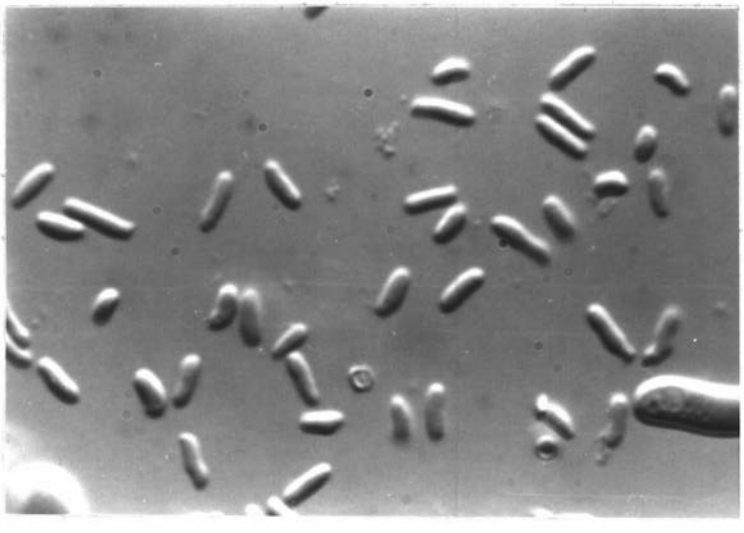

FIG. 25: Morphology of microconidia from host tissue. X 1,200.

TOP: *M. brunnea* ex *P.* x *euramericana* cv. Robusta, Dublin, Ireland.

CENTRE: *M. castagnei* ex *P. alba* cv. Dublin, Ireland.

BOTTOM: *M. populi* ex *P. nigra* cv. Italica, Dublin, Ireland. Note that microconidia of the three species are morphologically indistinguishable.

FIG. 27: Location of microconidiophores in host tissue. X 550.

TOP: *M. brunnea; P.* x *euramericana* cv. NL 2194, Palmerston North, New Zealand. Vertical section of leaf showing intraepidermal location of microconidiophores.

CENTRE: *M. castagnei; P. alba,* Dublin, Ireland, Vertical section of leaf showing intraepidermal location of microconidiophores.

BOTTOM: *M. populi; P. nigra* cv. Italica, Dublin, Ireland, Vertical section of leaf showing simultaneous formation of conidia and microconidia in a single acervulus (intraepidermal).

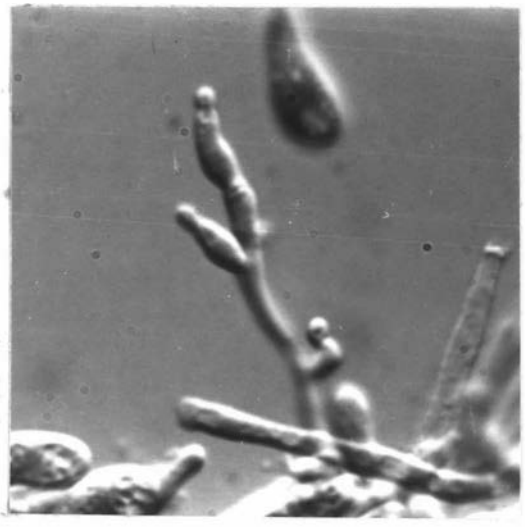

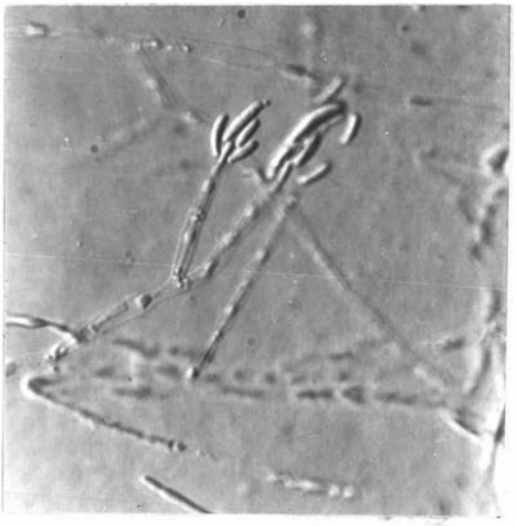

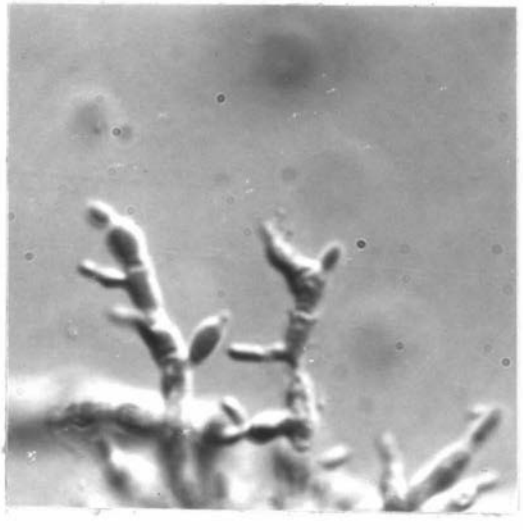

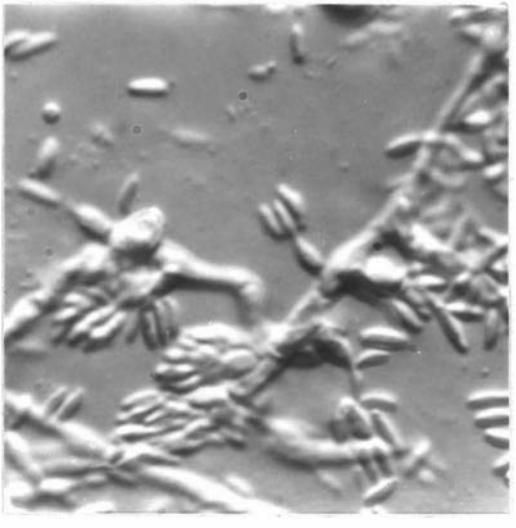

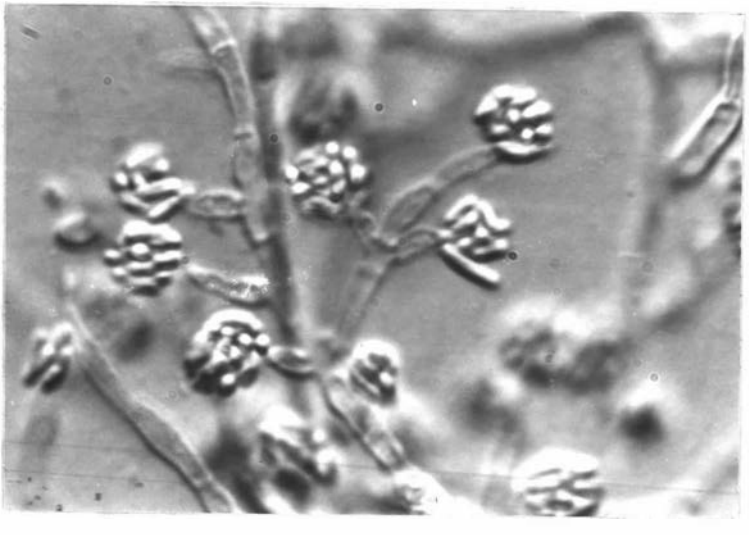

FIG. 28: Formation of microconidia in culture (15%V8) following 12 days dark incubation at 20°C. X 1,200.

TOP LEFT: *M. castagnei* (Cs 3). Ampulliform microconidiophores.

TOP RIGHT: *M. populi* (Po 1). Microconidiophores with accumulated microconidia.

CENTRE LEFT, CENTRE RIGHT & BOTTOM: *M. brunnea* (Br 5). Ampulliform microconidiophores with accumulated microconidia at their apices.

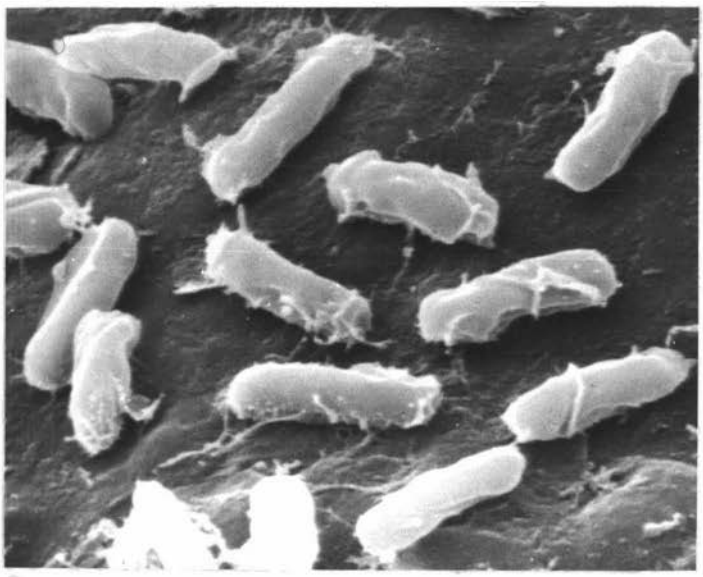

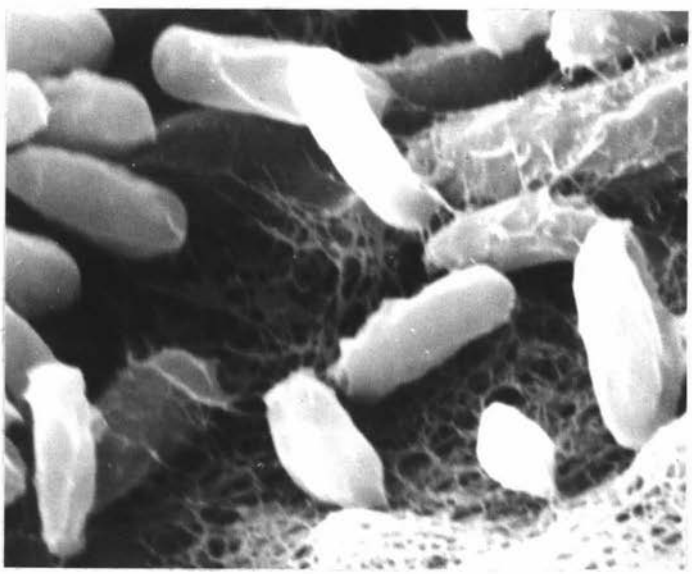

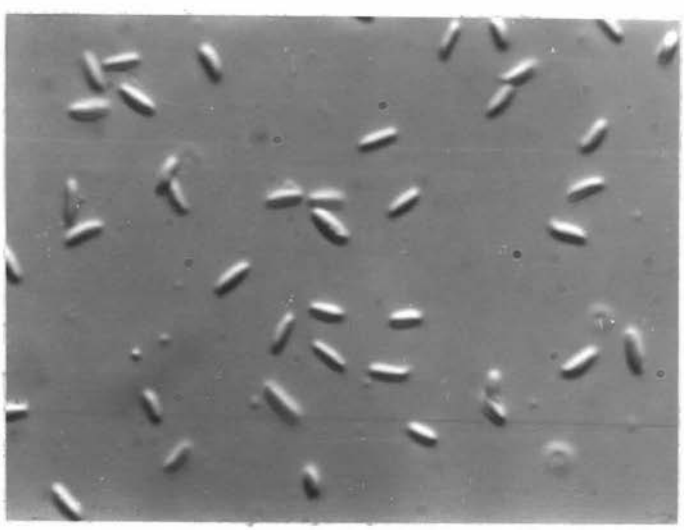

FIG. 29: Morphology of microconidia (*M. brunnea*) formed in the laboratory on *P. nigra* cv. Italica 'Aurea' and 15%V8 agar.

TOP: *P. nigra* cv. Italica 'Aurea'. X 8,000.

CENTRE: 15%V8 agar. X 8,000.
Note that on both substrates microconidia are smooth walled and bacillate.

BOTTOM: Microconidia formed on 15%V8. X 1,200.

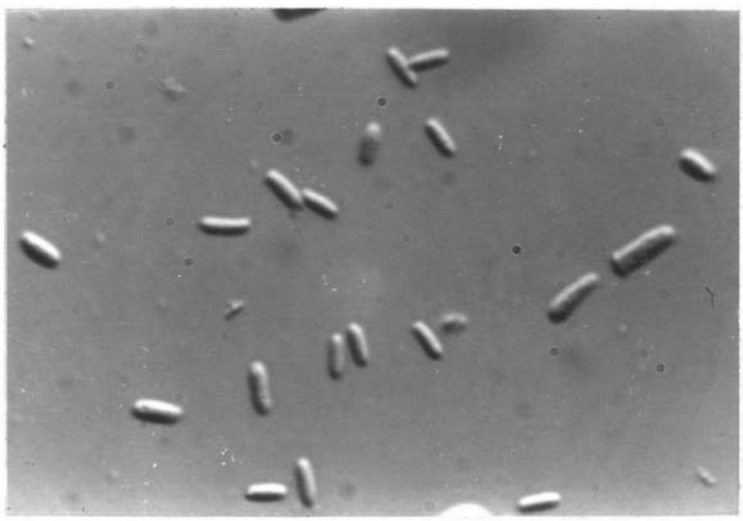

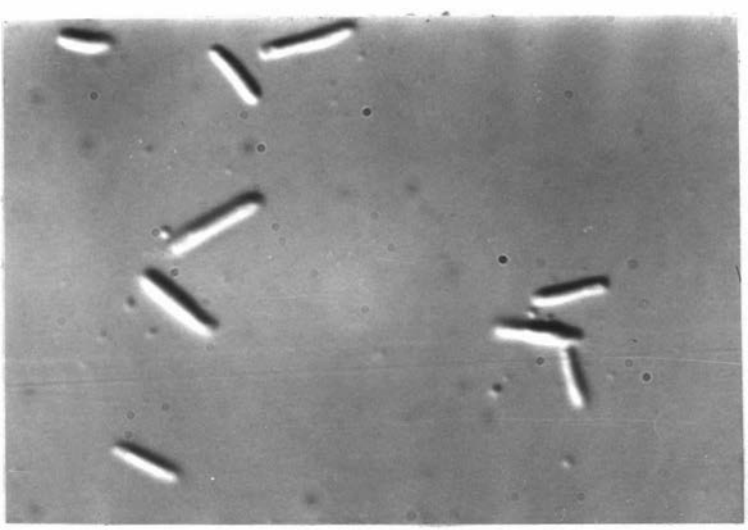

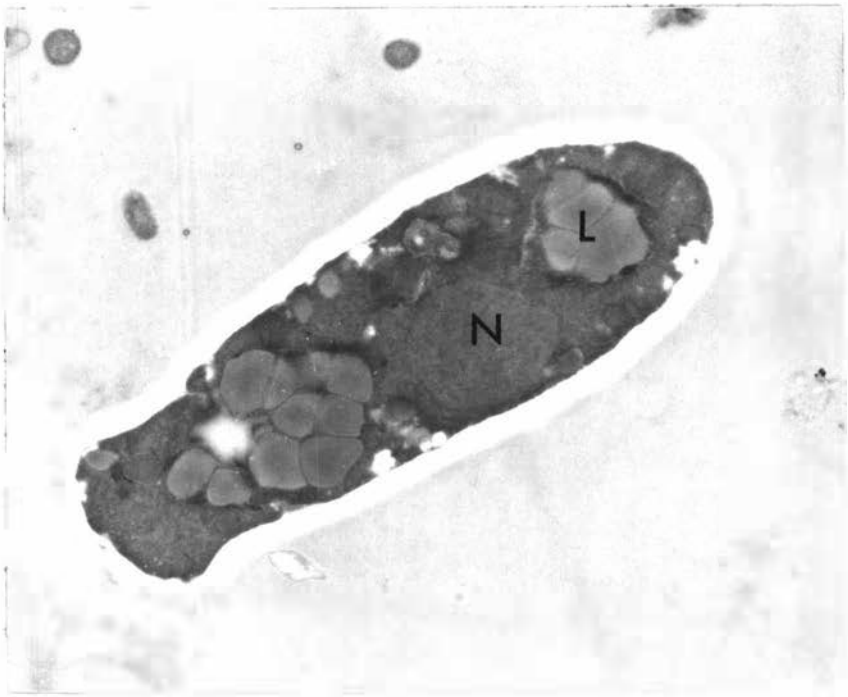
L
N

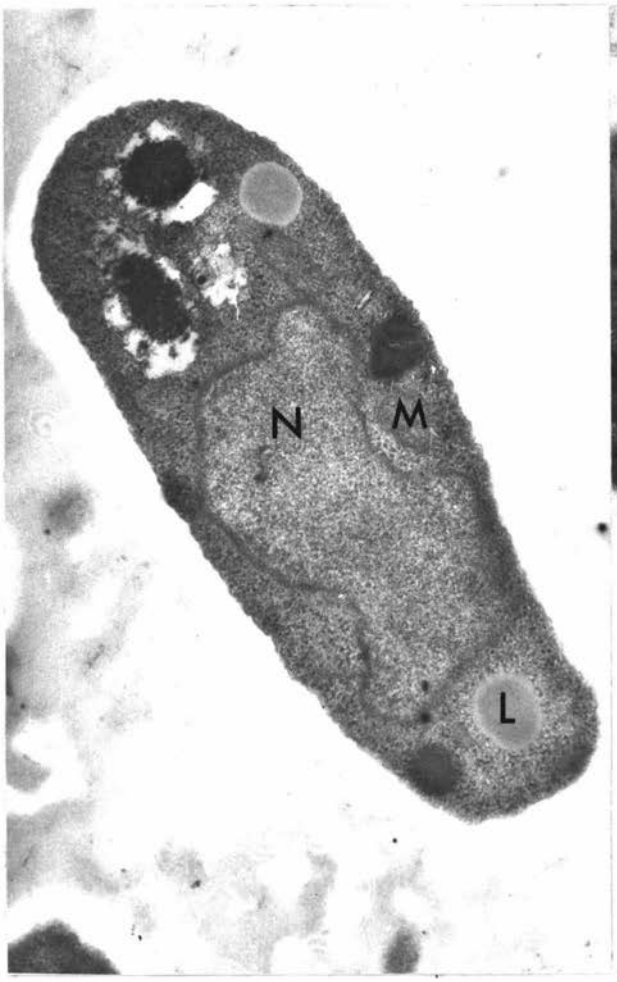
N
M
L

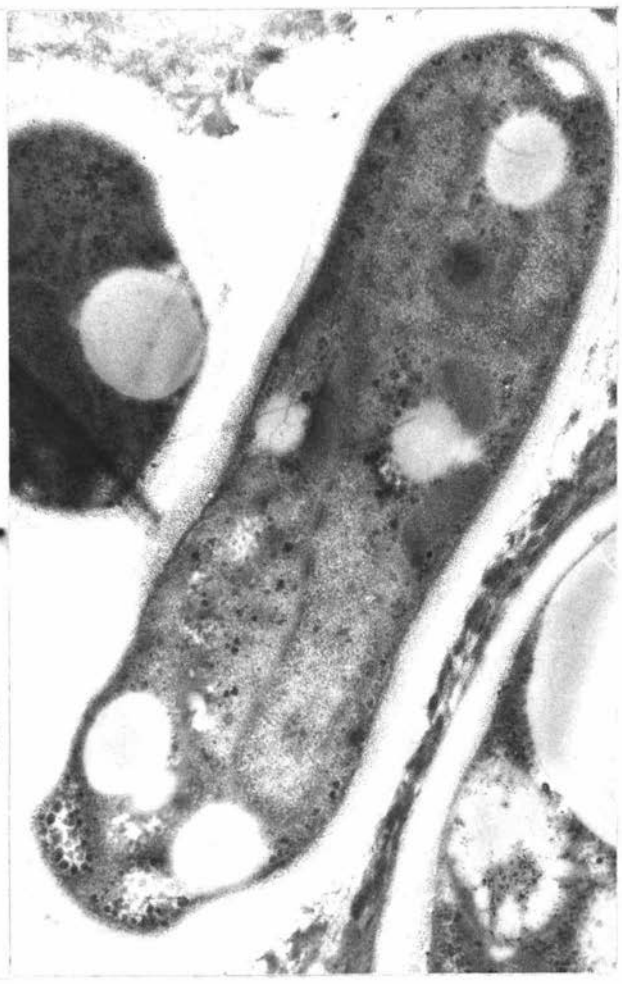

FIG. 30: Comparison of microconidia formed on *P. nigra* cv. Italica 'Aurea' by the normal and the 'large conidium variant' of *M. populi*. X 1,200.

TOP: Microconidia formed by *M. populi* Po 1.

BOTTOM: Microconidia formed by *M. populi* Po 1L.

Note that microconidia of *M. populi* Po 1L are significantly longer than those of *M. populi* Po 1.

FIG. 32: Ultrastructure of microconidia.

TOP: *M. brunnea*. *P.* x *euramericana* cv. NL 2195, Palmerston North, New Zealand. Note the inconspicuously bilayered electron opaque outer wall, the single central nucleus (N) and lipid globules (L). X 10,500.

BOTTOM LEFT: *M. populi*. *P. nigra* cv. Italica, Dublin, Ireland. Note the large central nucleus (N), lipid globules (L), mitochondria (M) and the dense granulated cytoplasm. X 22,000.

BOTTOM RIGHT: *M. populi* (Po 1L) 15%V8 agar. Note the dense granulated cytoplasm and the lipid globules. X 22,000.

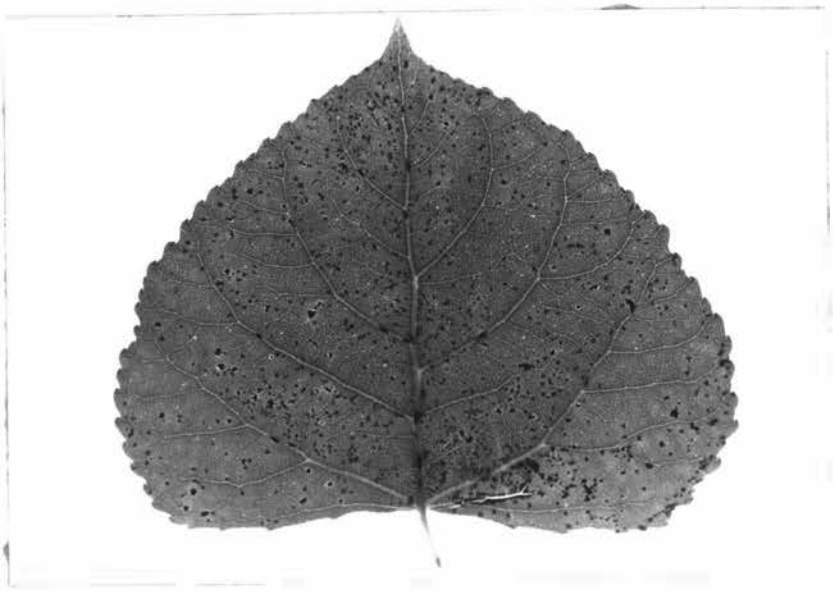

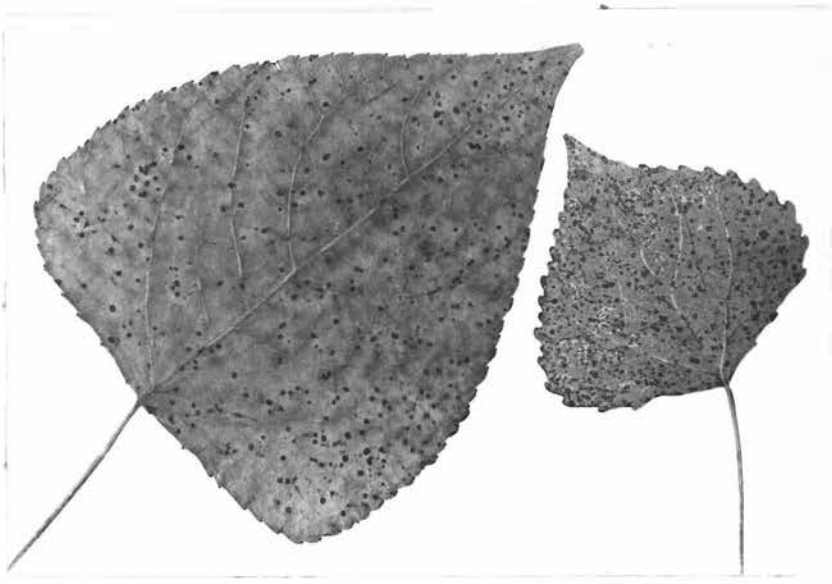

FIG. 33: Symptoms expressed by field collections of poplars infected with *M. brunnea*.

TOP: *P.* x *euramericana* cv. NL 2194, Palmerston North, New Zealand, 20.11.1979. Abaxial surface showing small (1.0mm diam.) discrete black angular punctiform spots.

CENTRE: *P. nigra*, Germany, collected by Zycha, 25.2.1965. Left adaxial surface; right abaxial surface, showing typical discrete punctiform spots of *M. brunnea*.

BOTTOM: *P.* x *euramericana*, Hungary, collected by Bertalan, 8.1.1979. Adaxial surface showing coalescence of spots to form irregular necrotic patches.

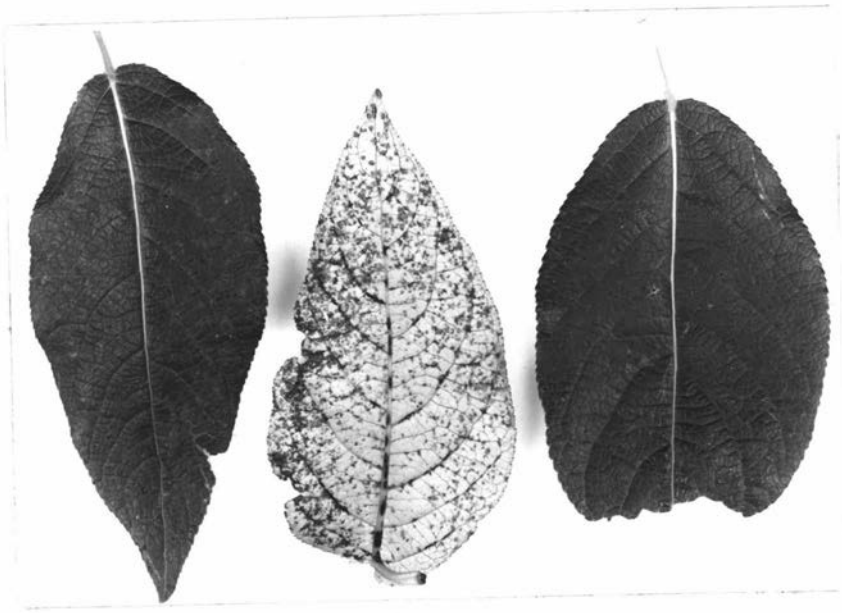

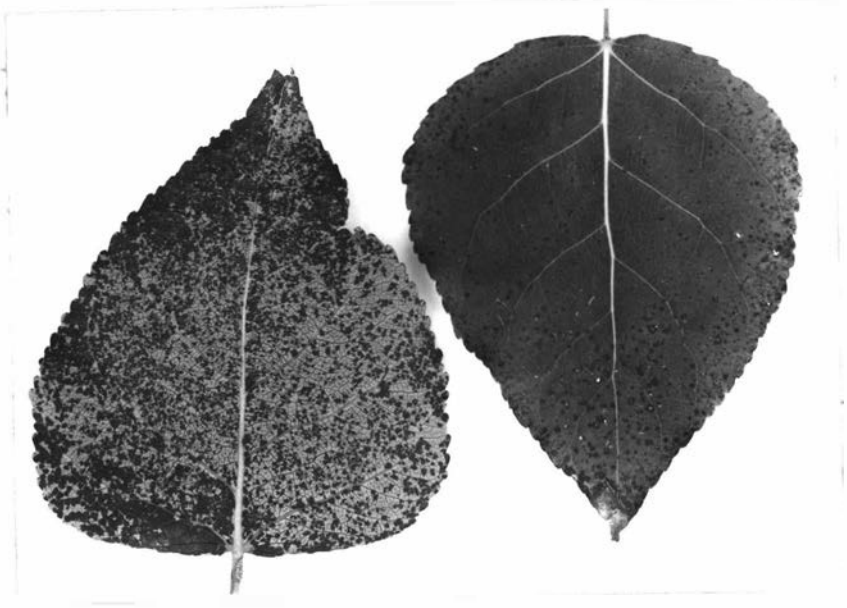

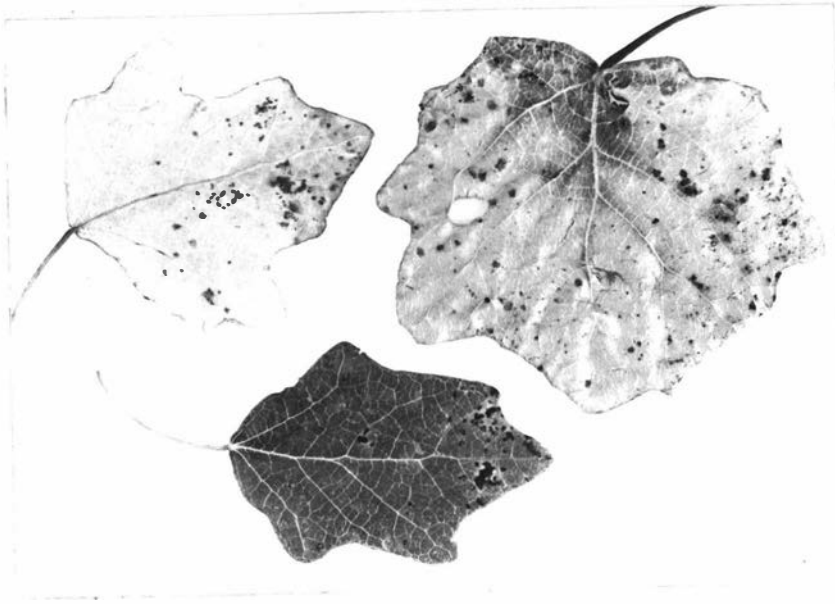

FIG. 34: Symptoms expressed by field collections of poplars infected with *M. brunnea*.

TOP: *P. koreana* x *P. trichocarpa*, Palmerston North, New Zealand, 26.2.1979, showing the higher infection level on the abaxial leaf surface and lesions on veins.

BOTTOM: *P. candicans*, Palmerston North, New Zealand, 26.2.1979, showing the higher infection level on the abaxial leaf surface (left). Note coalescence of lesions to form irregular necrotic patches.

FIG. 35: Symptoms expressed by field collections of poplars infected with *M. brunnea*. *P. alba*, British Columbia, collected by Harvey, 18.8.1961, showing punctiform black spots formed on both leaf surfaces.

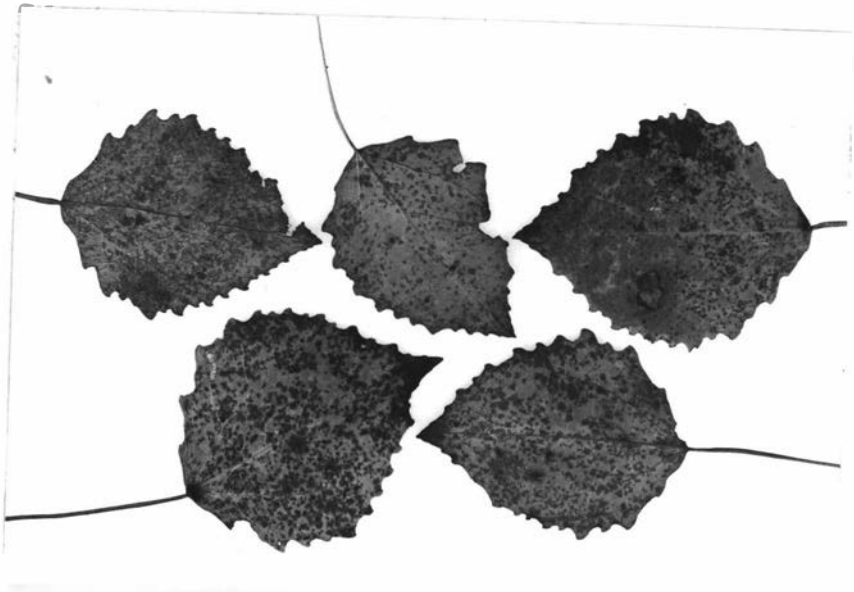

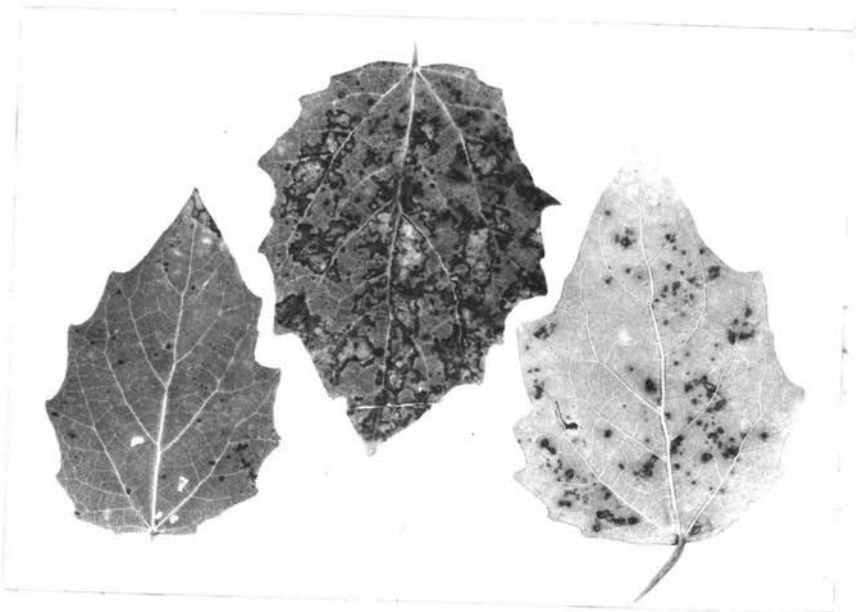

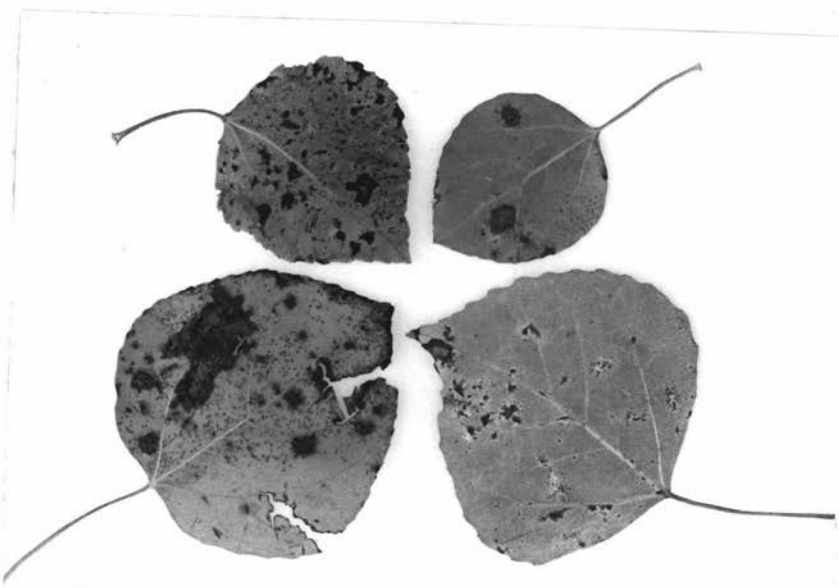

FIG. 36: Symptoms expressed by field collections of poplars infected with *M. brunnea*.

TOP: *P. tremula*. Brandenburg, Germany collected by Sydow, 21.9.1908, showing punctiform lesions and irregular blotches.

CENTRE: *P. grandidentata*, Ontario, Canada, collected by Dearness 1913, showing discrete punctiform lesions and necrotic blotches formed on the adaxial surface (left and centre). Sporulation was intense on the abaxial surface (right).

BOTTOM: *P. tremuloides*, Wyoming, USA collected by Solheim 16.9.1940. Abaxial surface showing discrete punctiform lesions and necrotic blotches covered with masses of conidia.

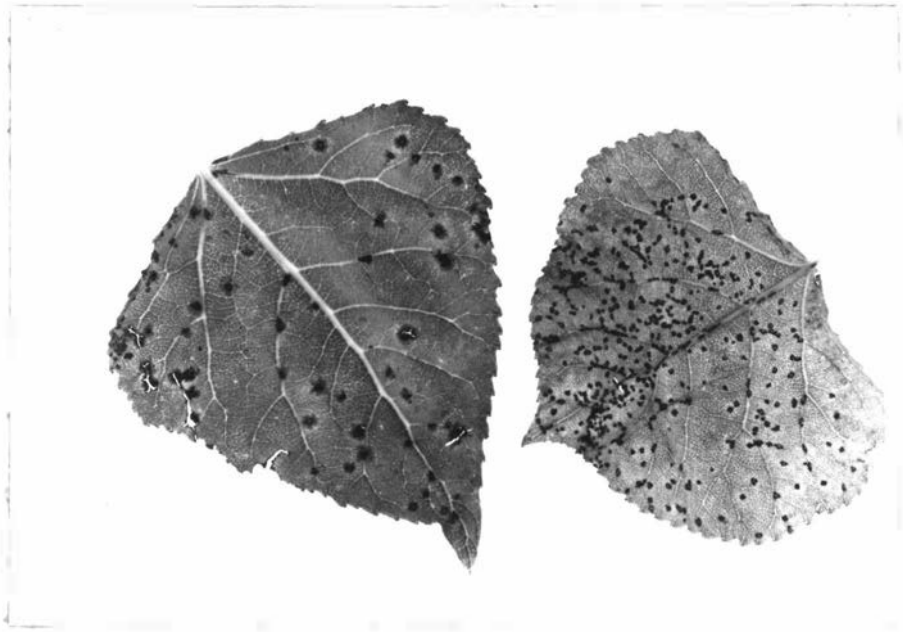

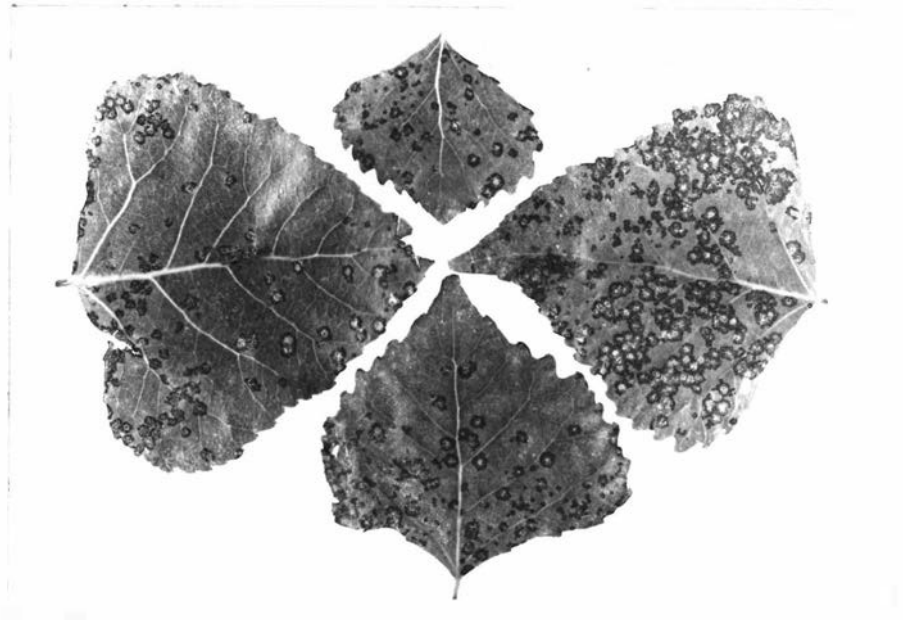

FIG. 37: Symptoms expressed by field collections of poplars infected with *M. brunnea*.

P. fremontii cv. 6 1/48, Palmerston North, New Zealand, 25.1.1978.

TOP: Left, abaxial leaf surface showing reverse of blotch symptom.
Right, abaxial surface showing amphigenous spots. Note the abundant sporulation.

BOTTOM: Adaxial leaf surface showing large (5-7mm diam.) circular tan blotches dotted with white punctiform acervuli. Note coalescence of blotches to form extensive necrotic patches.

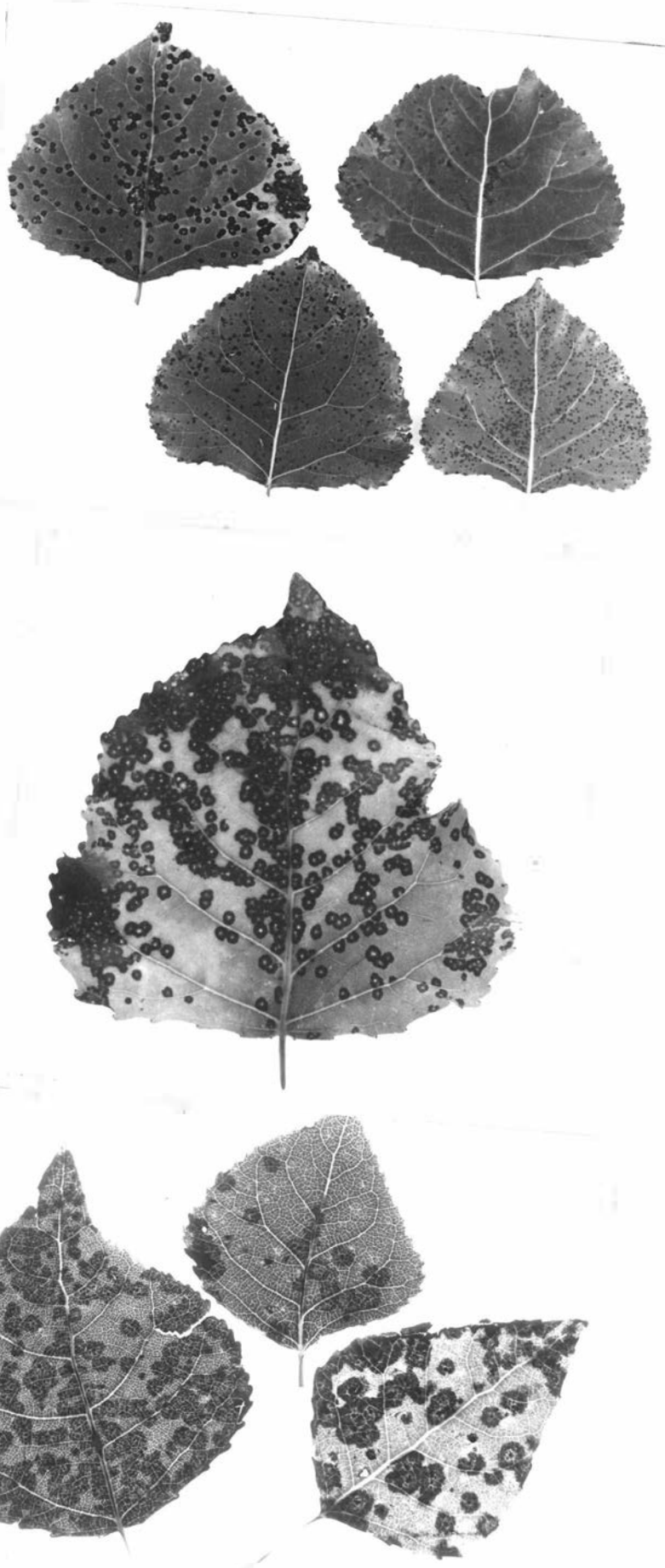

FIG. 38: Symptoms of the microconidial state expressed by field collections of poplars infected with *M. brunnea*.

TOP: *P.* x *euramericana* cv. NL 2194, Palmerston North, New Zealand, 24.4.1978.

Top-left and right, epiphyllous microconidial blotches.

Bottom-left and right, amphigenous microconidial spots.

CENTRE: *P. deltoides* seedling, Palmerston North, New Zealand, 27.4.1978, showing epiphyllous circular blotches coalesced to form irregular necrotic patches.

BOTTOM: *P. deltoides* x *P. trichocarpa* cv. NL 1647, Palmerston North, New Zealand 24.4.1978, showing large epiphyllous circular to irregular blotches coalesced to form large irregular necrotic patches.

FIG. 39: Symptoms expressed by field collections of poplars infected with *M. brunnea*.

TOP: *P. simonii* x *P. deltoides* angulata cv. I69/55 seedling, Palmerston North, NZ, 27.11.1979, showing lesions on herbaceous shoots.

BOTTOM: *P. deltoides* seedling no. 75/105/9, showing black circular lesions on one year old wood.

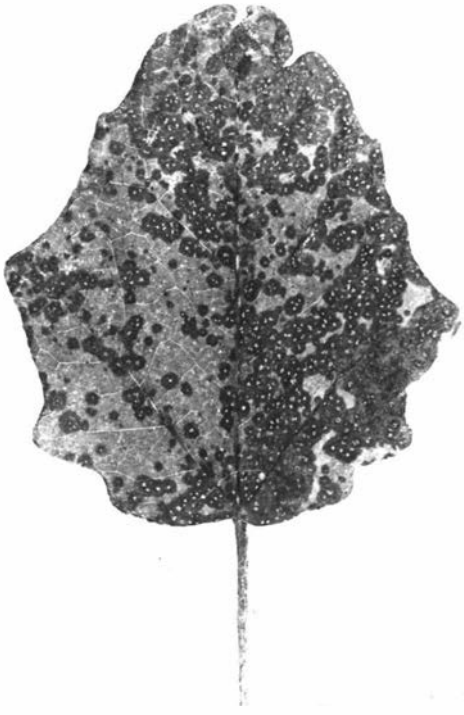

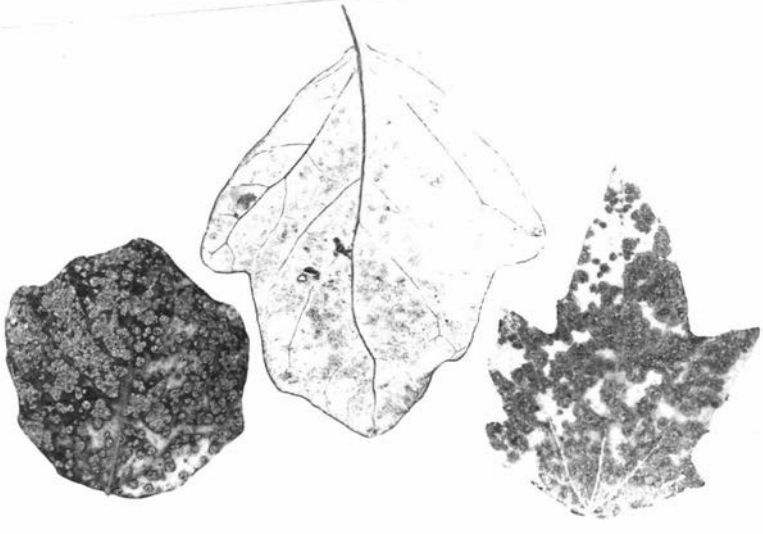

FIG. 40: Symptoms expressed by field collections of poplars infected with *M. castagnei*.

TOP: *P. alba*, Nurnberg Germany, collected by Starcs 6.9.1948, showing discrete circular lesions and irregular necrotic patches dotted with punctiform whitish acervuli.

BOTTOM: *P. alba*, Norway, collected by Nannfeldt 1930, showing coalescence of lesions to form extensive necrotic patches dotted with punctiform whitish acervuli. Note the diffuse dark patches on the adaxial leaf surface (centre).

FIG. 41: Symptoms expressed by field collections of poplars infected with *M. populi*.

TOP: *P. simonii*, Rothenburg Germany, collected by Zycha 17.8.1966, showing circular to angular lesions with some coalescence (spot symptom).

BOTTOM: *P. balsamifera*, Lake Timagami USA, collected by Thompson 25.8.1931, showing the spot symptom and extensive necrotic blotches dotted with whitish punctiform acervuli.

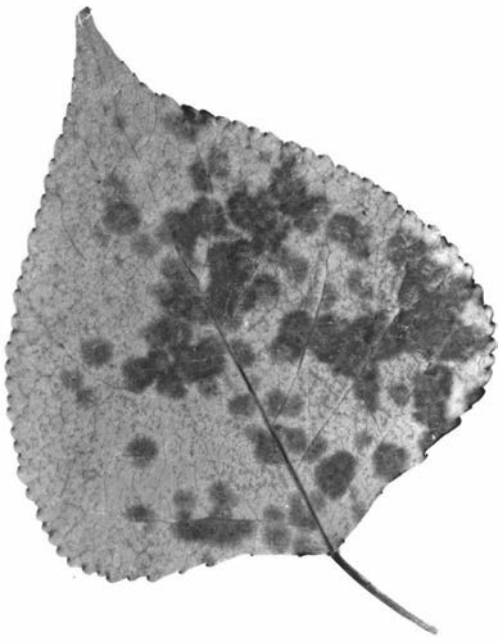

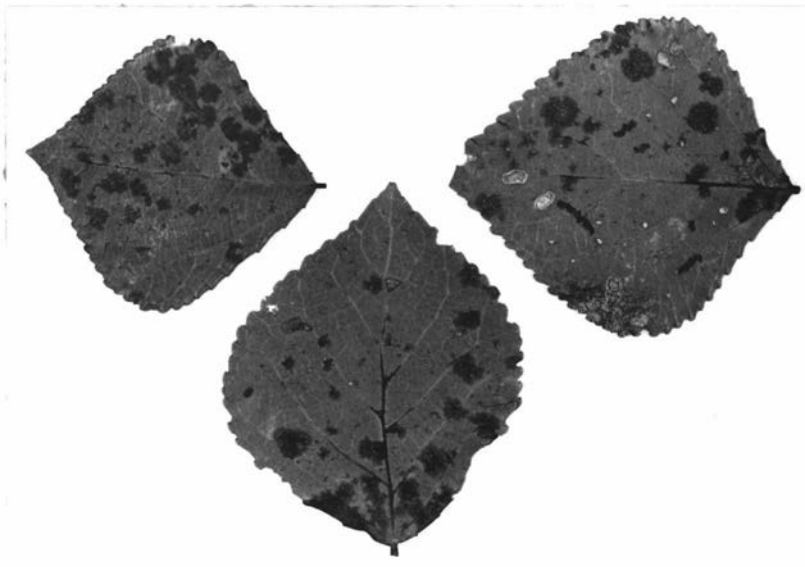

FIG. 42: Symptoms expressed by field collections of poplars infected with *M. populi*.

TOP: *P. marilandica*, Hannovers Munden Germany, collected by Butin 20.8.1955, showing the blotch symptom with coalescence.

BOTTOM: *P. nigra*, Niederdonau Germany, collected by Petrak 1939, showing circular blotches dotted with whitish punctiform acervuli.

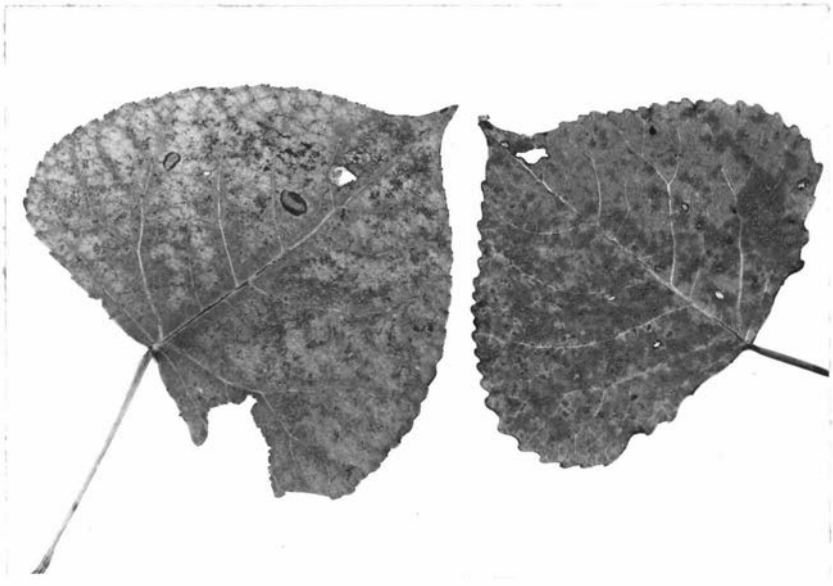

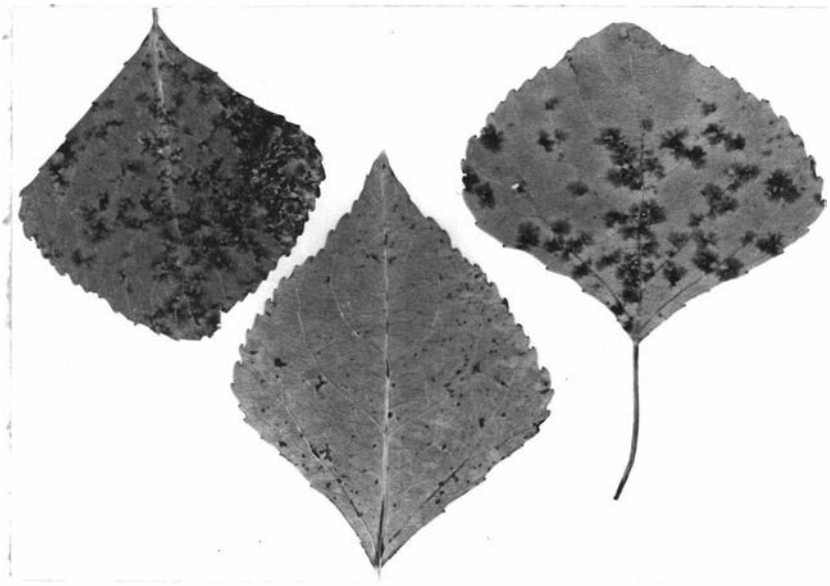

FIG. 43: Symptoms expressed by field collections of poplars infected with *M. populi*.
P. tremuloides, British Columbia Canada, collected by Andrews 18.7.1961, showing circular dendritic blotches.

FIG. 44: Symptoms expressed by field collections of poplars infected with *M. populi*.

TOP: *P. nigra*, Zurich Switzerland, collected by Rimpau 3.8.1960, showing fine dendritic threads (left).

BOTTOM: *P. nigra*, Stockholm Sweden, collected by Eriksson 1884, showing dendritic blotches on the adaxial leaf surface (left and right).

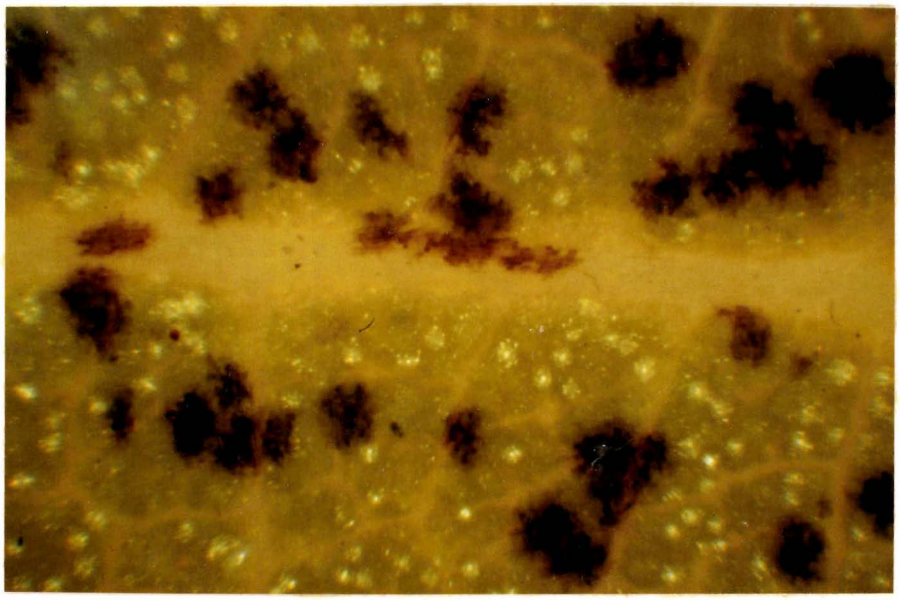

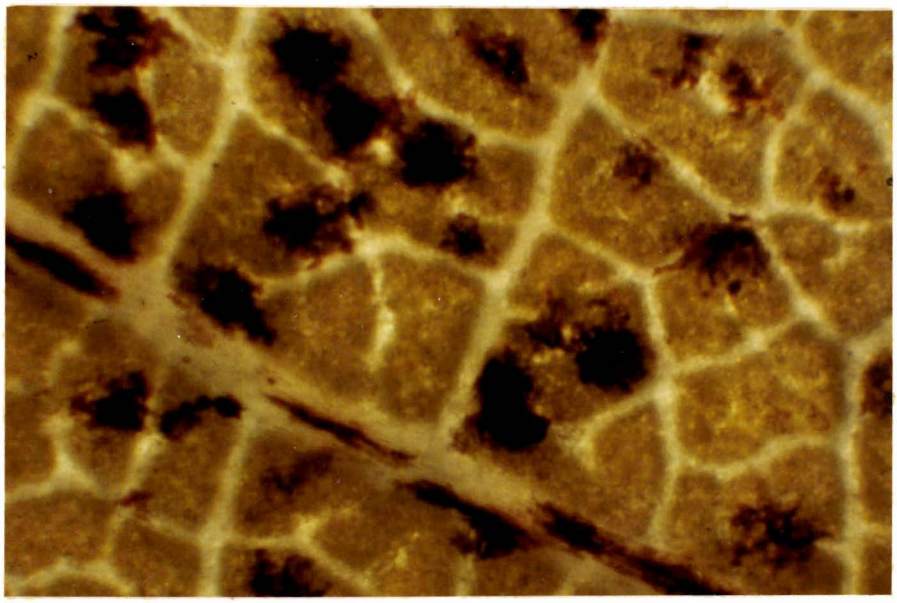

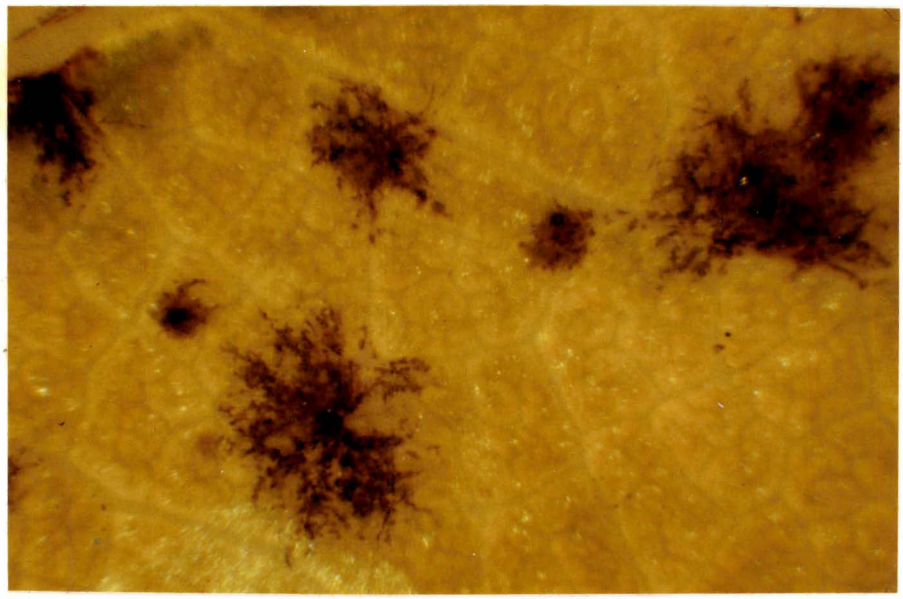

FIG. 45: Symptoms expressed on *P. nigra* cv. Italica 'Aurea' in laboratory inoculations with *Marssonina* species.

TOP: *M. brunnea:* small (1-2mm diam.), discrete punctiform black lesions.

CENTRE: *M. castagnei:* small (1-2mm diam.), discrete punctiform black lesions.

BOTTOM: *M. populi:* large (>5mm diam.), circular 'ink drop' like blotches.

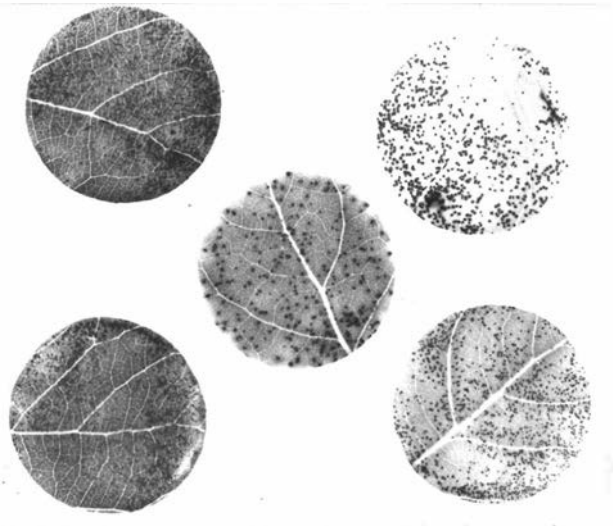

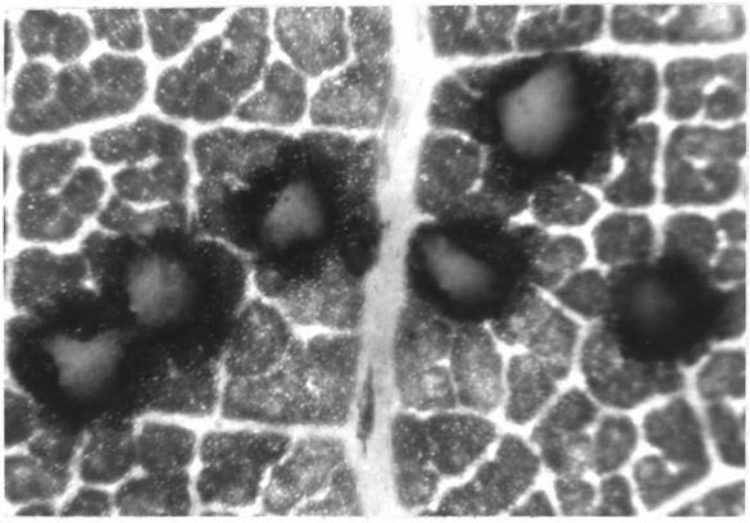

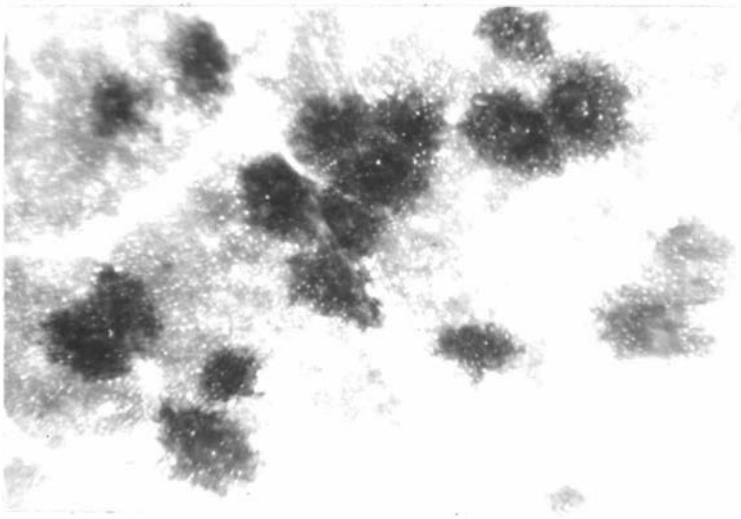

FIG. 46: Symptoms expressed on leaf discs in laboratory inoculations with *M. brunnea*.

TOP: Left - *P. nigra* cv. Vert de Garonne,
Centre - *P.* x *euramericana* cv. Robusta
Right - *P. nigra* cv. Italica 'Aurea'.

All clones exhibiting typical small (0.5-2.0mm diam.), circular to angular punctiform spots of *M. brunnea*.

Note with heavy infection the coalescence of lesions.

CENTRE: *P.* x *euramericana* cv. Robusta: circular to angular punctiform spots. Note the large white masses of conidia.

BOTTOM: *P. simonii:* discrete circular punctiform spots showing some coalescence.

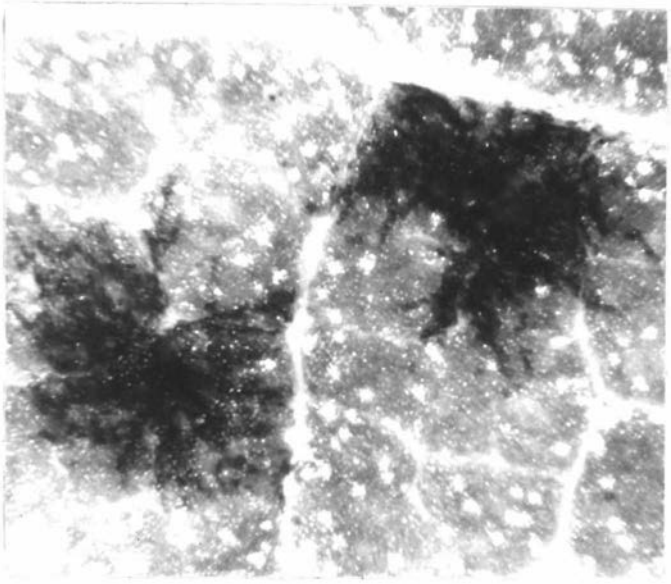

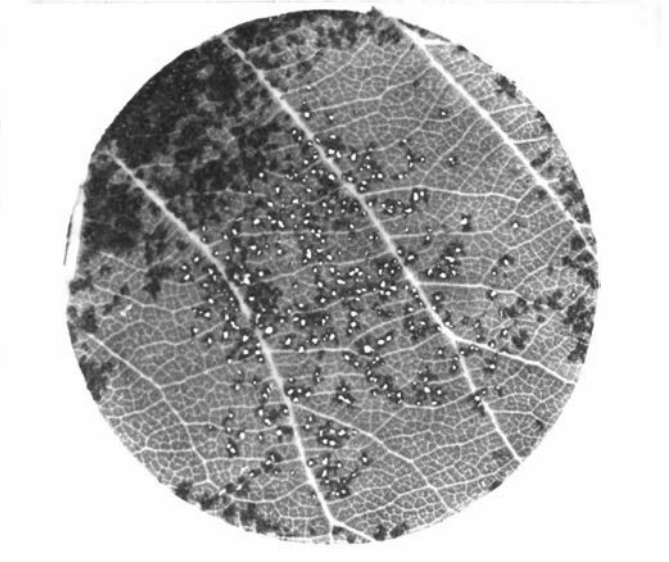

FIG. 47: Symptoms expressed on leaf discs in laboratory inoculations with *M. populi*.

TOP: *P. simonii:* irregular spots with dendritic margins.

CENTRE: *P.* x *euramericana* cv. Robusta.

BOTTOM: *P.* x *euramericana* cv. Schiavone.

Both showing irregular spots and coalescence.

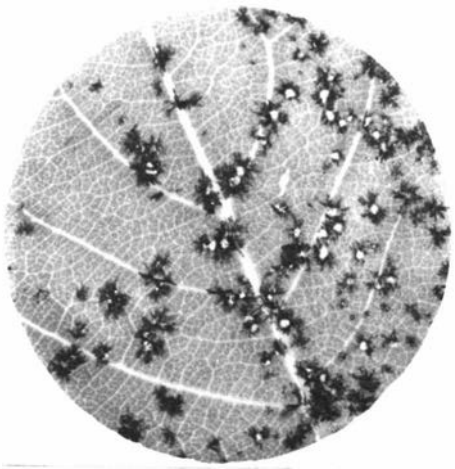

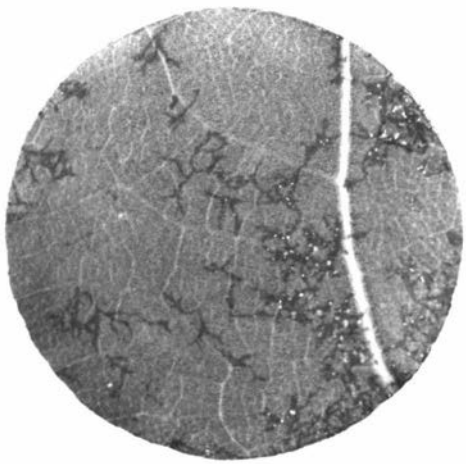

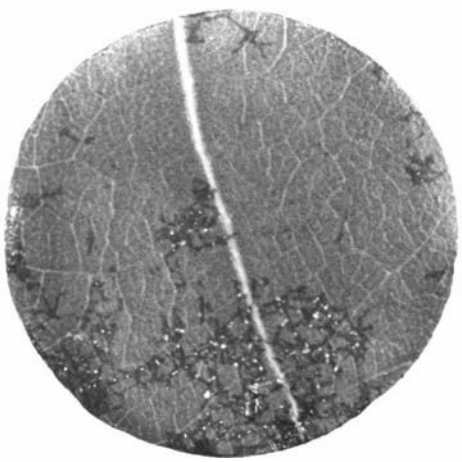

FIG. 48: Symptoms expressed on leaf discs in laboratory inoculations with *M. populi*.

TOP: *P. nigra* cv. Italica 'Aurea': 'ink drop' like spots with radial dendritic threads.

CENTRE: *P.* x *euramericana* cv. Bellini.

BOTTOM: *P. nigra* cv. Y83/66.

Both - showing branched dendritic threads covered with white masses of conidia.

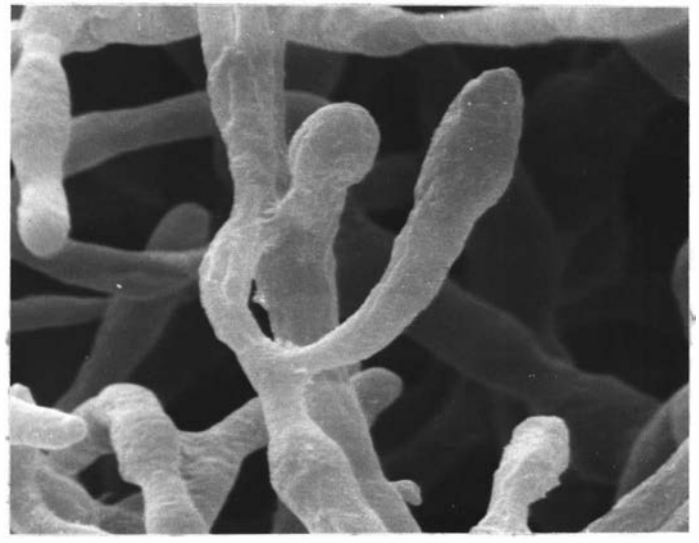

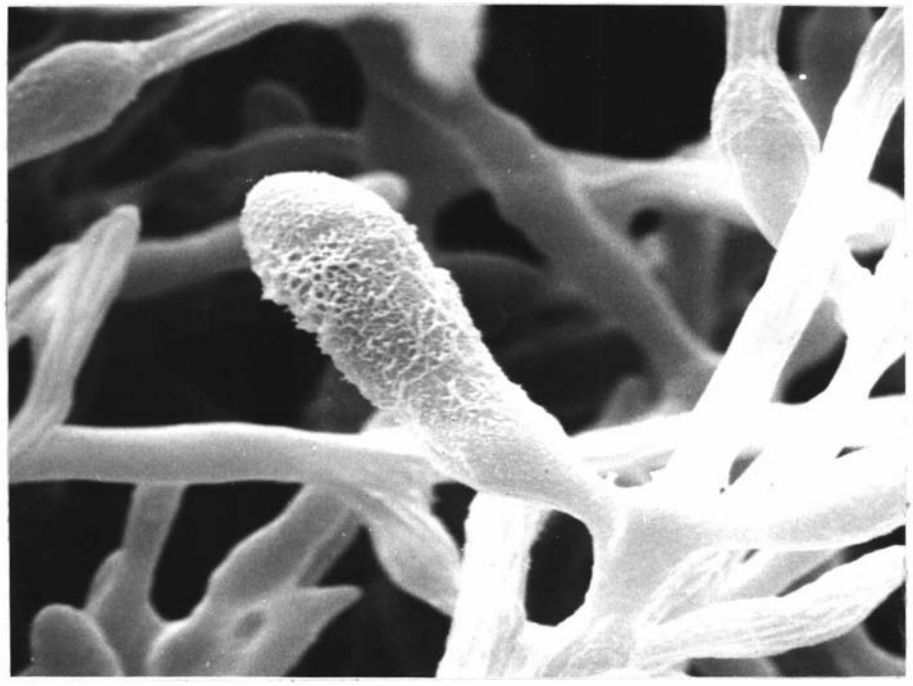

FIG. 50: *Marssonina brunnea:* scanning electron micrographs of conidium formation (15%V8, 10 days).

TOP: Initiation of primary conidium initial. X 12,000.

CENTRE: Holoblastic development of expanding primary conidium initial. X 3,200.

BOTTOM: Almost fully expanded primary conidium initial X 3,800.

Note 1: The smooth continuous wall between primary conidium initial and conidiophore which is indicative of holoblastic primary conidium formation.

Note 2: The deposit (possibly polysaccharide) on the conidium initial wall formed as an artifact of freeze drying.

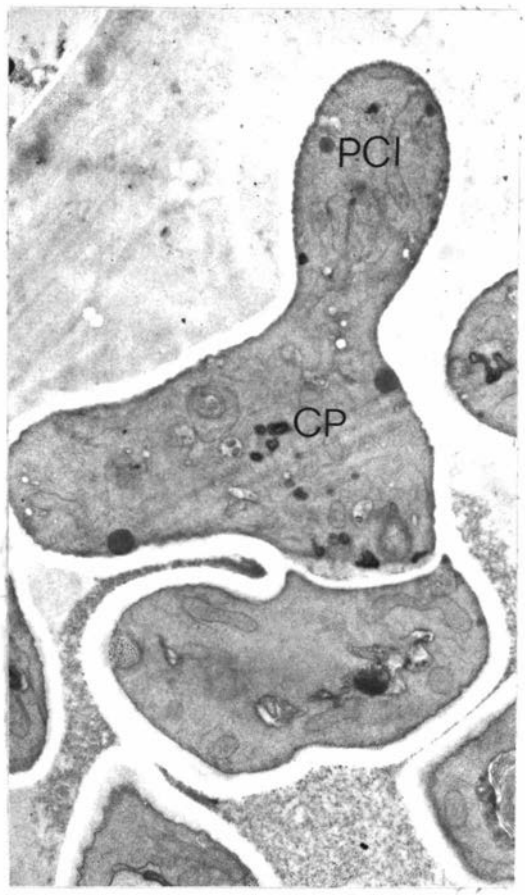
PCl
CP

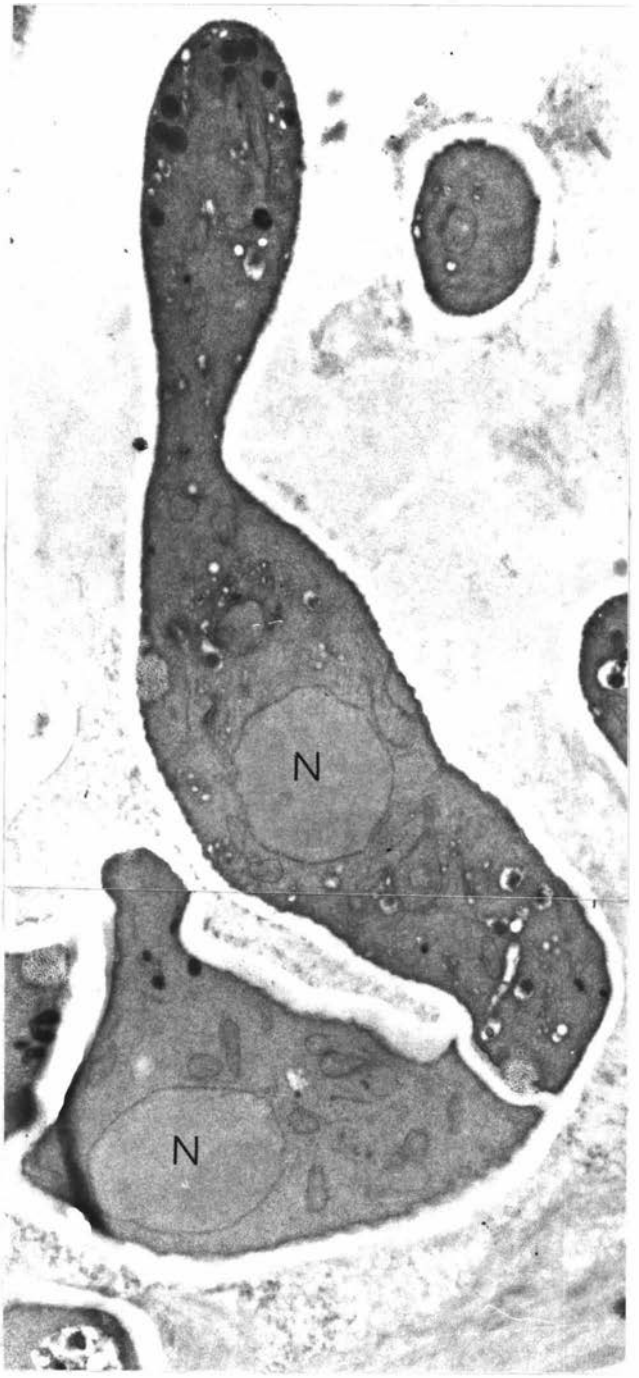
N
N

FIG. 51: *Marssonina castagnei:* electron micrographs of conidium formation (*P. alba* cv. NZ Old Clone 10 days). X 10,500.

LEFT: Holoblastic extension of primary conidium initial (PCI) from the conidiophore (CP).

RIGHT: Holoblastic extension of primary conidium initials from ampulliform conidiophores.

Note nuclei (N) in the base of the conidiophores.

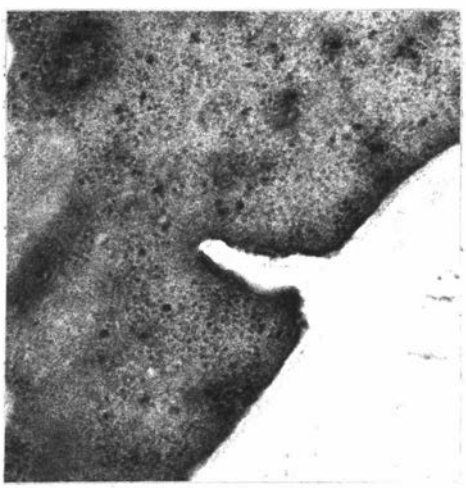

FIG. 52: *Marssonina castagnei*, *P. alba* 'Morocco' x *P. nigra* Sempervirens cv. Mareg 2.

TOP: Delimitation of primary conidium initial from the conidiophore by centripetal invagination of the plasmalemma leading to formation of a bilayered conidium delimiting septum. X 8,100.

BOTTOM: Septum initial and invaginated plasmalemma. X 46,000.


N


N
N

FIG. 53: *Marssonina brunnea:* formation of septum within the primary conidium initial following its delimitation from the conidiophore (*P. nigra* cv. Vert de Garonne).

LEFT: The primary conidium initial nucleus has divided (mitosis) and one daughter nucleus (N) has migrated to the base of the primary conidium initial. The septum within the conidium initial is forming by invagination of the plasmalemma. Note the perforate conidium delimiting septum. X 13,500.

RIGHT: The septum within the primary conidium initial has formed, both cells of the conidium enclosing a single nucleus (N).

The primary conidium initial is close to secession. X 13,500.


O
N

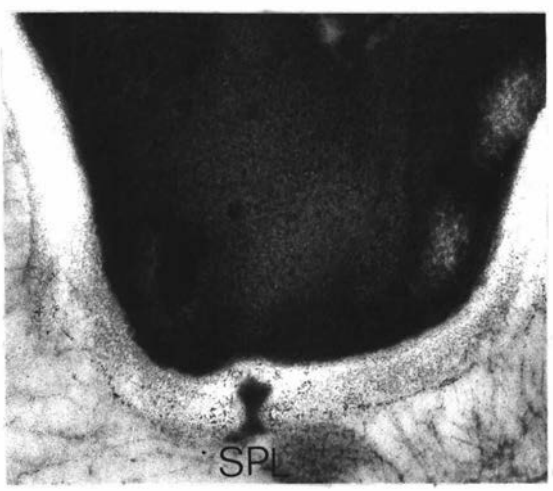
SPL

FIG. 54: *Marssonina castagnei*, *P. alba* NZ old clone.

LEFT: Formation of septum within primary conidium initial following delimitation of conidium initial from the conidiophore. The nucleus within the primary conidium initial has divided (mitosis) and one daughter nucleus (N) has migrated to the base of the conidium initial. X 8,100.

TOP RIGHT: Recently seceded conidium with a single nucleus within each cell of the conidium, and a septal plug embedded in the conidium base. X 10,500.

BOTTOM RIGHT: Plugged septal pore in base of seceded conidium.

Note 1: Deposition of further wall material on the inside of the septal plug (SPL).

Note 2: Inconspicuous basal frill on the conidium base. X 46,000.

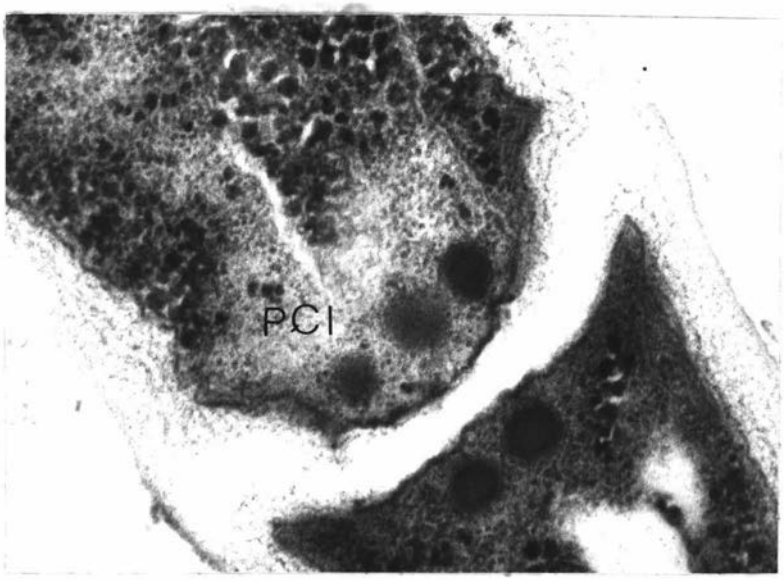
PCI

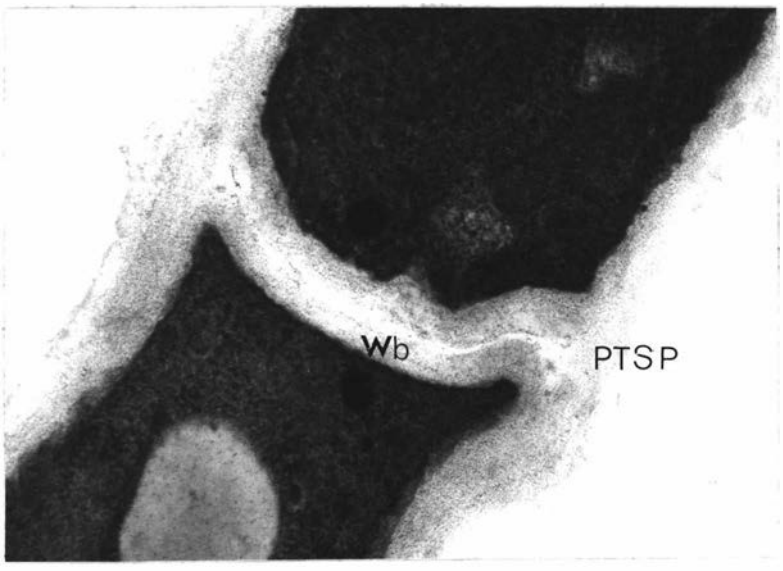
Wb
PTSP

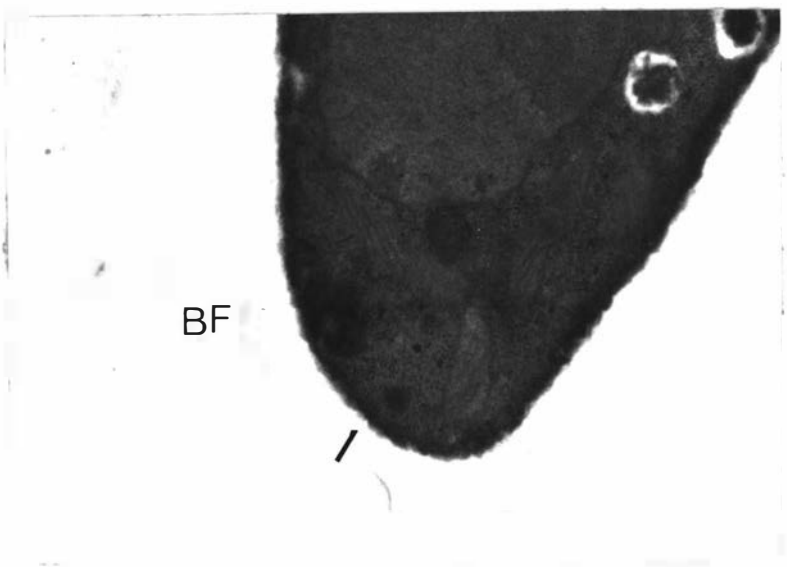
BF

FIG. 55: *Marssonina populi:* primary conidium initial delimiting septum (*P. nigra* cv. Italica).

TOP & CENTRE: Conidium delimiting septum between primary conidium initial and conidiophore. X46,000.

Note 1: Continuous outer wall which is single layered opposite the junction between the conidiophore and the primary conidium initial.

Note 2: The triangular pockets adjacent to the periclinal walls (periclinal triangular septal pockets, PTSP).

Note 3: (Centre) Woronin bodies (Wb) within primary conidium initial and conidiophore.

BOTTOM: *Marssonina populi* recently seceded conidium showing conspicuous basal frill (BF) and single layered wall (↗) at the base of the conidium. X 40,000.

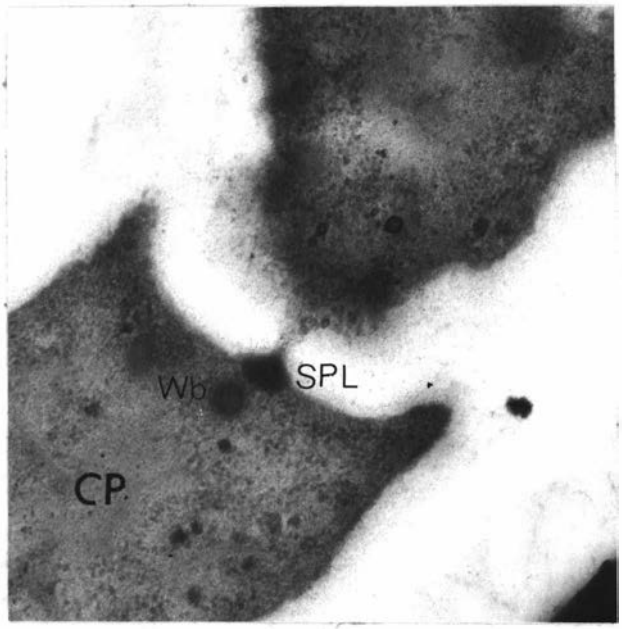
Wb
SPL
CP

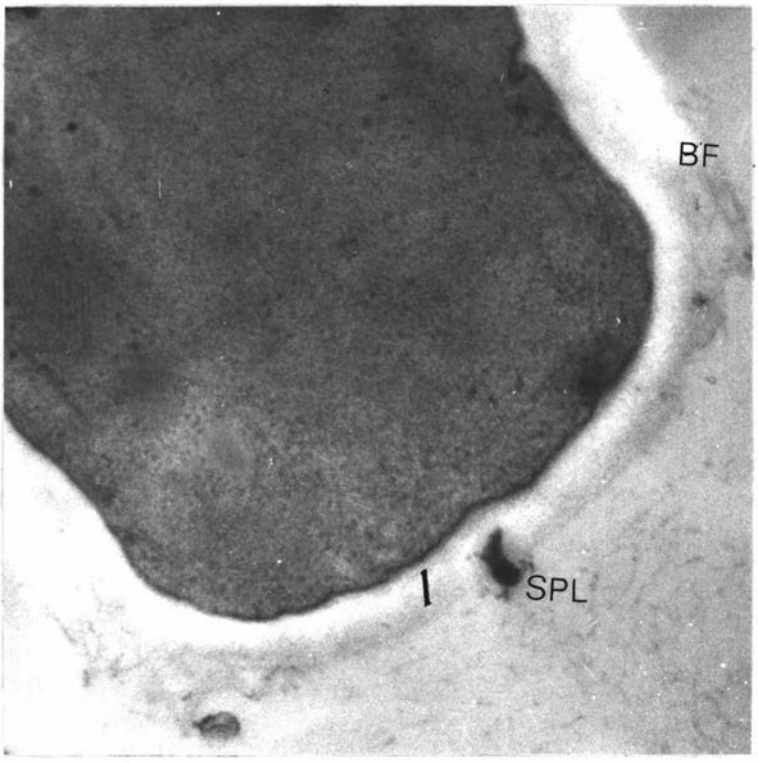
BF
SPL

FIG. 56: *Marssonina populi:* conidium secession.

TOP: *P.* x *euramericana* cv. Robusta. Septum between primary conidium initial and conidiophore (CP) prior to septum plugging and conidium secession.

Note 1: Septal plug (SPL) entering septal pore from the conidiophore and two Woronin bodies (Wb) within the conidiophore. X46,000.

BOTTOM: *P. nigra* cv. Vert de Garonne. Plugged septal pore in base of seceded conidium.

Note 1: Deposition of additional wall material on the inside of the septal plug (SPL).

Note 2: The single layered wall at the base of the conidium (|).

Note 3: The inconspicuous basal frill (BF) on the conidium base and the bilayered wall above the basal frill. X 46,000.

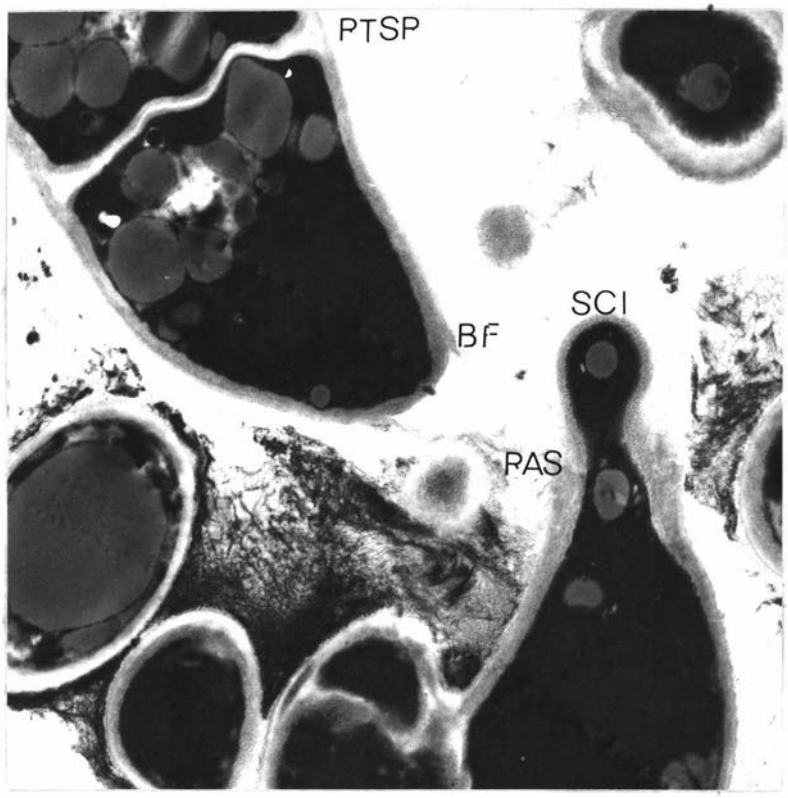
PTSP
SCI
BF
PAS


SCI
CP

FIG.57: *Marssonina brunnea:* conidium secession (15%V8 agar).

TOP: Release of primary conidium from the conidiophore and enteroblastic extension of secondary conidium initial (SCI) through the conidiophore apex.

Note 1: Basal frill (BF) on conidium base and corresponding primary annular scar (PAS) on the conidiophore.

Note 2: Central splitting of the bilayered conidial septum (*f*) and the triangular pockets adjacent to the periclinal walls (periclinal triangular septal pockets, PTSP). X13,500.

BOTTOM: Release of primary conidium from the conidiophore without formation of prominent basal frills on the conidium base and primary annular scars on the conidiophore (CP).

Note formation of secondary conidium initial (SCI) enteroblastically from inside the base of the primary annular scar (*f*). X25,000.

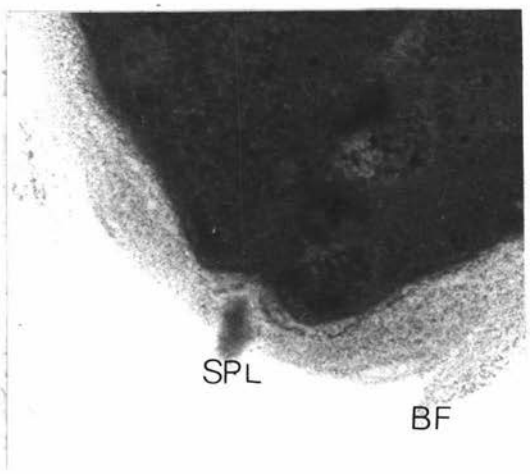
SPL
BF

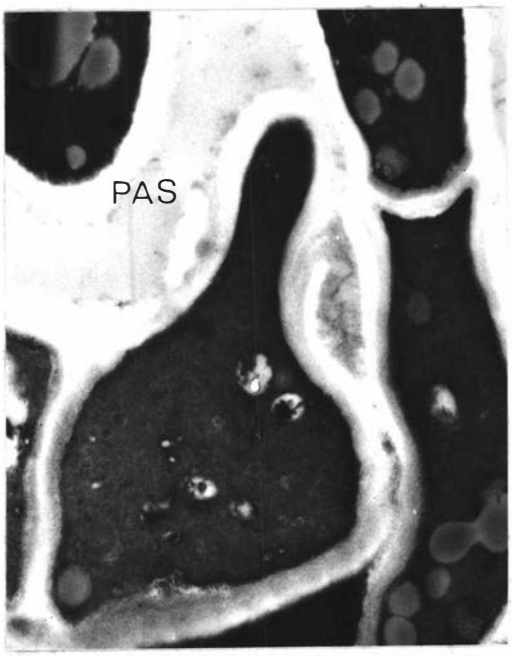
PAS

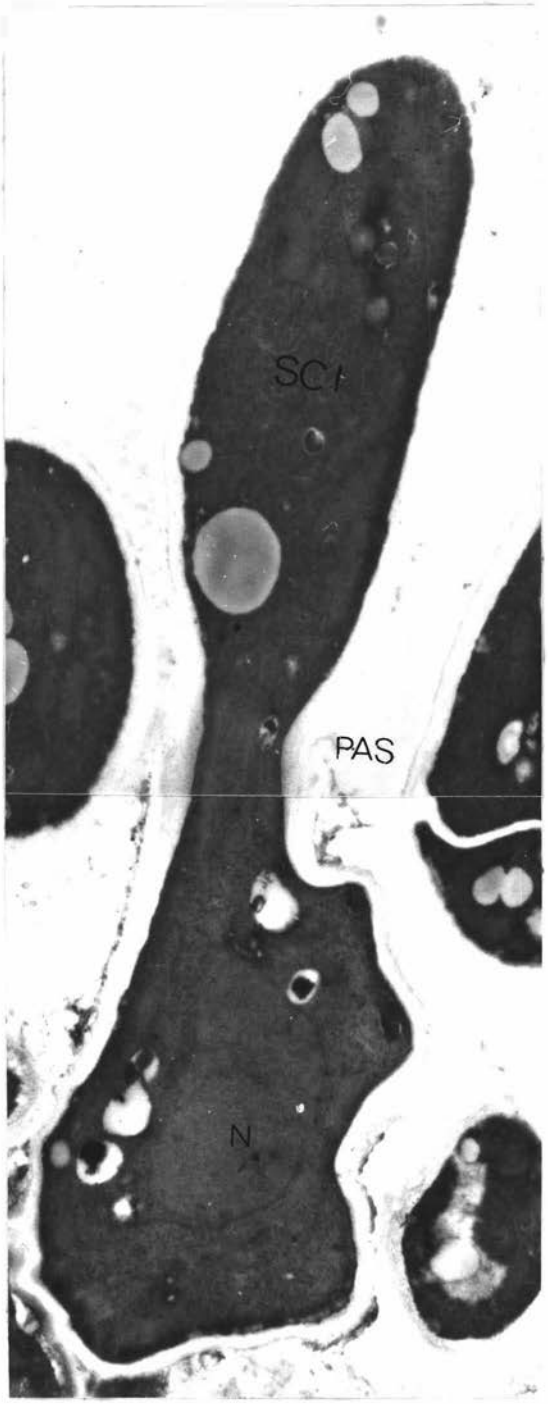
SC
PAS
N

FIG. 58: *Marssonina brunnea:* Conidium secession and formation of secondary conidium initial.

TOP LEFT: Recently seceded conidium (see Fig.57) showing septal pore plug (SPL) and conspicuous basal frill (BF). (15%V8 agar).

Note 1: Deposition of further wall material on the inside of the septal plug.

Note 2: The single layered basal conidium wall. X61,000.

BOTTOM LEFT: Enteroblastic extension of secondary conidium initial (SCI) from conidiophore soon after secession of primary conidium as indicated by the primary annular scars (PAS).

(*P. nigra* cv. Vert de Garonne). X13,500.

RIGHT: Almost fully expanded secondary conidium initial (SCI) as indicated by the primary annular scars (PAS).

Note possible division (mitotic) of the conidiophore nucleus (N) prior to migration of a daughter nucleus into the secondary conidium initial.

(*P.* x *euramericana* cv. I-154). X13,500.


B
L
N
SCI
C
N
A
N

FIG. 59: *M. brunnea:* formation and delimitation of secondary conidium initials. (*P. nigra* cv. Vert de Garonne). X10,500.

A. Conidiophore 'blowing out' secondary conidium initial following secession of primary conidium.

B. Fully expanded secondary conidium initial (SCI) following delimitation from the conidiophore prior to division (mitotic) of the conidium initial nucleus (N) and formation of the conidial septum. Note the lipid globules (L) in the conidium initial.

C. Slightly later stage than B. The nucleus within the secondary conidium initial has divided and one daughter nucleus (N) has migrated to the conidium base, but as yet the conidium septum has not formed.

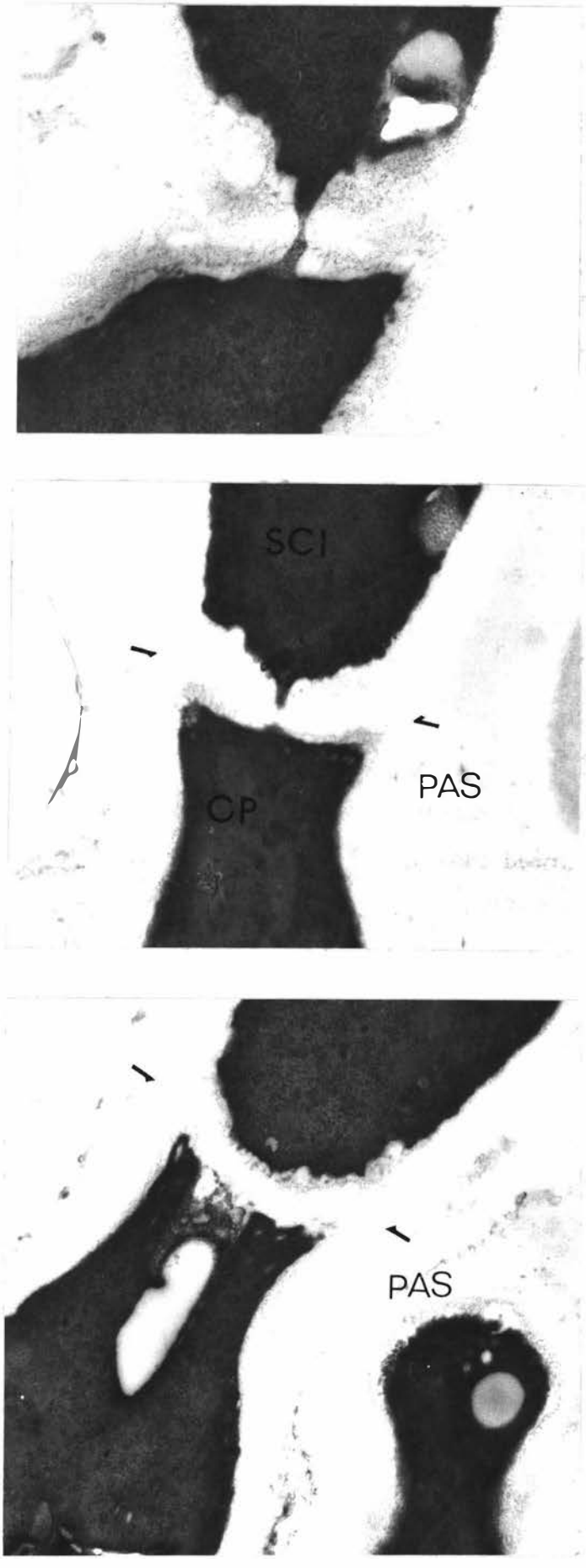
SCI
CP
PAS
PAS

FIG. 60: *Marssonina brunnea:* the delimiting septum between the secondary conidium initial (SCI) and the conidiophore (CP).

TOP: Bilayered conidium delimiting septum showing simple septal pore. (*P.* x *euramericana* cv. Robusta). X25,000.

CENTRE & BOTTOM: Secondary conidium delimiting septum showing delimitation of the second formed conidium at a higher level on the conidiophore apex than the first formed conidium (arrows ↑ mark possible point of secession).

Note 1: Bilayered septum and the inconspicuous periclinal triangular septal pockets.

Note 2: Primary annular scar (PAS) formed on secession of primary conidium.

(*P. nigra* cv. Vert de Garonne). X25,000.

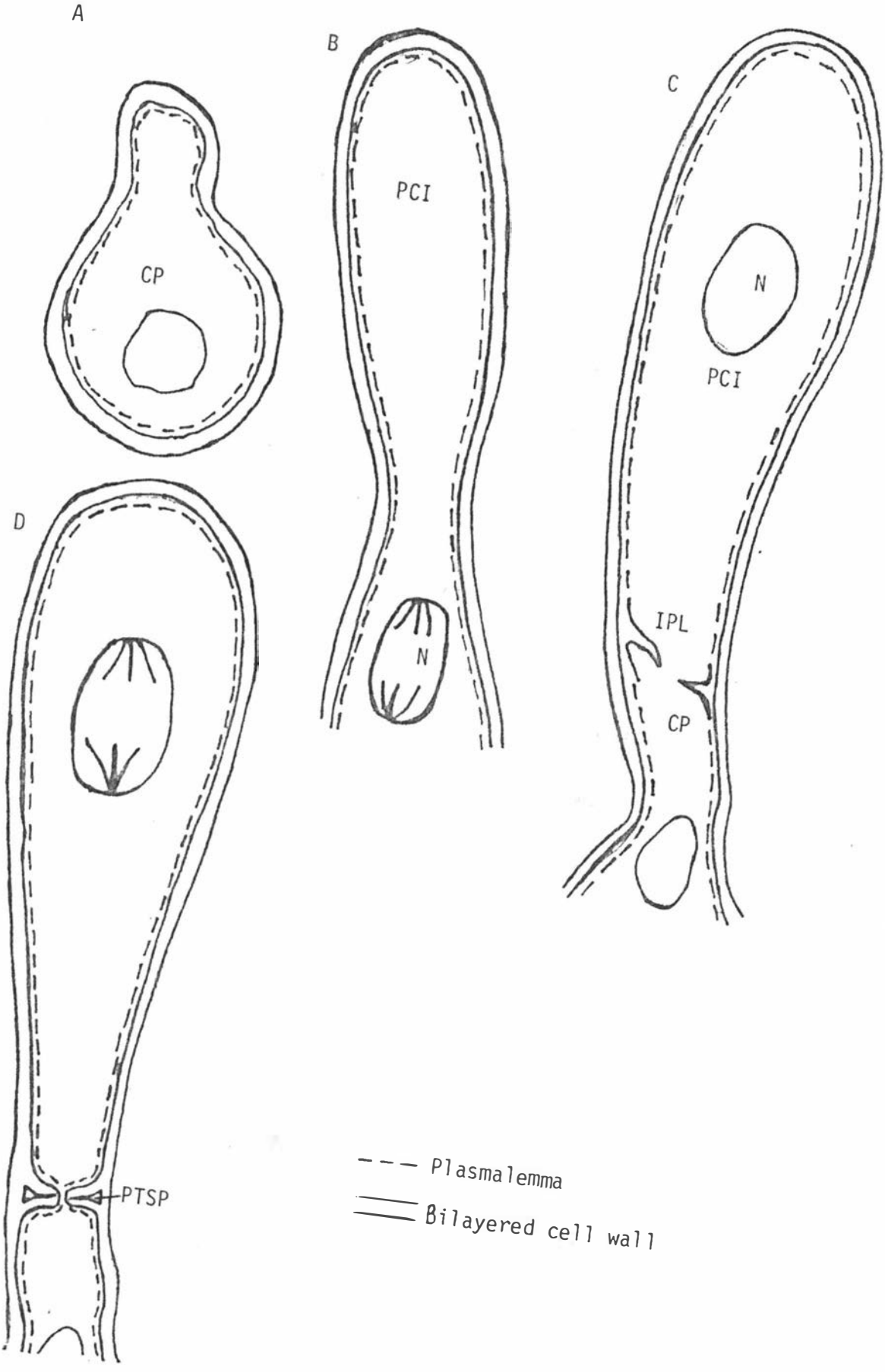
A
B
C
D
CP
PCI
N
PCI
N
IPL
CP
PTSP
Plasmalemma
Bilayered cell wall

FIG. 61: A-I Diagrammatic interpretation of conidiogenesis of *M. brunnea*, *M. populi* and *M. castagnei*. Approx. X13,000.

A. Initiation of conidiogenesis by apical extension of the conidiophore (CP).

B. Holoblastic extension of the conidiophore wall to form the primary conidium initial (PCI). The wall between the conidiophore and the primary conidium initial is continuous and inconspicuously bilayered. Prior to full extension of the primary conidium initial the single nucleus (N) within the conidiophore divides mitotically.

C. One daughter nucleus (N) migrates into the fully expanded primary conidium initial (PCI) and the conidium initial becomes delimited from the conidiophore (CP) by formation of a septum. Septation is initiated by centripetal invagination of the plasmalemma (IPL invaginating plasmalemma).

D. The conidium delimiting septum is perforate and bilayered with the periclinal triangular septal pockets (PTSP). Soon after formation of the conidium delimiting septum the single conidium initial nucleus divides mitotically.

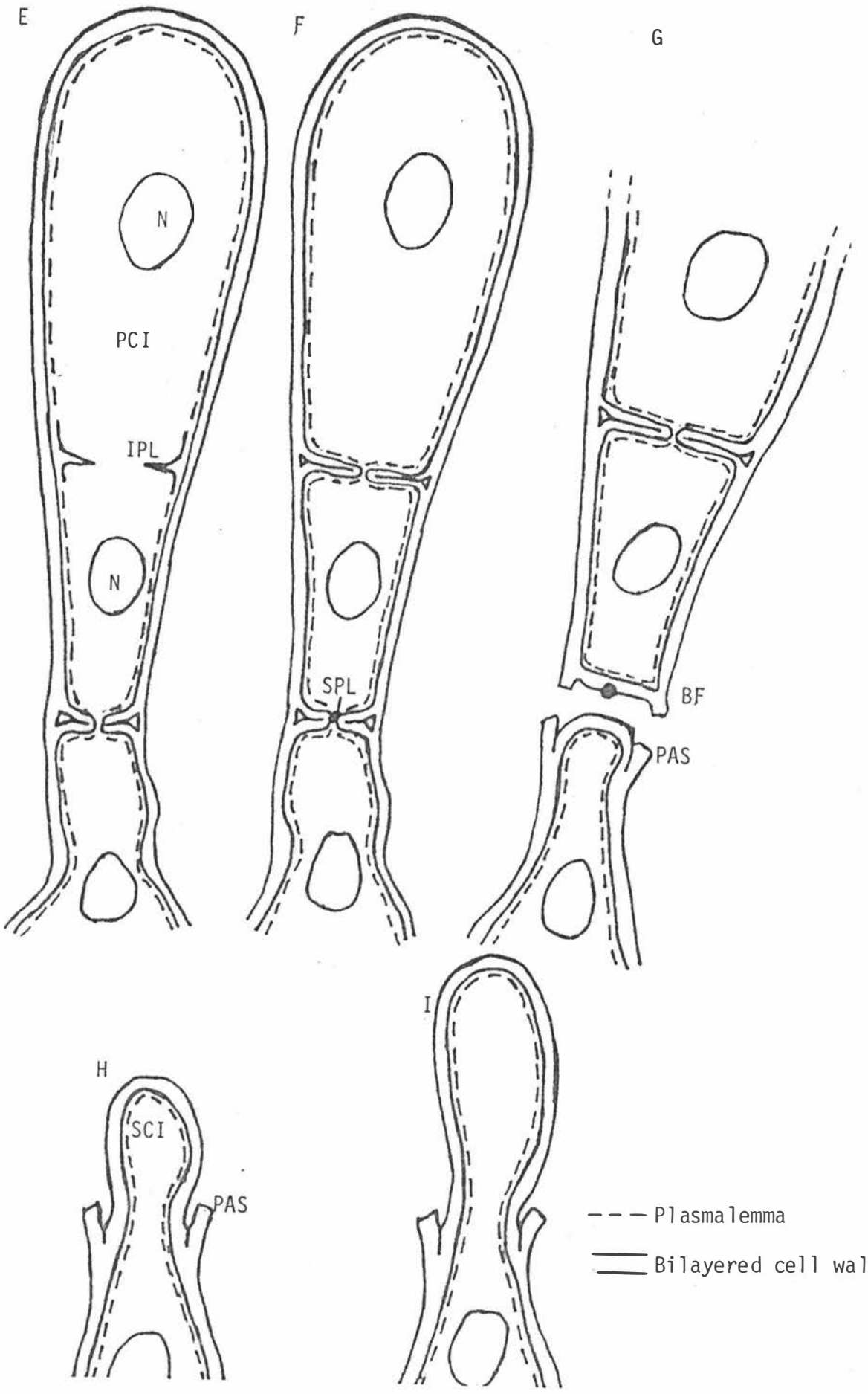
E
F
G
N
PCI
IPL
N
SPL
BF
PAS
H
SCI
PAS
I
Plasmalemma
Bilayered cell wal

FIG. 61:

E. Following nuclear division a daughter nucleus (N) migrates to the base of the primary conidium initial (PCI) and formation of the conidial septum is initiated by centripetal invagination of the plasmalemma (IPL).

F. The perforate septum within the primary conidium initial is fully formed. The septal pore of the conidium delimiting septum is plugged within an electron dense deposit, the septal plug (SPL).

G. Conidium secession by central splitting of the bilayered conidium delimiting septum commencing at the triangular pockets adjacent to the periclinal walls (PTSP) and circumscissle rupture of the periclinal wall adjacent to the septum. The broken outer wall forms a basal frill (BF) on the conidium base and primary annular scars (PAS) on the conidiophore apex.

Note the septal plug embedded in the base of the seceded conidium.

H & I: The secondary conidium initial (SCI) 'blowing out' enteroblastically through the conidiophore apex from inside the primary annular scars (PAS) until the secondary conidium initial is fully formed, repeating the steps outlined for the primary conidium initial.

FIG. 62: Diagrammatic interpretation of the conidium delimiting septum between the primary and secondary conidium initial and the conidiophore. Approx. X25,000.

A. Conidium delimiting septum between the primary conidium initial (PCI) and the conidiophore (CP).

Note 1: The simple septal pore (SP) and the periclinal triangular septal pockets (PTSP).
Note 2: The continuous outer wall which is single layered opposite the periclinal septal pockets.

B. Conidium delimiting septum between the secondary conidium initial (SCI) and the conidiophore (CP).

Note 1: The simple septal pore and the periclinal triangular septal pockets (PTSP).
Note 2: The primary annular scars (PAS) on the conidiophore formed by secession of the primary conidium initial.
Note 3: Delimitation of secondary conidium initial at a higher level on the conidiophore than the primary conidium initial.

C. Secession of secondary conidium initial (SCI) from the conidiophore (CP).

Note 1: Basal frill (BF) and septal plug (SPL) in base of seceded conidium.
Note 2; The single layered conidium base and conidiophore apex.
Note 3: The primary and secondary annular scars (PAS, SAS) on the apex of the conidiophore.

D. Enteroblastic extension of tertiary conidium initial (TCI) from inside the base of the secondary annular scar (SAS).

Note the annellated conidiophore.

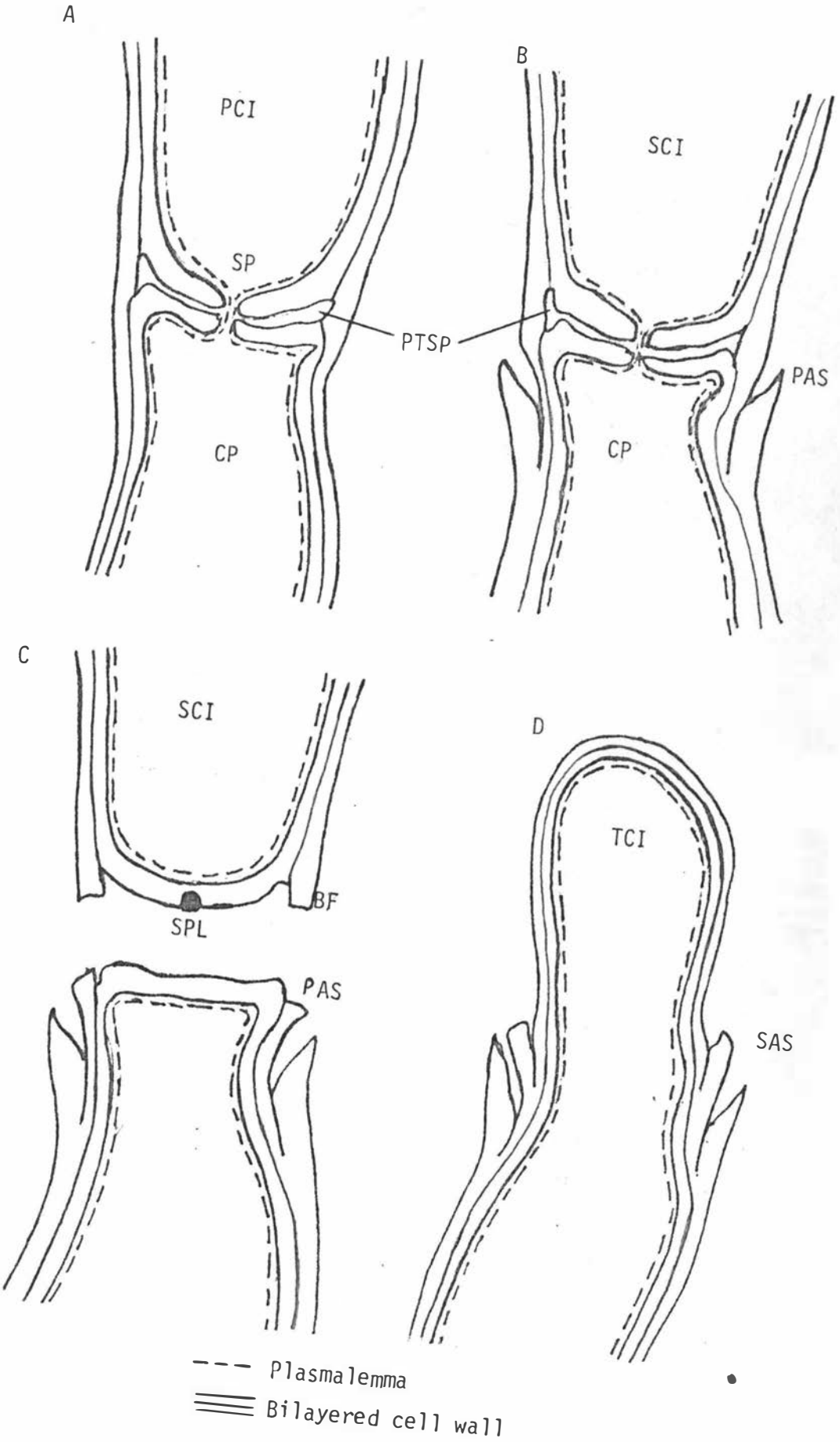
A
PCI
SP
PTSP
CP
B
SCI
PAS
CP
C
SCI
BF
SPL
PAS
D
TCI
SAS
Plasmalemma
Bilayered cell wall

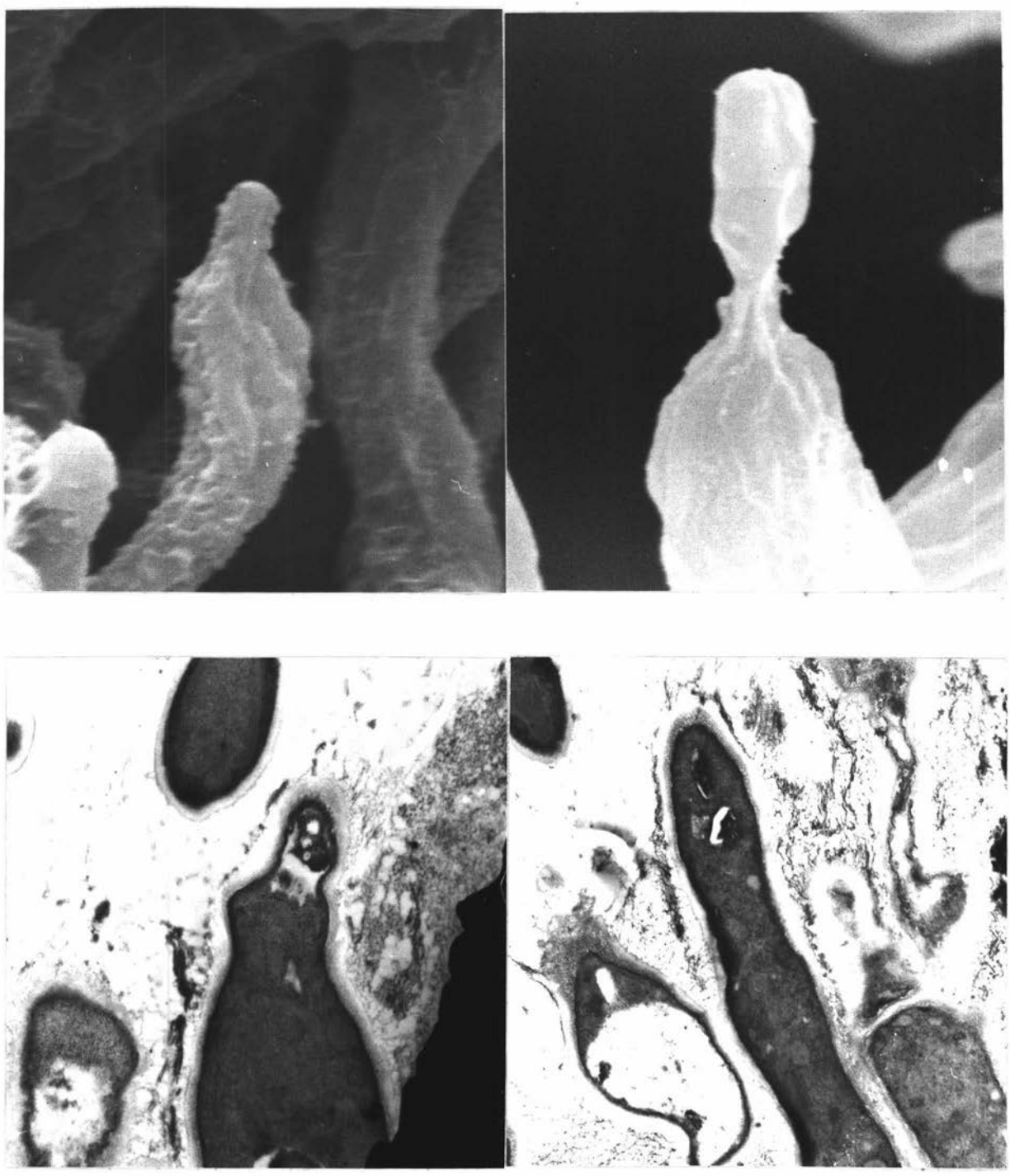

FIG. 63: *Marssonina brunnea:* microconidium formation.

TOP LEFT: Initiation of the primary microconidium initial (15%V8 agar). X8,000.

TOP RIGHT: Developing primary microconidium initial (15%V8 agar). X8,000.

BOTTOM LEFT & RIGHT: Holoblastic extension of microconidiophore to form primary microconidium initial (*P.* x *euramericana* cv. NL 2194). X 17,000.

FIG. 64: *Marssonina populi:* microconidium formation.

TOP: Almost fully formed primary microconidium initial (15%V8 agar). X10,000.

Note smooth continuous wall between primary microconidium initial and microconidiophore.

BOTTOM: Holoblastic extension of microconidiophore to form primary microconidium initial (*P. nigra* cv. Italica). X6,400.

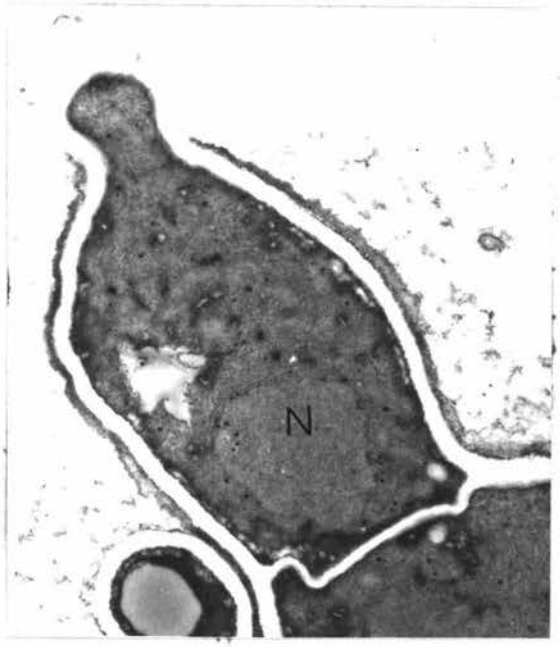
N


N

FIG. 65: *Marssonina brunnea:* formation and delimitation of primary microconidium initial (15%V8 agar).

TOP LEFT: Formation of primary microconidium initial by apical extension of the microconidiophore.

Note the basal nucleus (N) in the microconidiophore. X11,000.

BOTTOM LEFT: Almost fully expanded primary microconidium initial.

Note the continuous outer wall. X20,000.

RIGHT: Fully formed primary microconidium following delimitation from the microconidiophore.

Note single central nucleus (N) within the primary microconidium. X22,000.

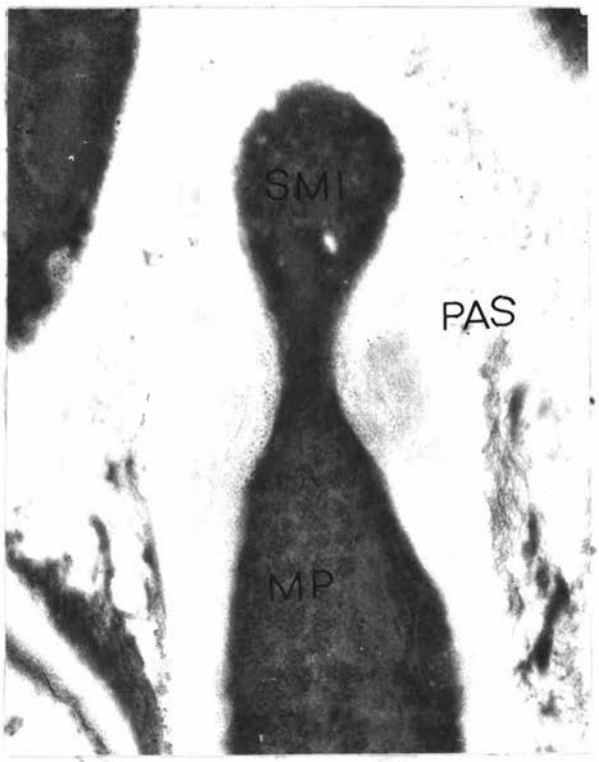
SMI
PAS
MP


PAS

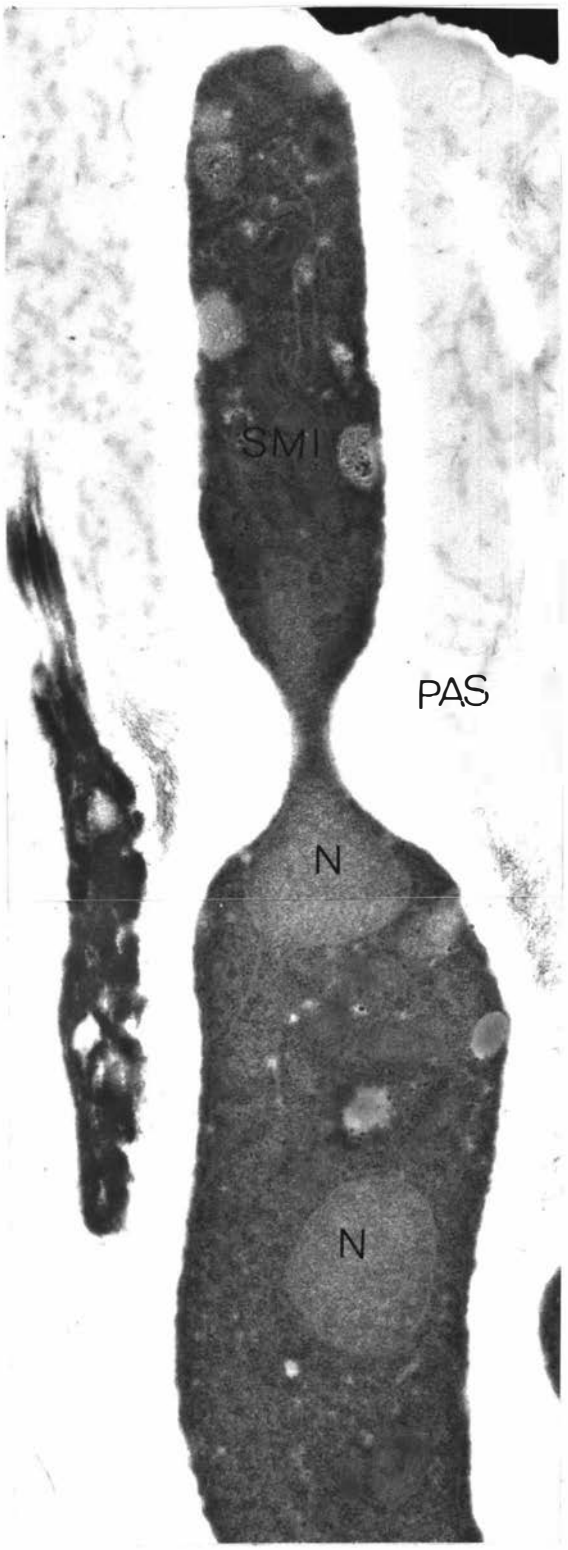
SMI
PAS
N
N

FIG. 66: *Marssonina populi:* formation of the secondary microconidium initial.

TOP LEFT: Enteroblastic extension of secondary microconidium initial (SMI) from the microconidiophore (MP) soon after secession of the primary microconidium.

Note the large primary annular scars (PAS) formed by secession of primary microconidium (15%V8 agar). X25,000.

BOTTOM LEFT: Secession of primary microconidium and enteroblastic extension of secondary microconidium initial from the microconidiophore.

Note the basal frill (BF) on the conidium base and the corresponding primary annular scar (PAS) on the apex of the microconidiophore (*P. nigra* cv. Italica). X17,500.

RIGHT: An almost fully expanded secondary microconidium initial (SMI) as indicated by the presence of primary annular scars (PAS) on the apex of the microconidiophore.

Note that the microconidiophore nucleus has divided (mitotically) and a daughter nucleus (N) is migrating through the narrow channel in the apex of the microconidiophore to enter the secondary microconidium initial (15%V8 agar). X22,500.

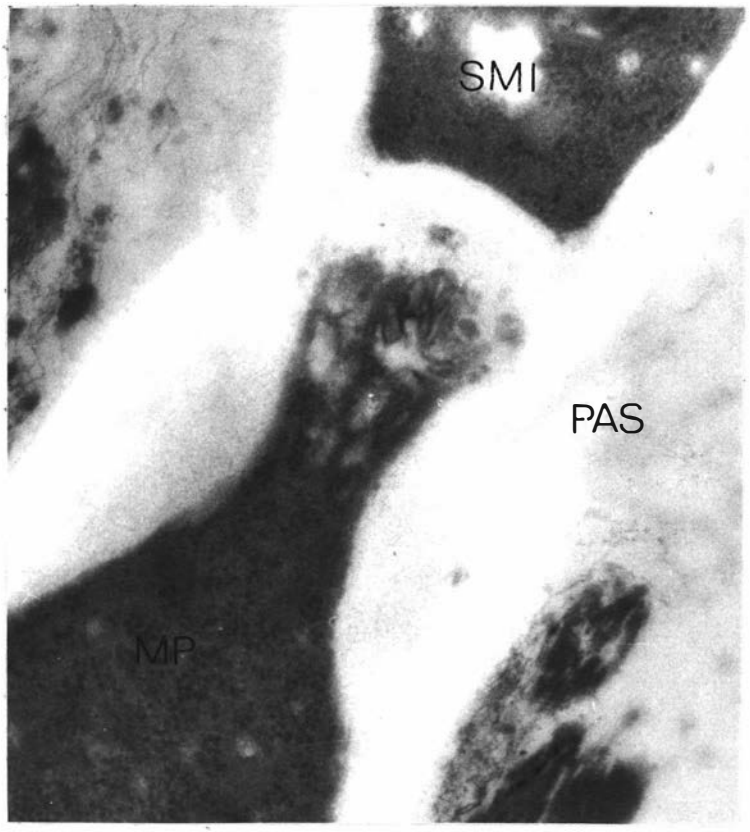
SMI
PAS
MP

FIG. 67: *Marssonina populi:* the delimiting septum between the secondary microconidium initial (SMI) and the microconidiophore (MP).

Note 1: The prominent primary annular scars (PAS) on the microconidiophore.

Note 2: The formation of the secondary microconidium initial delimiting septum at a higher level on the conidiophore than previously for the primary microconidium (15%V8 agar). X46,000.

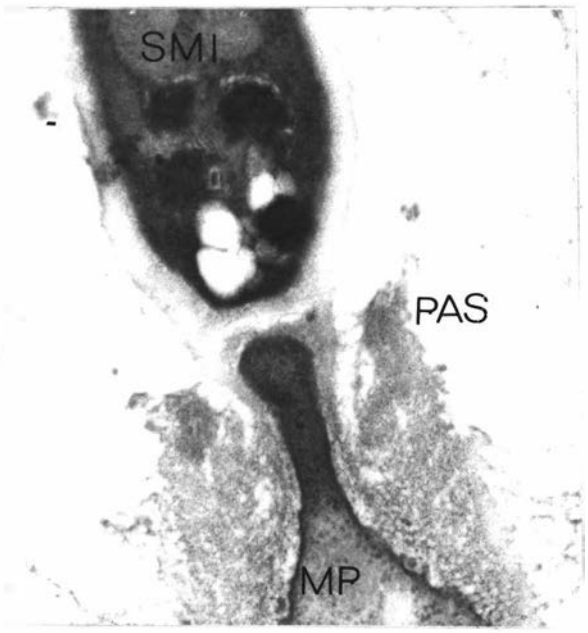
SMI
PAS
MP

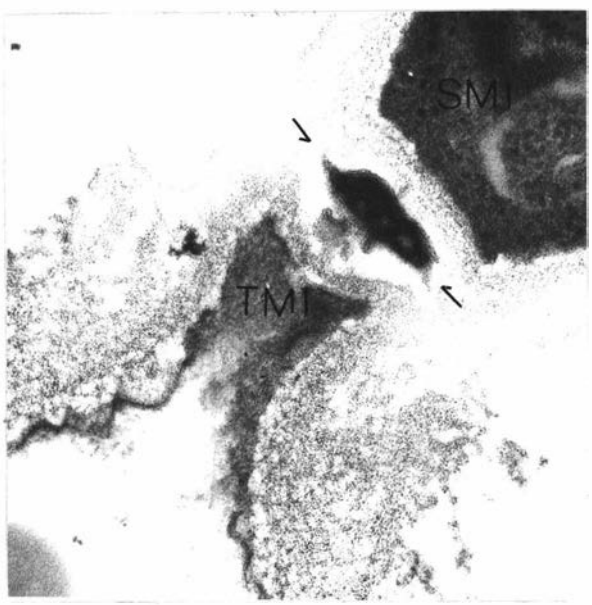
SMJ
TMI

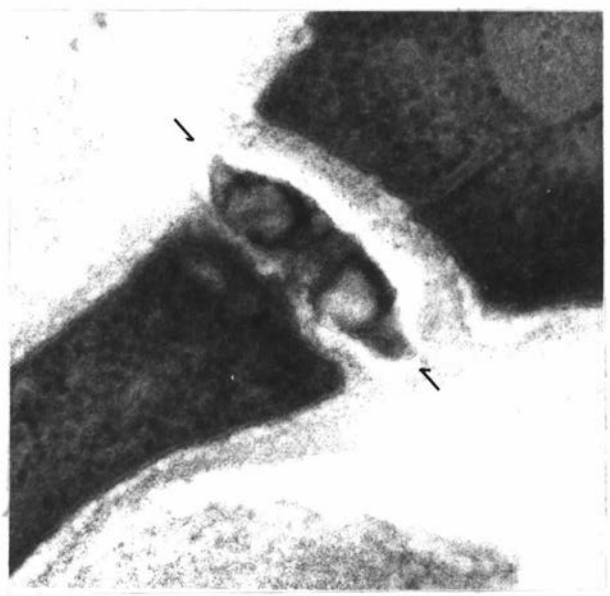

FIG. 68: *Marssonina brunnea:* microconidium delimiting septum between secondary microconidium initial and microconidiophore (*P.* x *euramericana* cv. NL 2194).

TOP LEFT: Atypical mode of septation involving independent development of the basal microconidium wall and the wall of underlying microconidium initial.

Note the entrapped pool of cytoplasm. X34,000.

TOP RIGHT: Common mode of septation involving the formation of a common bilayered septum between the microconidiophore (MP) and the secondary microconidium initial (SMI). Note the large primary annular scars (PAS). X34,000.

BOTTOM LEFT & RIGHT: Atypical mode of septation.

Note 1: The basal wall of the secondary microconidium initial (SMI) and the apex of the next formed tertiary microconidium initial (TMI) are single layered, possibly as a result of their independent formation.

Note 2: The entrapped pool of cytoplasm. The arrows indicate the possible line of microconidium secession.

LEFT: X61,000
RIGHT: X82,500.

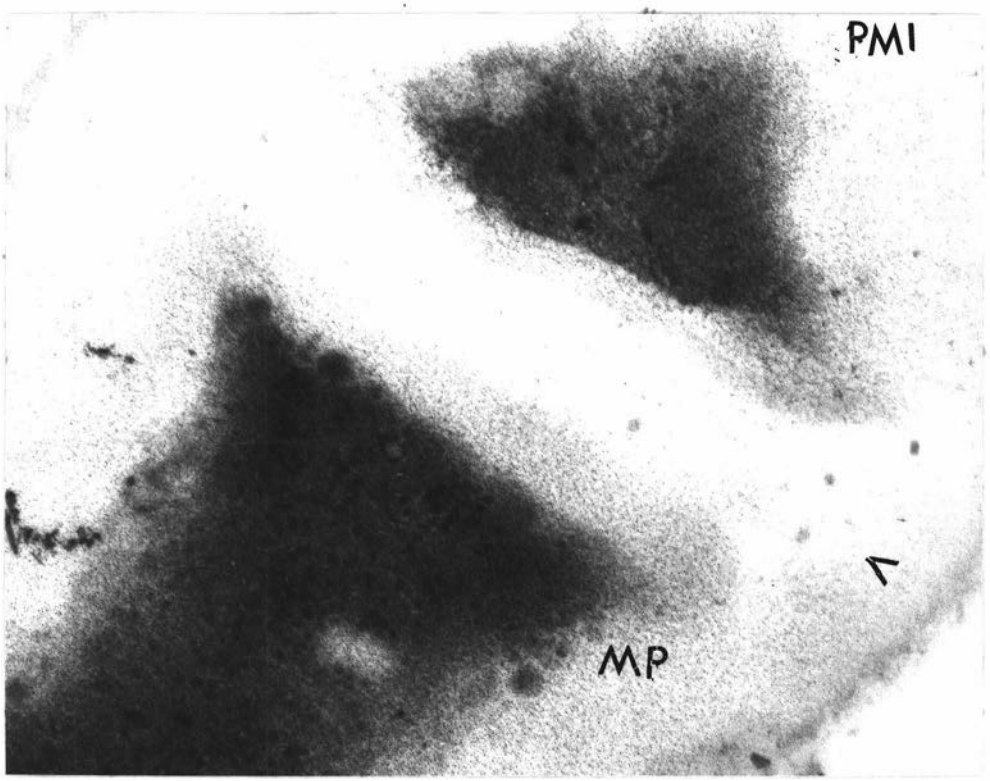
PMI
MP

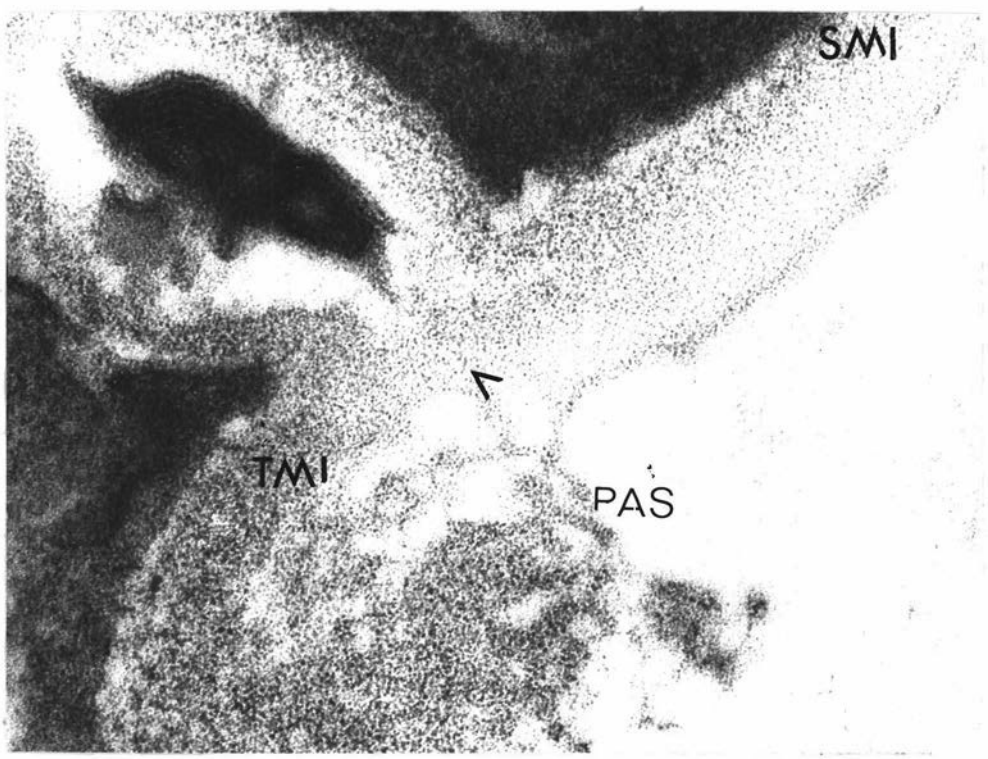
SMI
TMI
PAS

FIG. 69: *Marssonina brunnea:* comparison of the two types of microconidium delimiting septa (*P.* x *euramericana* cv. NL 2194).

TOP: Most common method of septation between the primary microconidium initial (PMI) and microconidiophore (MP) involving the formation of a common bilayered septum. Note the mid line separation of the two wall layers of the septum and the single layered periclinal wall, X160,000.

BOTTOM: Atypical septum, this instance formed between the secondary microconidium initial (SMI) and the microconidiophore (MP).

Note 1: The walls at the base of the secondary microconidium initial (SMI) and the underlying apex of the tertiary microconidium initial (TMI) are single layered.

Note 2: The single layered periclinal wall at the possible point of secession (↑).

Note 3: The primary annular scar (PAS). X140,000. For a lower magnification see Fig. 68 bottom left.

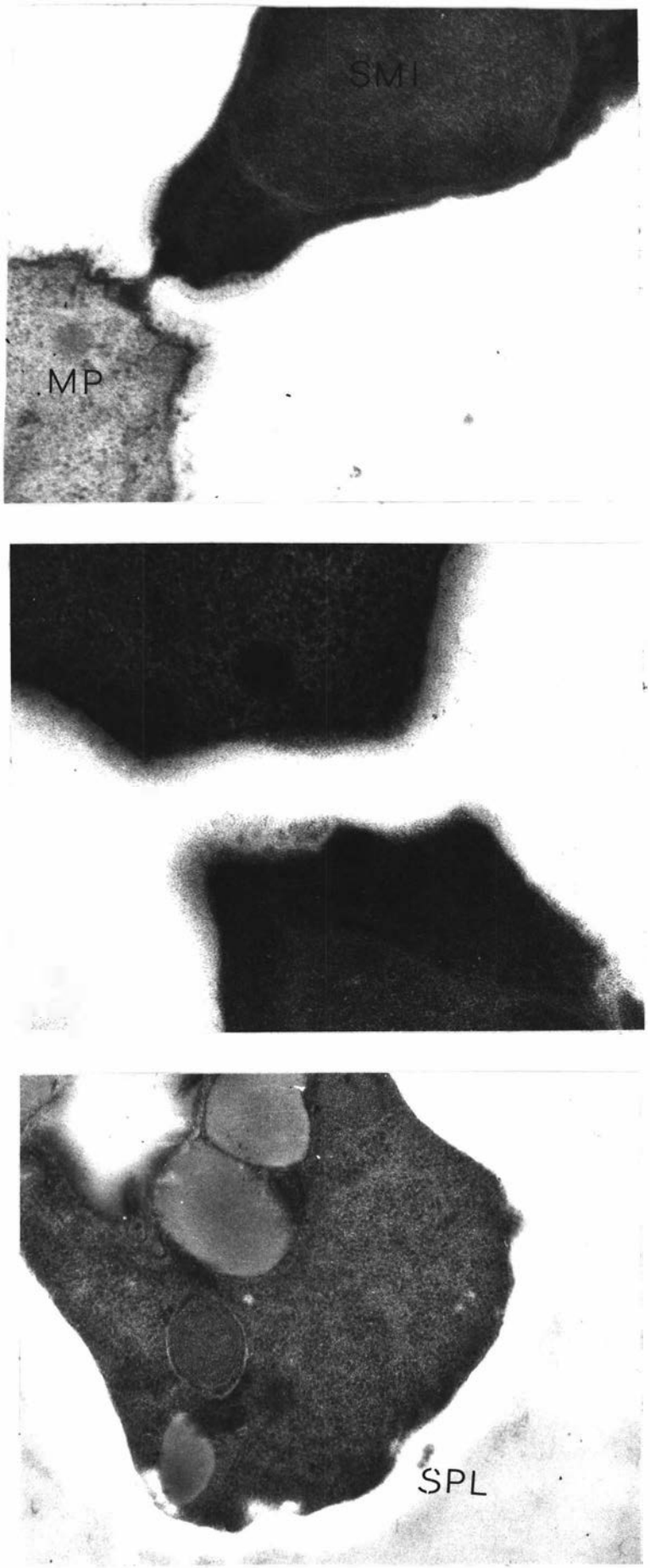
SMI
MP
SPL

FIG. 70: *Marssonina brunnea:* microconidium delimiting septum between the secondary microconidium initial (SMI) and the microconidiophore (MP). (*P.* x *euramericana* cv. NL 2194).

TOP: Bilayered microconidium delimiting septum showing simple septal pore.

Note the possible septal plug entering the septal pore from the secondary microconidium initial (SMI). X46,000.

CENTRE: Presence of Woronin bodies in the secondary microconidium initial and the microconidiophore following formation of the delimiting septum. X82,500.

BOTTOM: Recently seceded microconidium with a septal pore plug (SPL) embedded in the microconidium base. X34,000.

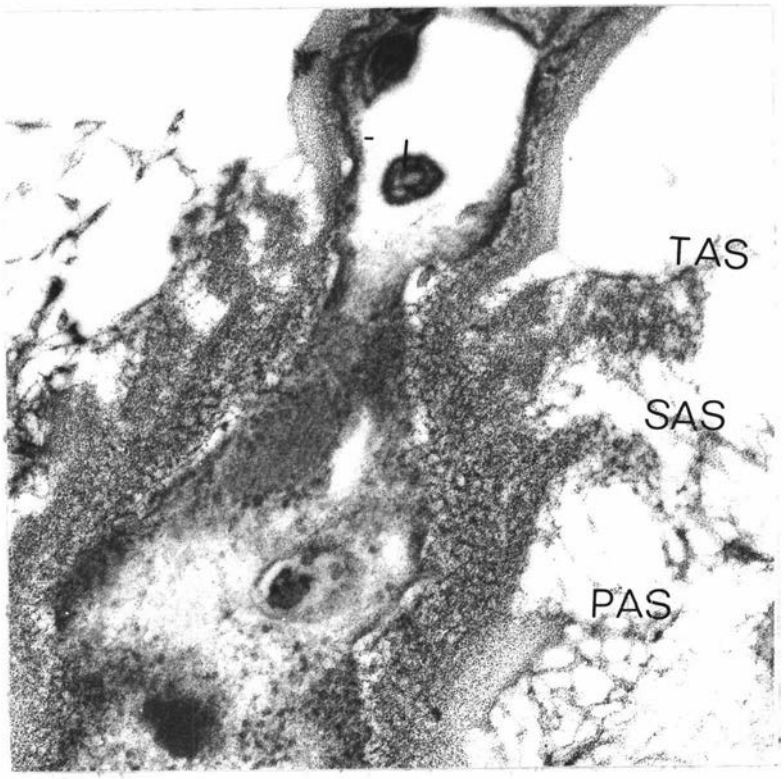
TAS
SAS
PAS

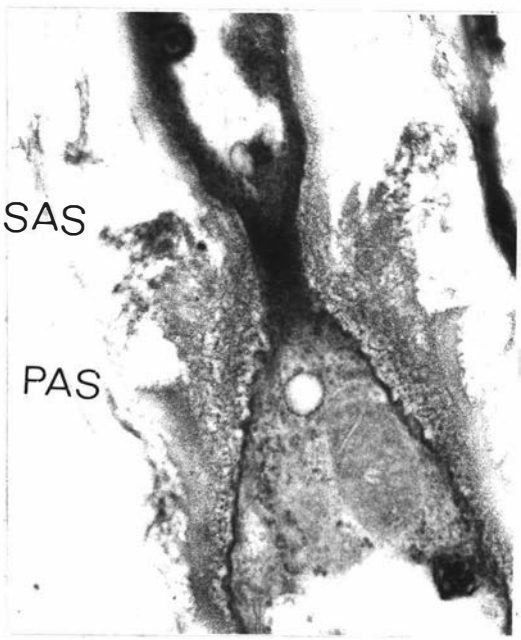
SAS
PAS

FIG. 71: *Marssonina brunnea* formation of annellations on the microconidiophore (*P.* x *euramericana* cv. NL 2194).

TOP: Development of the quarternary microconidium initial as indicated by the presence of primary (PAS), secondary (SAS) and tertiary annular scars (TAS) on the apex of the microconidiophore. X42,500.

BOTTOM LEFT & RIGHT: Development of the tertiary microconidium initial as indicated by the presence of primary (PAS) and secondary annular scars (SAS) on the microconidiophore.

LEFT: X24,000
RIGHT: X34,000.

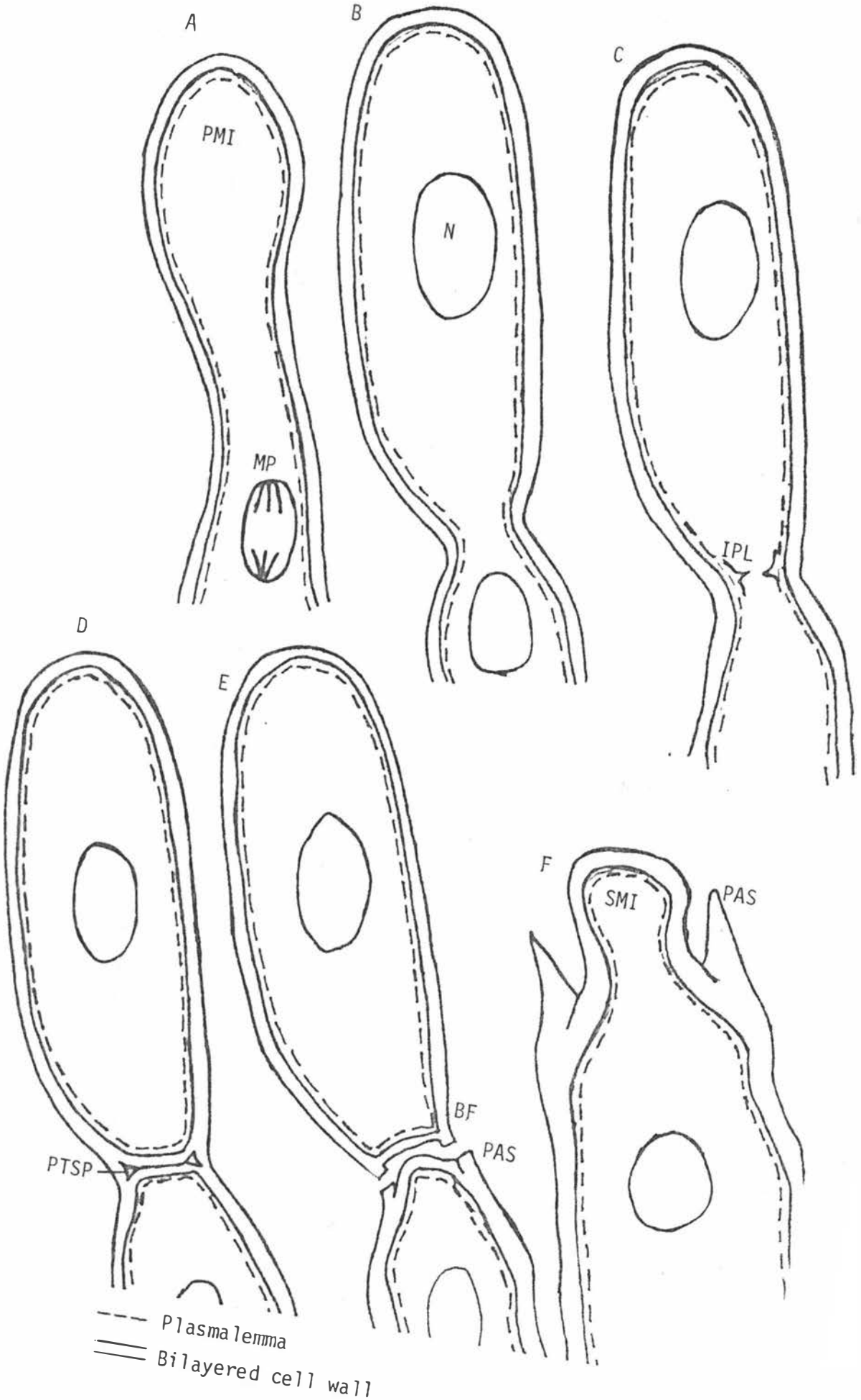
A
PMI
MP
B
N
C
IPL
D
PTSP
E
BF
PAS
F
SMI
PAS
Plasmalemma
Bilayered cell wall

FIG. 72 A-M: Diagrammatic interpretation of microconidiogenesis of *M. brunnea*, *M. populi* and *M. castagnei*. Approx. X20,000.

A. Holoblastic formation of the primary microconidium initial (PMI) by apical extension of the microconidiophore (MP), indicated by the wall between and the primary microconidium initial being continuous and inconspicuously bilayered. Prior to full extension of the primary microconidium initial the single conidiophore nucleus will divide mitotically.

B. The primary microconidium initial is fully expanded with a single nucleus (N) which has migrated from the microconidiophore.

C & D. Formation of a septum has delimitated the primary microconidium initial from the microconidiophore. Septation is initiated by centripetal invagination of the plasmalemma (IPL invaginating plasmalemma) (see c). The microconidium delimiting septum is perforate and bilayered with periclinal triangular septal pockets (PTSP).

E. Conidium secession by central splitting of the bilayered conidium delimiting septum commencing at the triangular pockets adjacent to the periclinal walls and circumscissle rupture of the periclinal walls adjacent to the septum. The broken outer wall forms a basal frill (BF) on the microconidium base and primary annular scars (PAS) on the microconidiophore apex.

F. The secondary microconidium initial (SMI) 'blowing out' enteroblastically through the microconidiophore apex from inside of the primary annular scars (PAS).

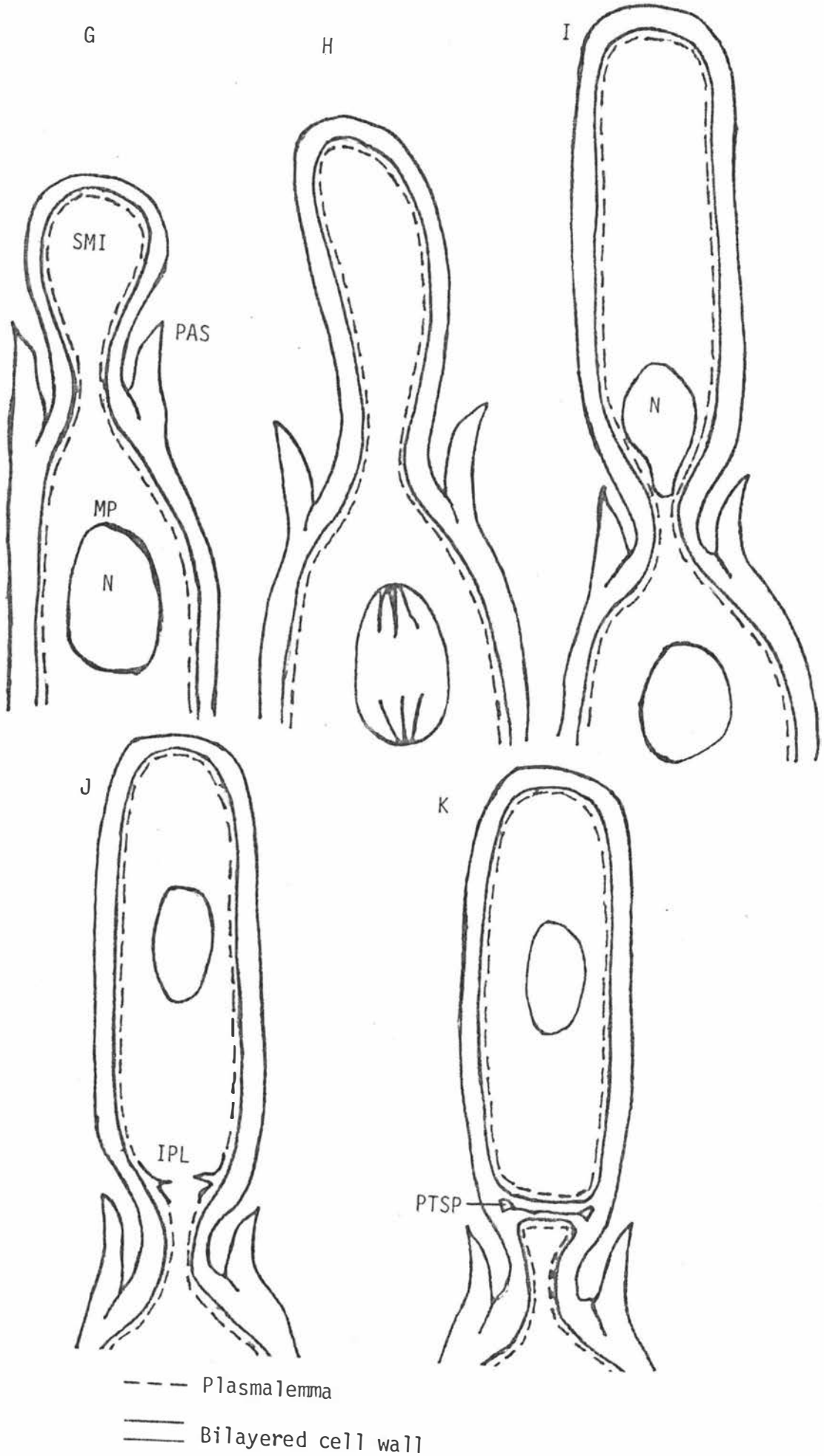
G
H
I
SMI
PAS
MP
N
N
J
K
IPL
PTSP
Plasmalemma
Bilayered cell wall

FIG. 72:

G, H & I. The secondary microconidium initial (SMI) continuing to 'blow out' through the microconidiophore (MP) apex until the secondary microconidium initial is fully formed. Prior to full extension, the basal microconidiophore nucleus (N) divides mitotically (H) and a daughter nucleus (N) migrates through the narrow microconidiophore apex (I).

Note the prominent primary annular scars (PAS) on the conidiophore formed by secession of the primary microconidium initial.

J & K. The secondary microconidium initial has delimited from the microconidiophore by centripetal invagination of the plasmalemma (IPL) resulting in the formation of a bilayered septum with periclinal triangular septal pockets (PTSP).

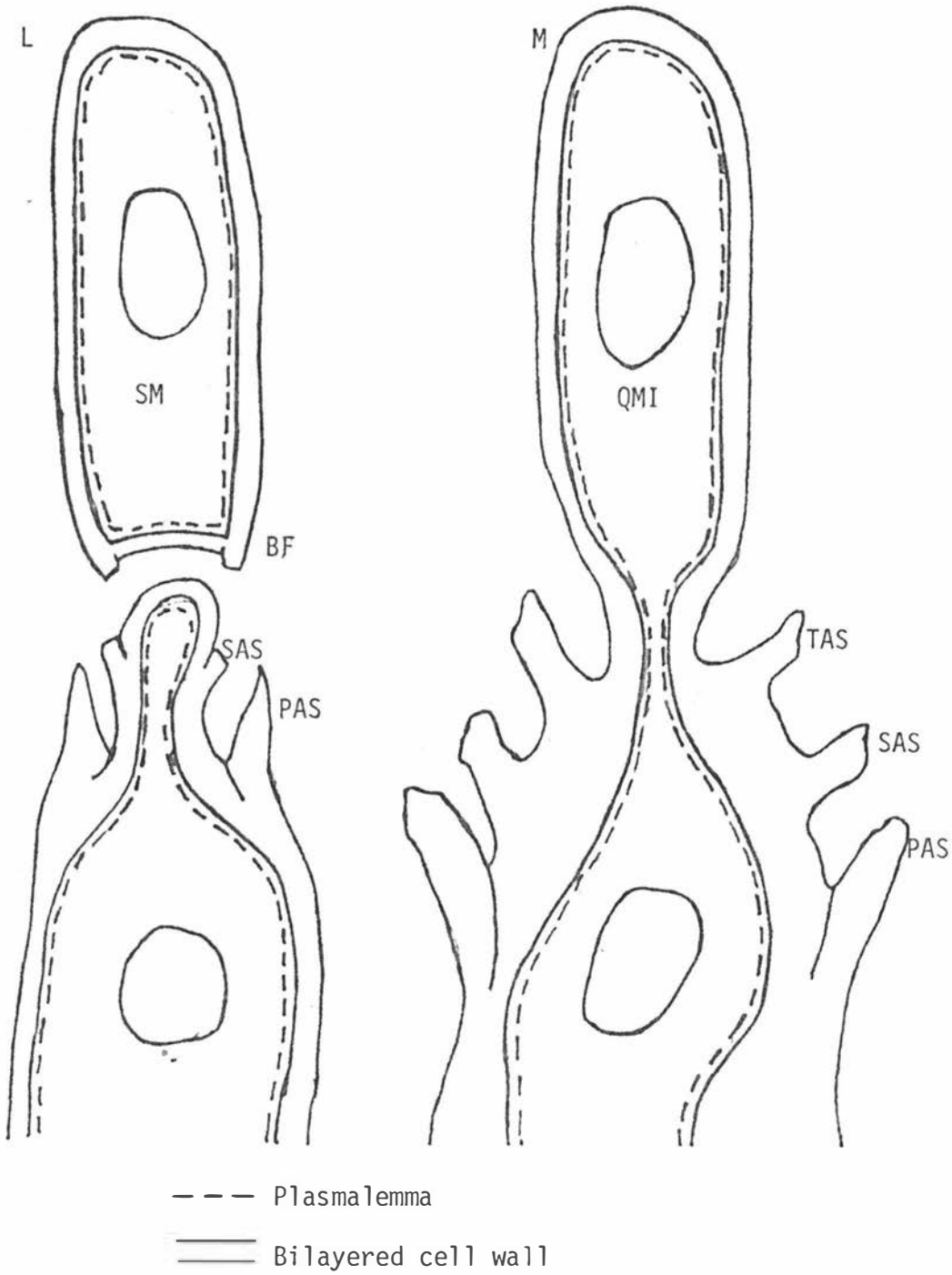
L
SM
BF
SAS
PAS
M
QMI
TAS
SAS
PAS
Plasmalemma
Bilayered cell wall

FIG. 72:

L. Secession of secondary microconidium (SM) from the microconidiophore (MP), resulting in the formation of secondary annular scars (SAS) on the conidiophore at a higher level than the primary annular scars (PAS) formed previously by secession of the primary microconidium.

Note the basal frills (BF) on the microconidium base which correspond to the secondary annular scars on the microconidiophore.

M. Quarternary microconidium initial (QMI) as indicated by the primary (PAS), secondary (SAS) and tertiary (TAS) annular scars (annellations) on the conidiophore.

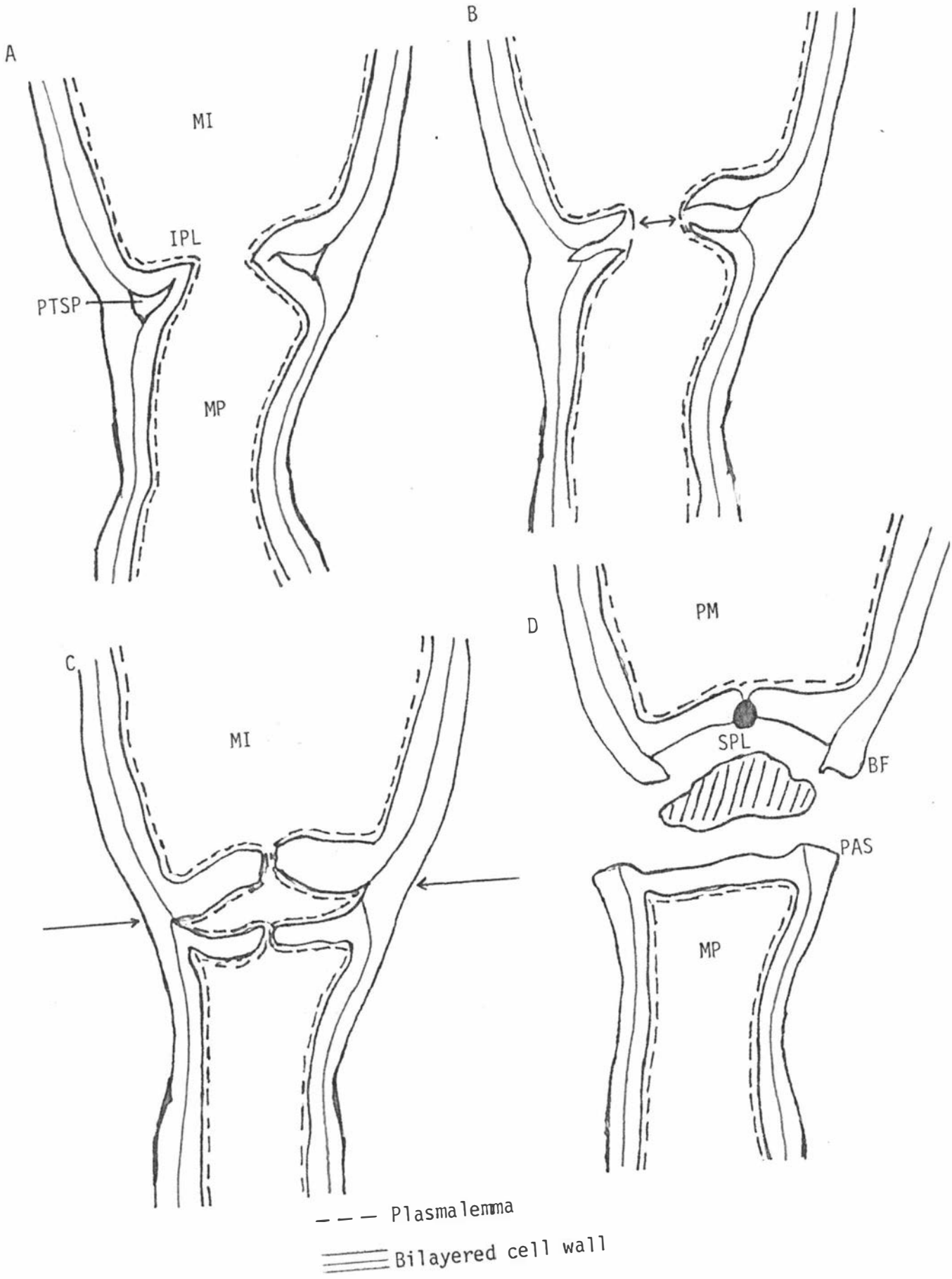
A
MI
IPL
PTSP
MP
B
C
MI
D
PM
SPL
BF
PAS
MP
Plasmalemma
Bilayered cell wall

FIG. 73: Diagrammatic interpretation of the steps involved in the formation of the 'atypical' microconidium delimiting septum, as exhibited by *M. brunnea* on *P.* x *euramericana* cv. NL 2194.

A. Initiation of septation by centripetal invagination of the plasmalemma (IPL) and inward growth of the bilayered cell wall, the two layers being separated by periclinal triangular septal pockets (PTSP).

B. The invaginating cell walls split and separate at their apices (↑), the plasmalemma lining the newly formed fork.

C. The now separate walls grow independently, the wall closest to the microconidium initial (MI) forming the base of the seceded microconidium the lower wall forming the apex of the next formed microconidium initial. Both walls are perforate. Arrows (↑) indicate the possible line of secession.

D. Secession of primary microconidium (PM) from the microconidiophore (MP) by circumsessile rupture of the periclinal wall, the septal pore in the base of the seceded microconidia being plugged with a septal plug (SPL), the pore in the apex of the secondary microconidium initial being sealed by wall growth. The entrapped pool of cytoplasm is lost on secession.

Note the basal frills (BF) formed on the base of the microconidium and the primary annular scars (PAS).

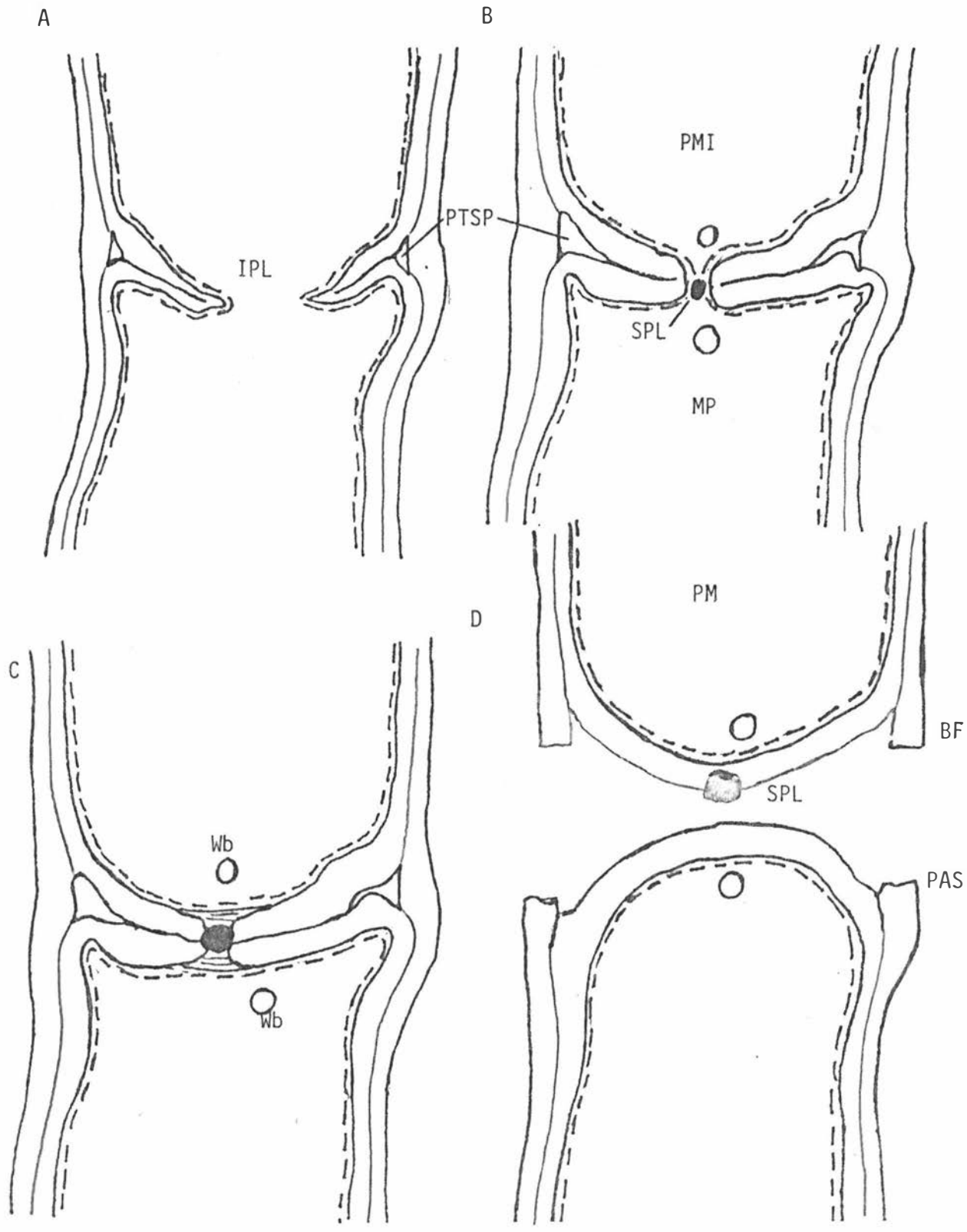
A
B
IPL
PTSP
PMI
SPL
MP
PM
D
C
BF
SPL
Wb
Wb
PAS
Plasmalemma
Bilayered cell wall

FIG. 74: Diagrammatic interpretation of the steps involved in the formation of a 'typical' microconidium delimiting septum, as exhibited by *M. brunnea*, *M. populi* and *M. castagnei*.

A. Initiation of septation by centripetal invagination of the plasmalemma (IPL) and inward growth of the bilayered cell wall, the two layers being separated by periclinal triangular septal pockets (PTSP).

B. By further growth the primary microconidium delimitating septum is fully formed and Woronin bodies are present both within the primary microconidium initial (PMI) and the microconidiophore (MP). Prior to microconidium secession an electron dense septal plug (SPL) enters the septal pore.

C. The septal plug is firmly lodged in the septal pore and additional wall material is deposited on both sides of the septal plug, both within the primary microconidium initial and the microconidiophore. Woronin bodies (WB) are present both within the primary microconidial initial and the microconidiophore. Note the presence of the periclinal triangular septal pockets.

D. Secession of primary microconidium (PM) from the microconidiophore occurring by central splitting of the bilayered septum starting at the periclinal triangular septal pockets and culminating in the rupture of the periclinal walls adjacent to the septum. The septal plug (SPL) remains embedded within the base of the seceded microconidium. The ruptured periclinal wall forms conspicuous basal frills (BF) on the microconidium base and primary annular scars (PAS) on the apex of the microconidiophore.

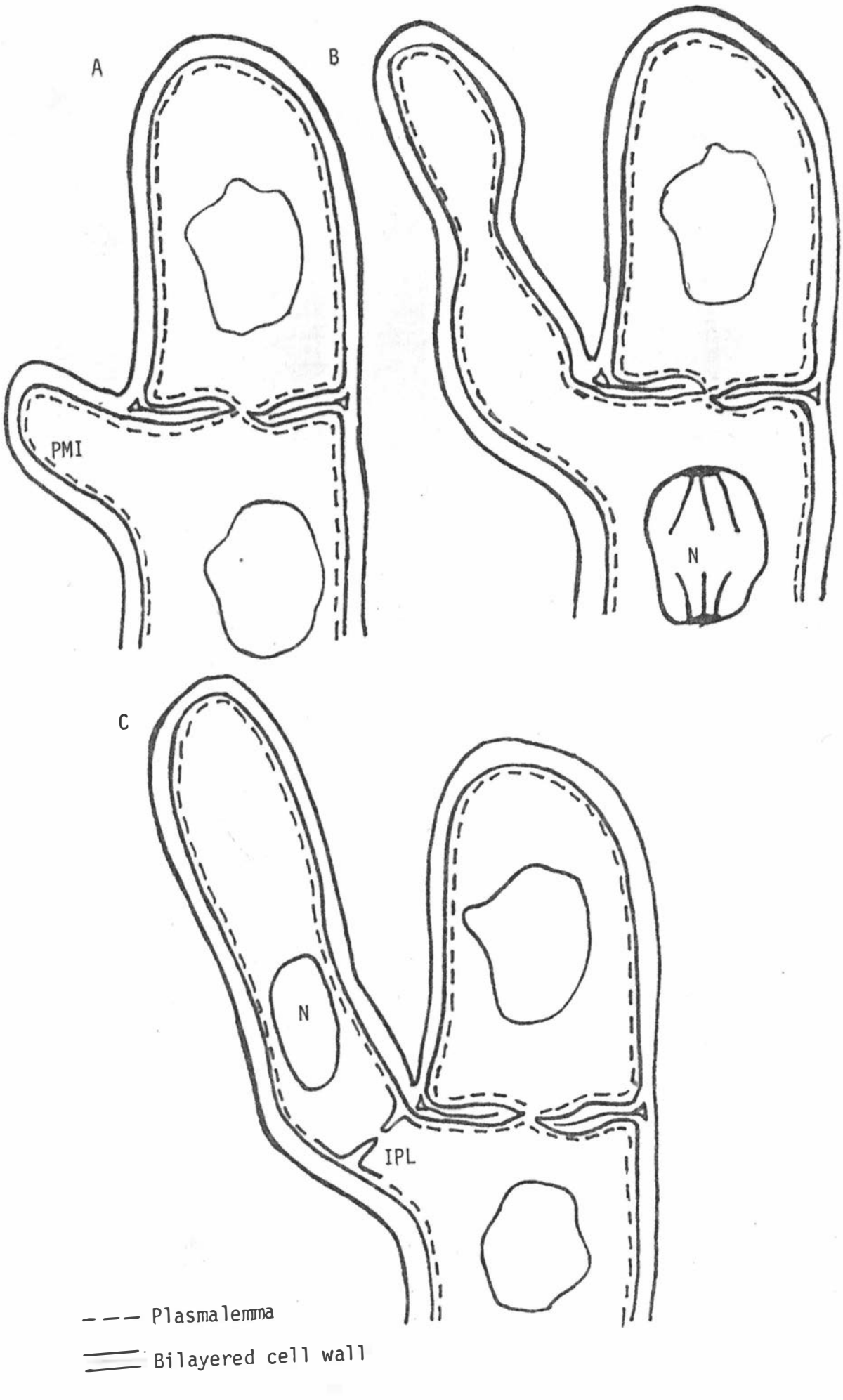
A
B
PMI
N
C
N
IPL
Plasmalemma
Bilayered cell wall

FIG. 75 A-E: Diagrammatic interpretation of the formation of microconidia by conidia of *M. brunnea*, *M. castagnei* and *M. populi*. Approx. X15,000.

A. Holoblastic extension of the conidium wall to form a primary microconidium initial (PMI).

B. Continued extension of the conidium wall, the conidium nucleus (N) dividing (mitotically) prior to full extension.

C. Migration of a daughter nucleus (N) into the primary microconidium initial and initiation of septation by centripetal invagination of the plasmalemma (IPL).

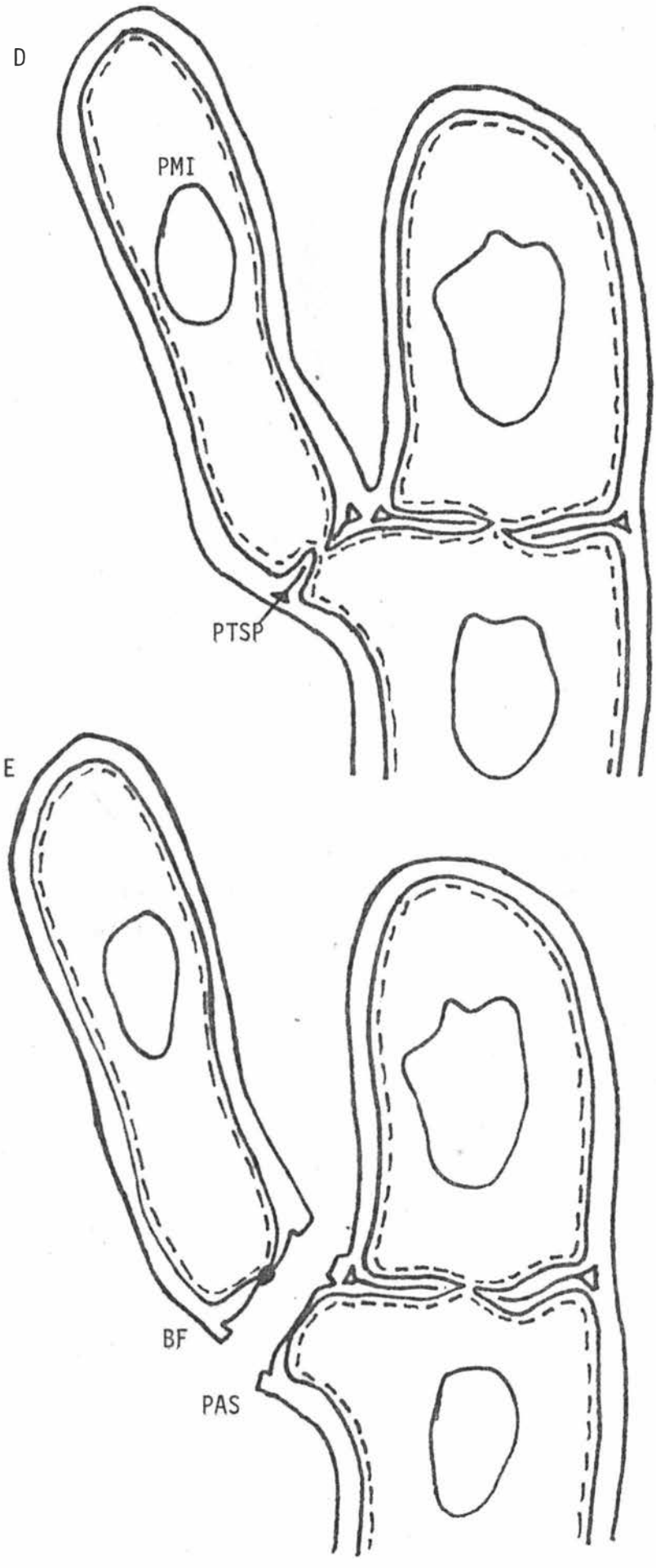
D
PMI
PTSP
E
BF
PAS
--- Plasmalemma
═══ Bilayered cell wall

FIG. 75:

D. Delimitation of the primary microconidium initial (PMI) from the conidium by formation of a perforate bilayered septum. Note the periclinal triangular septal pockets (PTSA).

E. Secession of primary microconidium by central splitting of the bilayered delimiting septum and circumscissle rupture of periclinal walls. Inconspicuous basal frills (BF) and primary annular scars (PAS) have formed on the microconidium and conidium respectively.

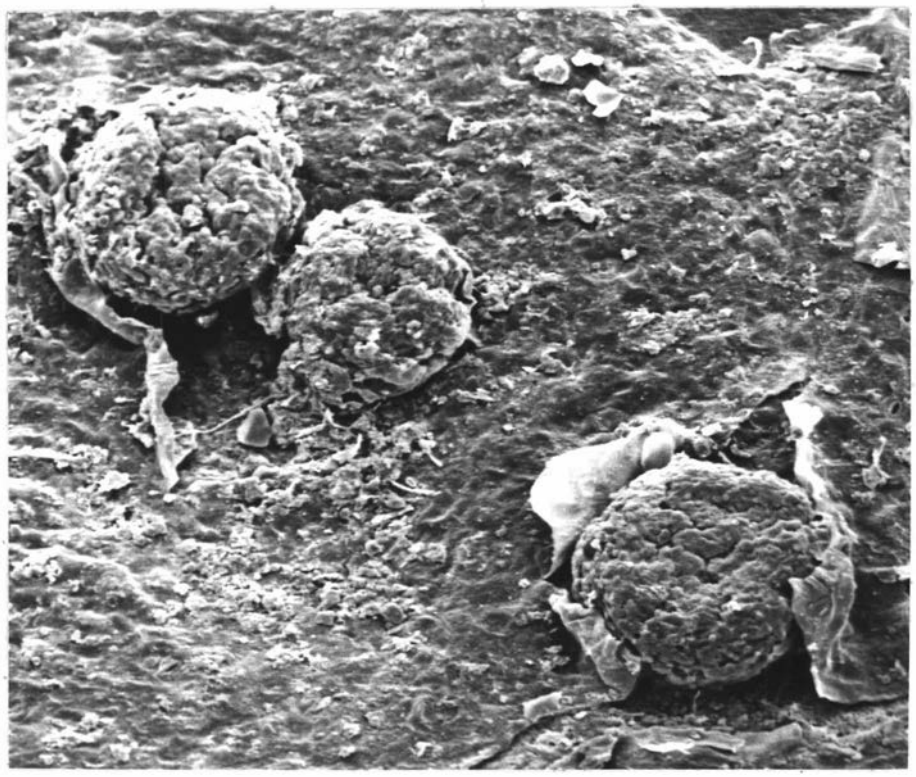

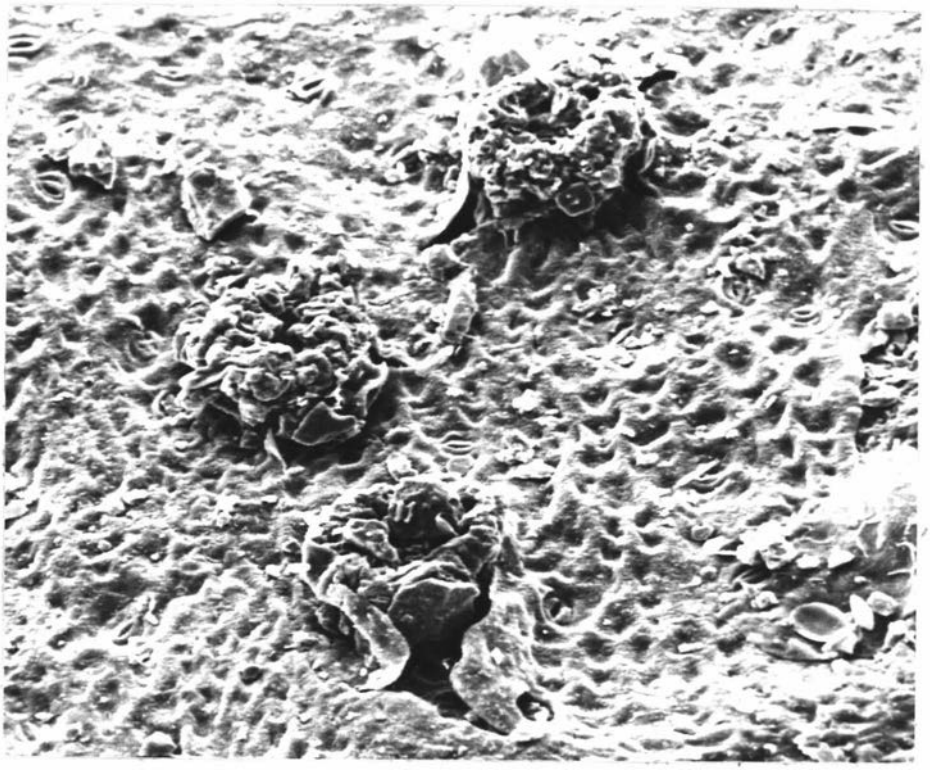

FIG. 76: External morphology of apothecia of *Drepanopeziza populorum*.

TOP: *P. nigra*, Zurich Switzerland, collected by Rimpau 7.5.1961. X 140.

BOTTOM: *P. nigra*, Brandenburg Germany, collected by Fahrendorff 10.5.1941. X 200.

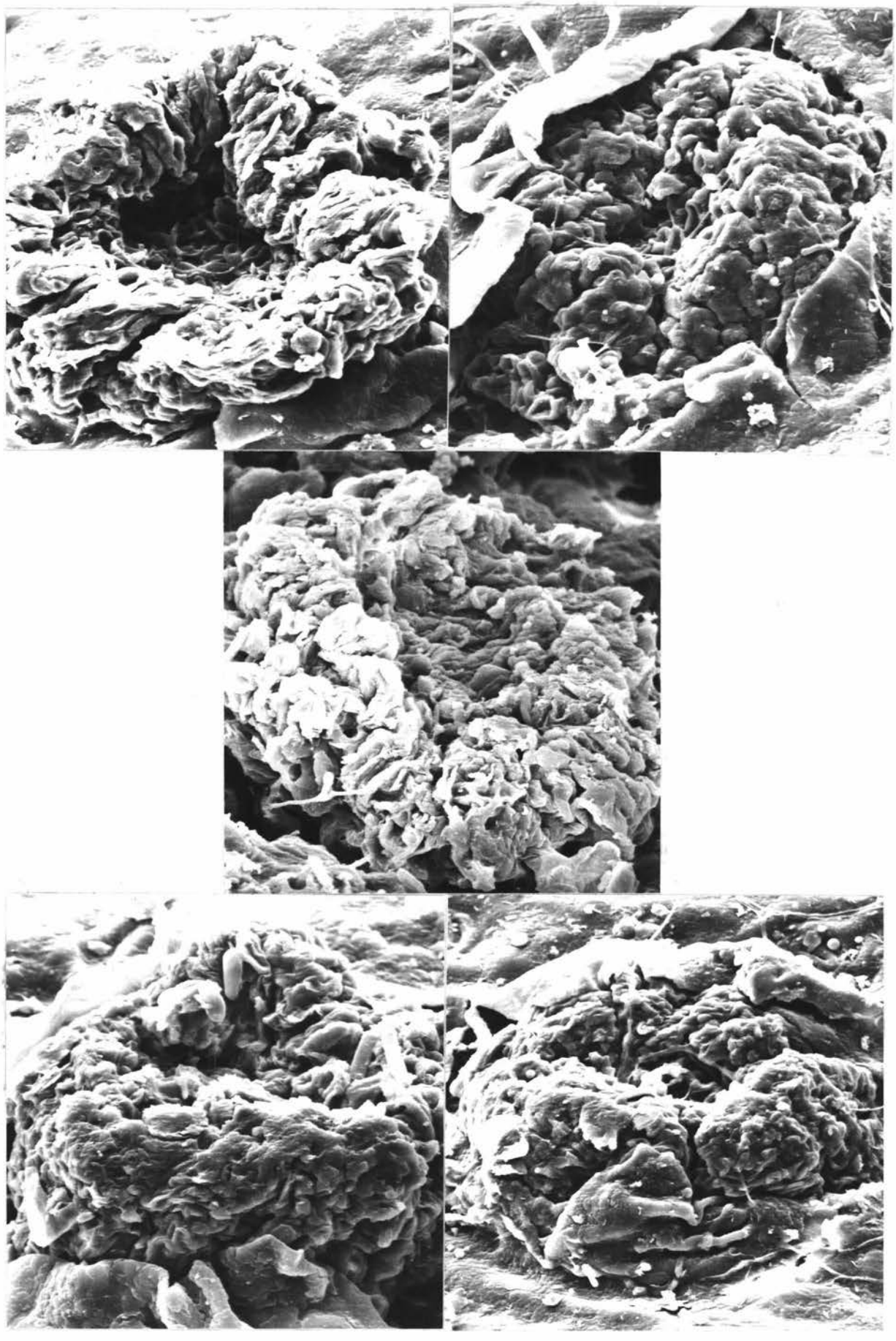

FIG. 77: External morphology of apothecia of *Drepanopeziza populorum*.

TOP LEFT: *P. nigra*, Westfalen Germany, collected by Ipse, 20.5.1938. X600.

TOP RIGHT: *P. nigra*, Westfalen Germany, collected by Ipse, 26.5.1938. X700.

CENTRE: *P. nigra*, France, collected by Desmazières, 1857. Type specimen X400.

BOTTOM LEFT: *P. nigra*, Brandenburg Germany, collected by Fahrendorff 10.5.1941. X700.

BOTTOM RIGHT: *P. canadensis*, Brandenburg Germany, collected by Vogel, 25.5.1932. X400.

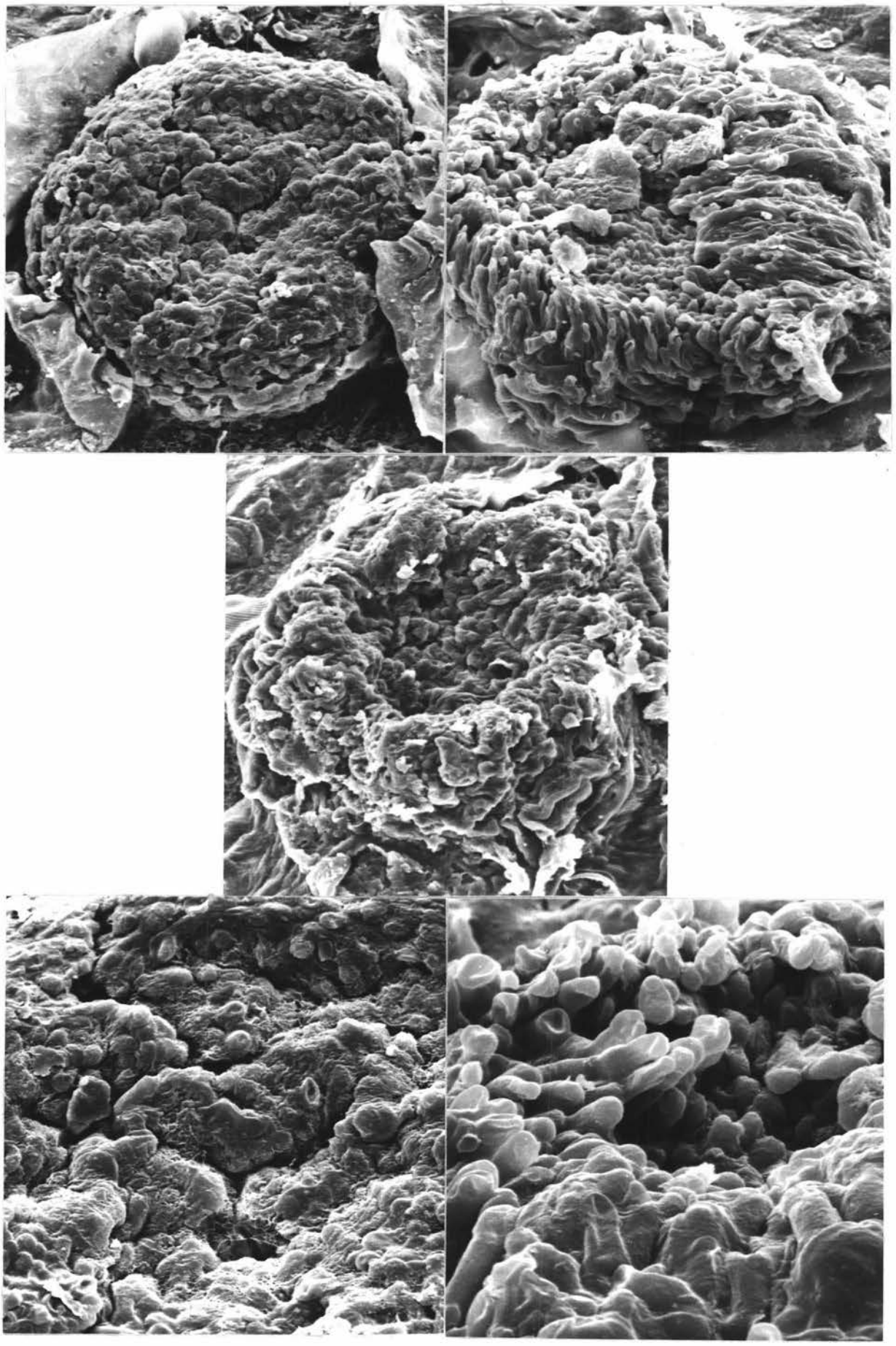

FIG. 78: External morphology of apothecia of *Drepanopeziza populorum*.

TOP RIGHT & LEFT: *P. nigra*, Zurich Switzerland, collected by Rimpau, 7.5.1961. Note the different external morphology of the two apothecia.
LEFT: X400.
RIGHT: X600.

CENTRE: *P. tacamahaca* x *P. trichocarpa* cv. 37, Kildare Co. Ireland, collected by O'Riordain, Autumn 1965. X400.

BOTTOM LEFT: Higher magnification of top left apothecium. X900.

BOTTOM RIGHT: Higher magnification of top right apothecium. X2,400.

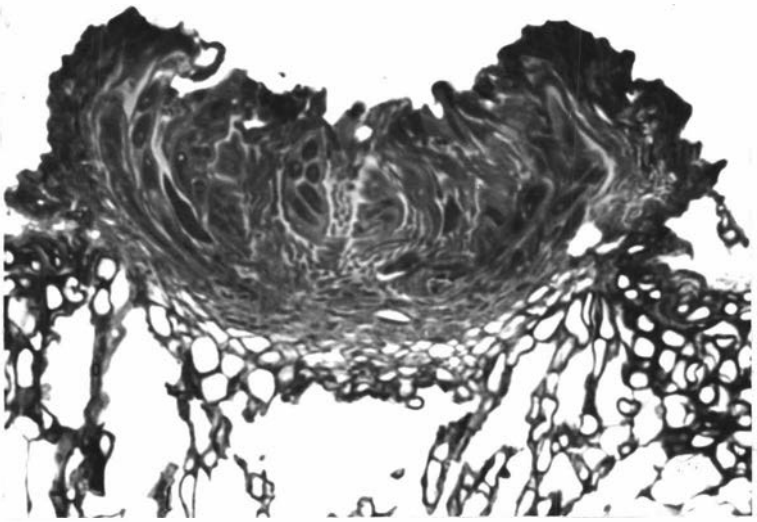

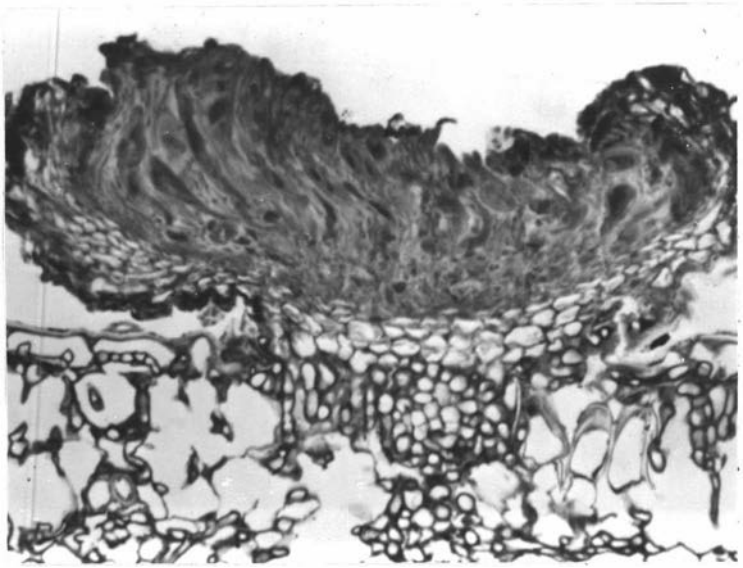

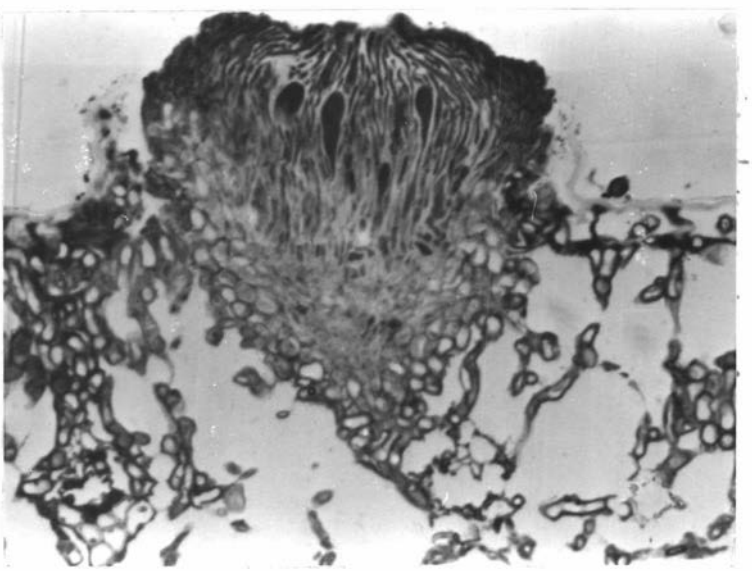

FIG. 79: Vertical sections through apothecia of *Drepanopeziza populorum*.

TOP: *P. nigra*, France, collected by Desmazieres, 1857 (type specimen). Note concave disc shape and well developed excipulum. X540.

CENTRE: *P. nigra*, Zurich Switzerland, collected by Rimpau, 7.5.1961. Note concave disc shape and well developed excipulum. X450.

BOTTOM: *P. nigra*, Zurich Switzerland, collected by Rimpau, 7.5.1961. Conical immature apothecium. X400.

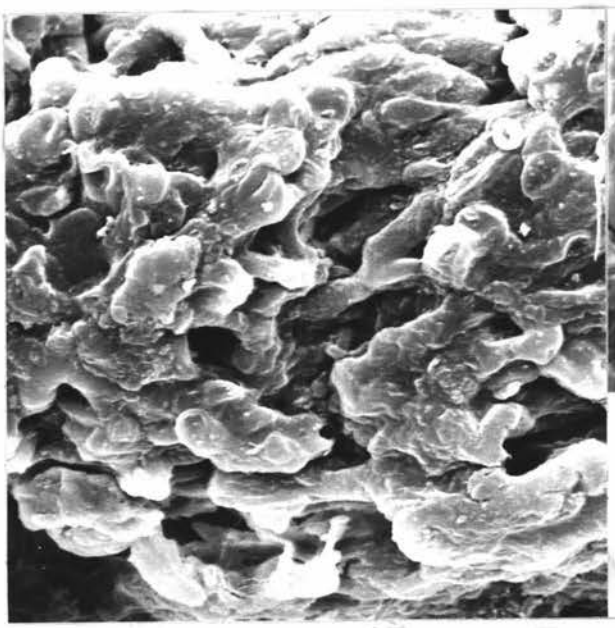

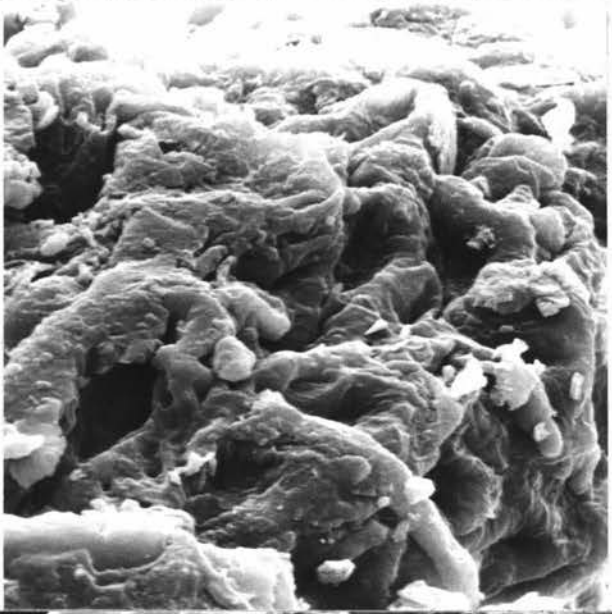

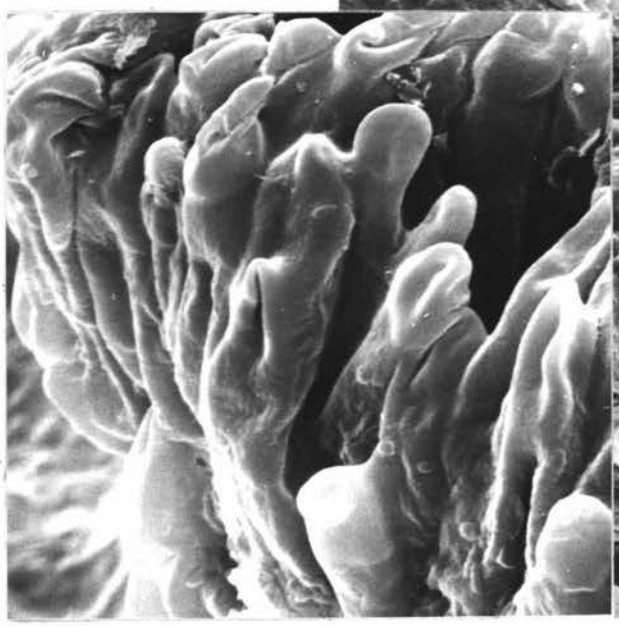

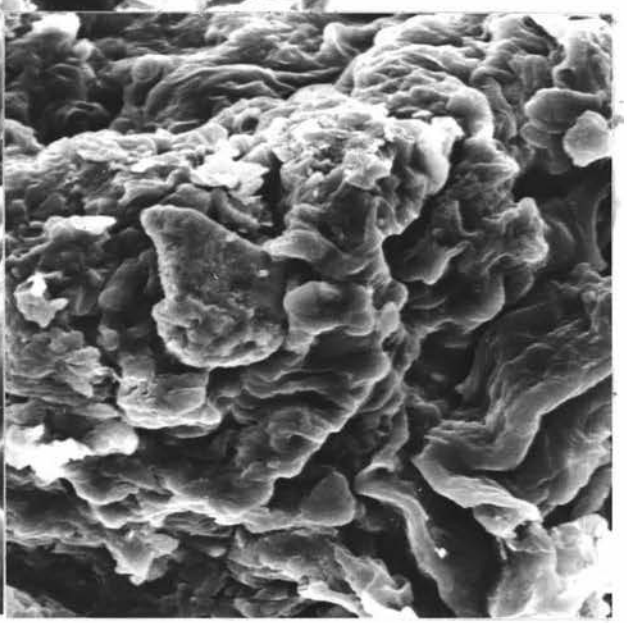

FIG. 80: External morphology of apothecia of *Drepanopeziza populorum*.

TOP LEFT: *P. nigra*, Zurich Switzerland, collected by Rimpau, 7.5.1961. Side of wall of apothecium showing lumpy texture. X400.

TOP RIGHT: *P. nigra*, Brandenburg Germany, collected by Fahrendorff, 10.5.1941. Apex of apothecial side wall X550.

CENTRE: As above, side wall. X 2,800.

BOTTOM LEFT: *P. nigra*, Zurich Switzerland, collected by Rimpau, 7.5.1961. Side wall showing fused vertical finger like processes. X 4,000.

BOTTOM RIGHT: *P. tacamahaca* x *P. trichocarpa* cv. 37, Kildare Co. Ireland, collected by O'Riordain, Autumn 1965. Side wall. X800.

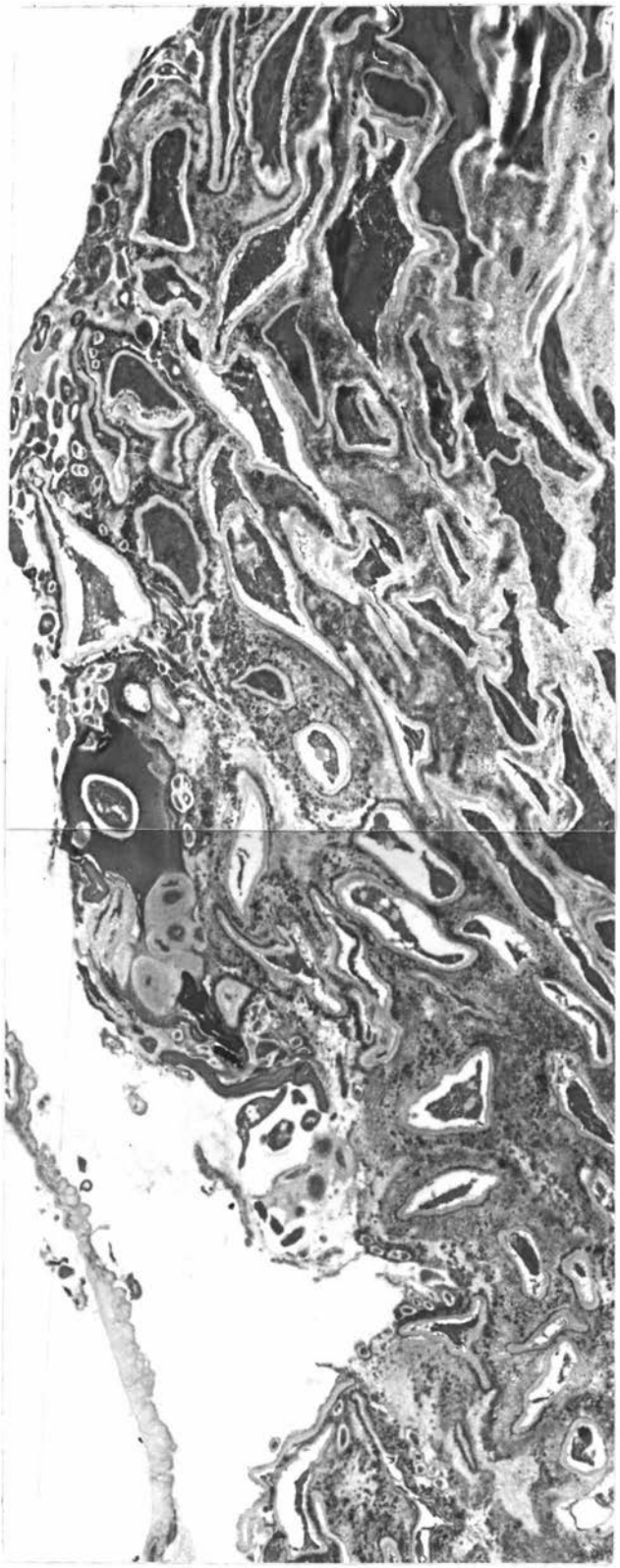

FIG 81: Ectal excipulum of *Drepanopeziza populorum*.

LEFT & RIGHT: *P. nigra*, Zurich Switzerland, (Rimpau, 7.5.1961). Outer layers of ectal excipulum consisting of irregular elongate cells embedded in a dark-pigmented matrix.
LEFT: X 4,700.
RIGHT: X 6,400.

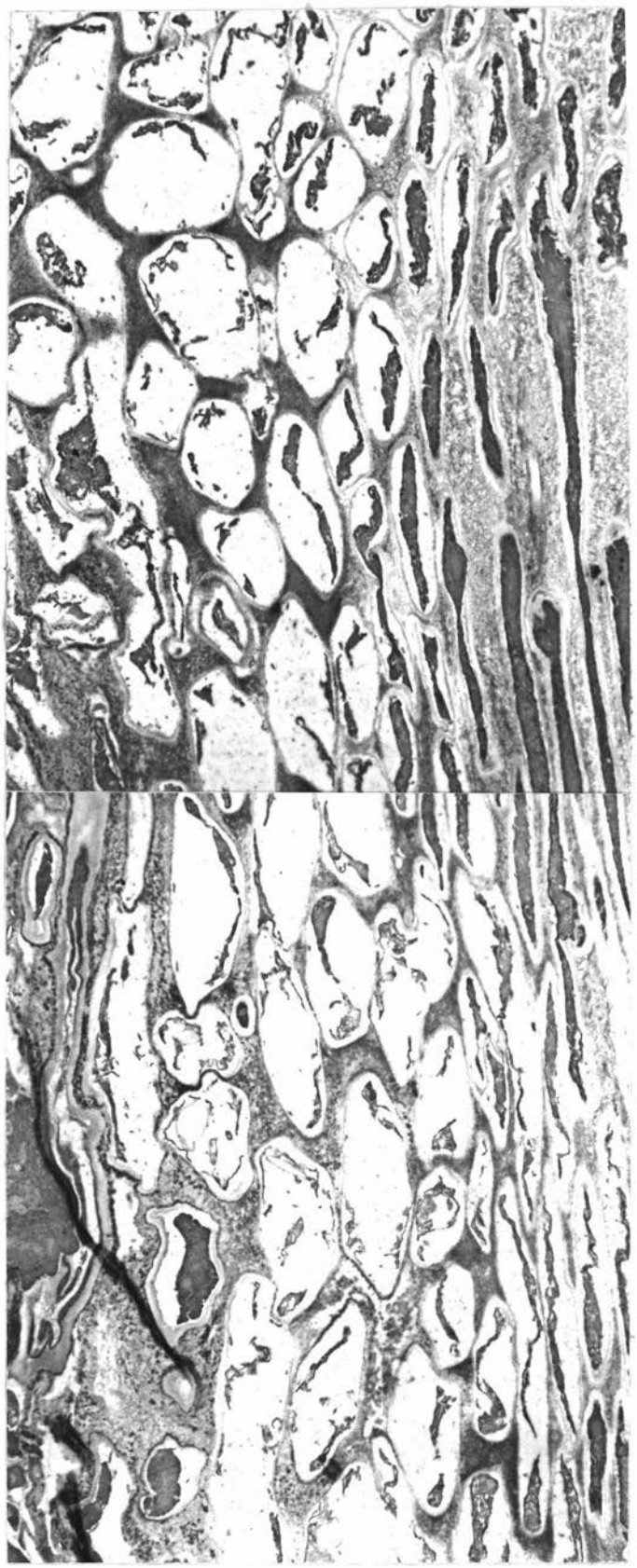

FIG. 82: Ectal excipulum of *Drepanopeziza populorum*.

LEFT: *P. nigra*, Zurich Switzerland, Rimpau, 7.5.1961. Inner layers of ectal excipulum comprising 3-4 rows of globular regularly arrayed cells bounded on the inside by septate paraphyses. X4,700.

RIGHT: As above showing septate paraphyses. X8,100.

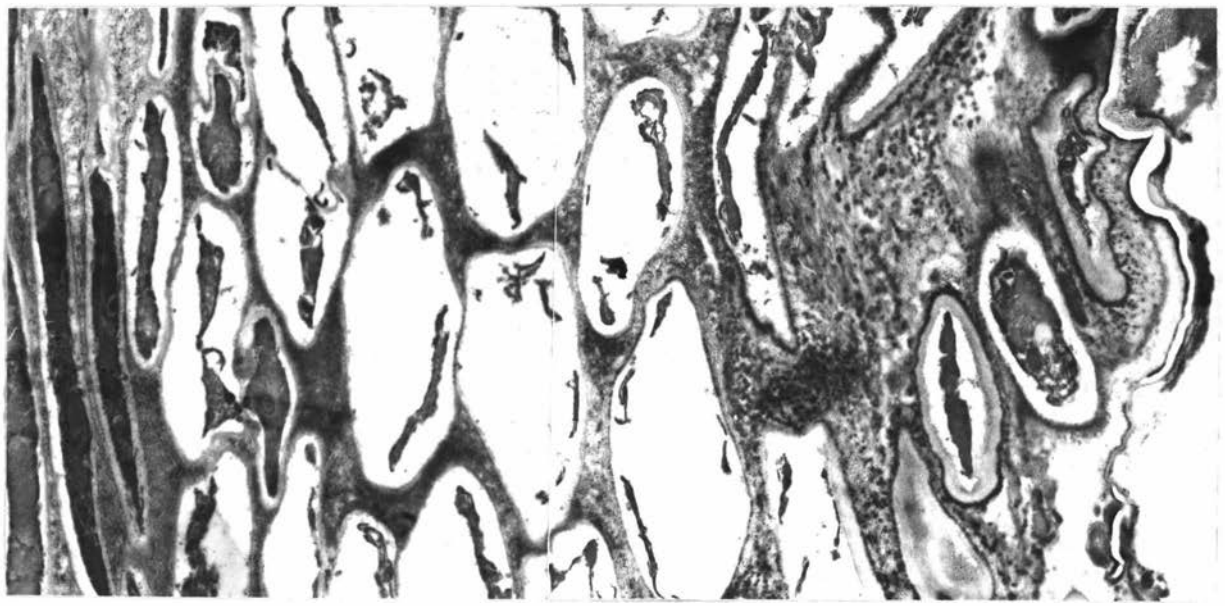

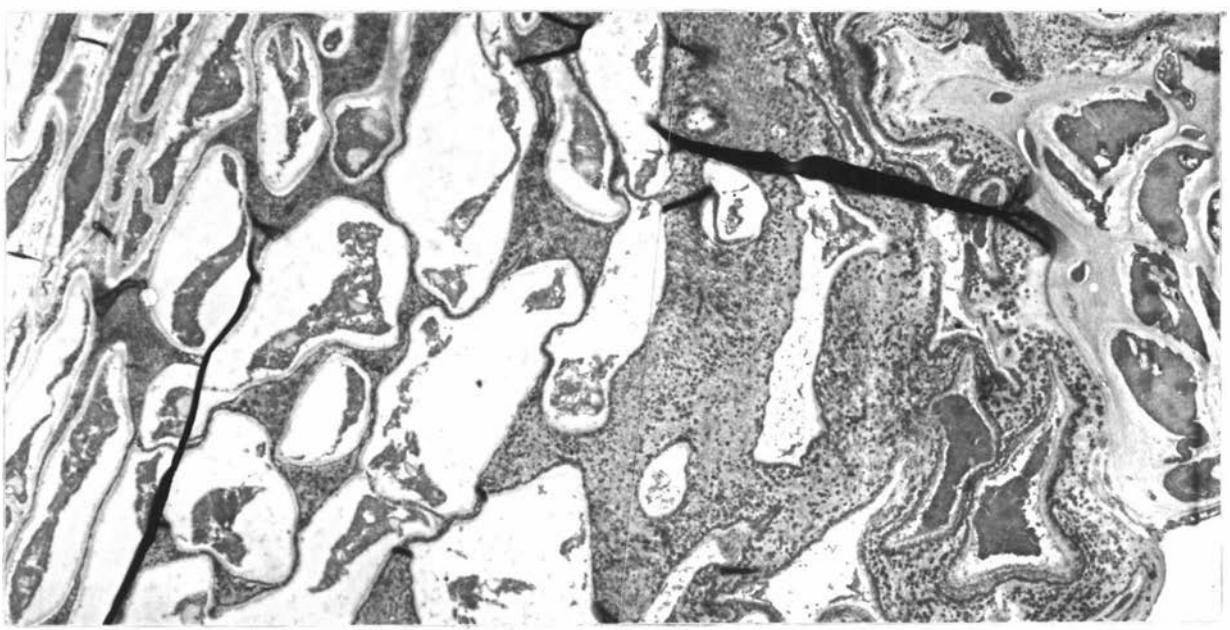

FIG. 83: Ectal excipulum of *Drepanopeziza populorum*.

TOP & BOTTOM: *P. nigra*, Zurich Switzerland, Rimpau, 7.5.1961. Vertical section through ectal excipulum showing outermost 2-3 layers of irregular cells embedded in a dark matrix; an inner layer of 3-4 rows of globular regularly arrayed cells bounded on the inside by paraphyses.

TOP: X10,500.
BOTTOM: X6,400

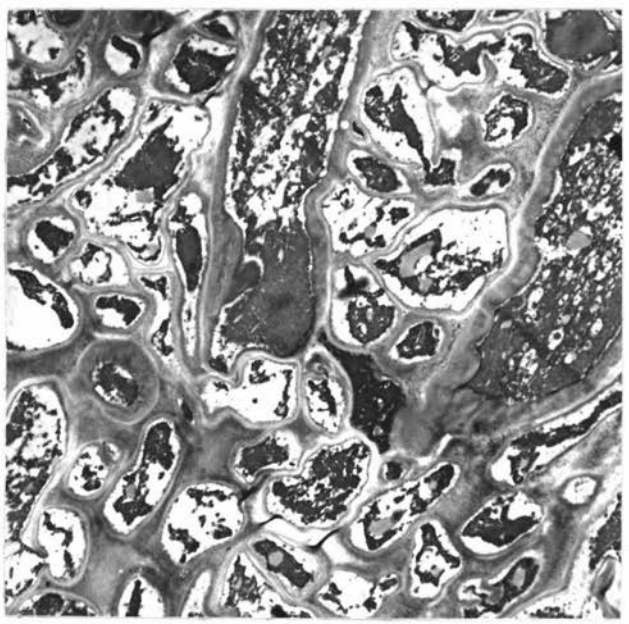

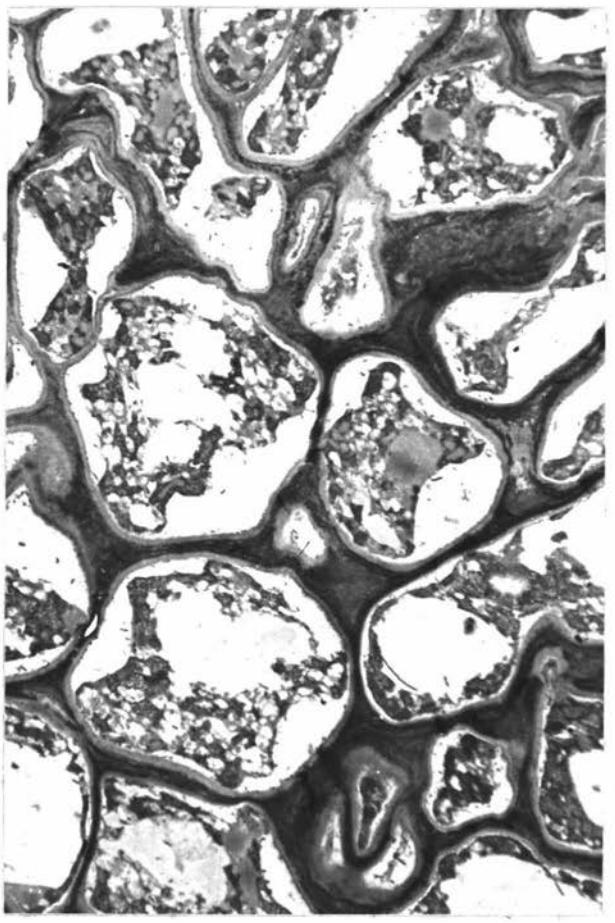

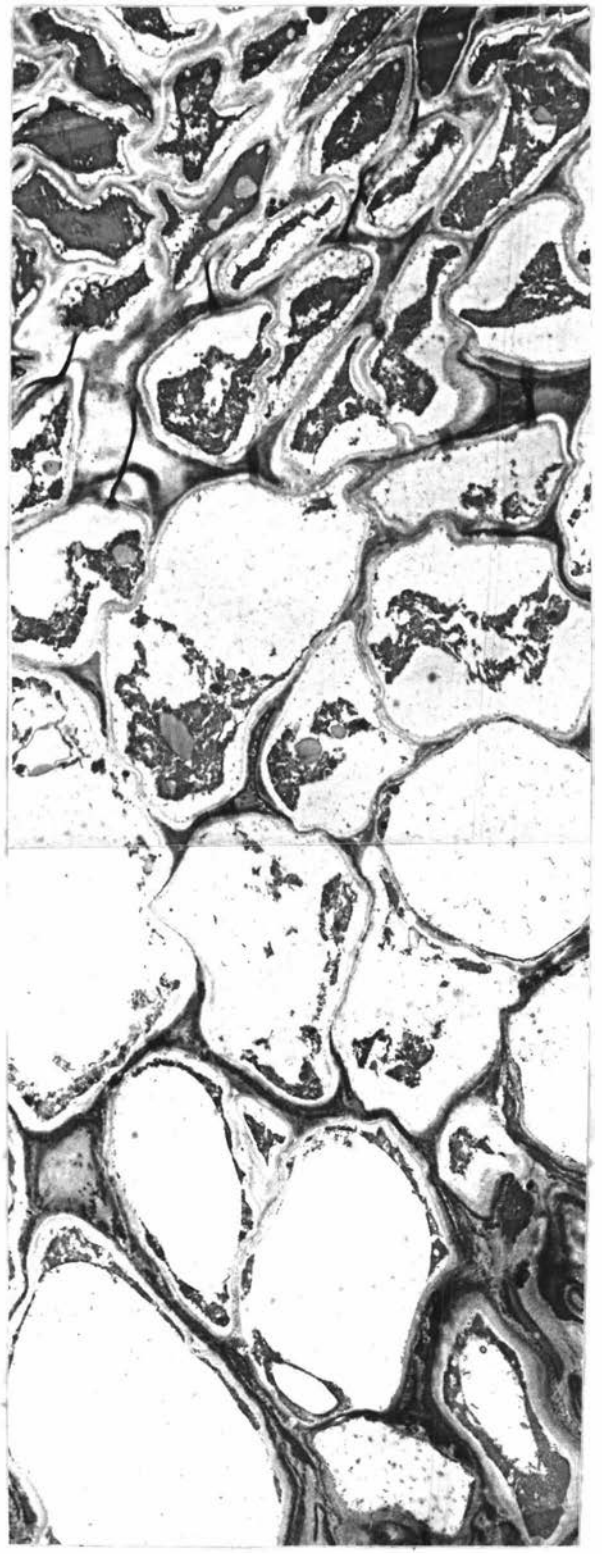

FIG. 84: Medullary excipulum and hypothecium of *Drepanopeziza populorum*. *P. nigra*, Zurich Switzerland, Rimpau, 7.5.1961.

TOP LEFT: Hypothecium comprised of small (3-4u diam.), globose to subglobose cells regularly arrayed around the bases of asci. X2,500.

BOTTOM LEFT: Large (5-7u diam.) angular globose to subglobose cells of the medullary excipulum. X3,400.

RIGHT: Vertical section through apothecium showing medullary epithecium and hypothecium. Note the sharp delimitation between the two tissues. X4,700.

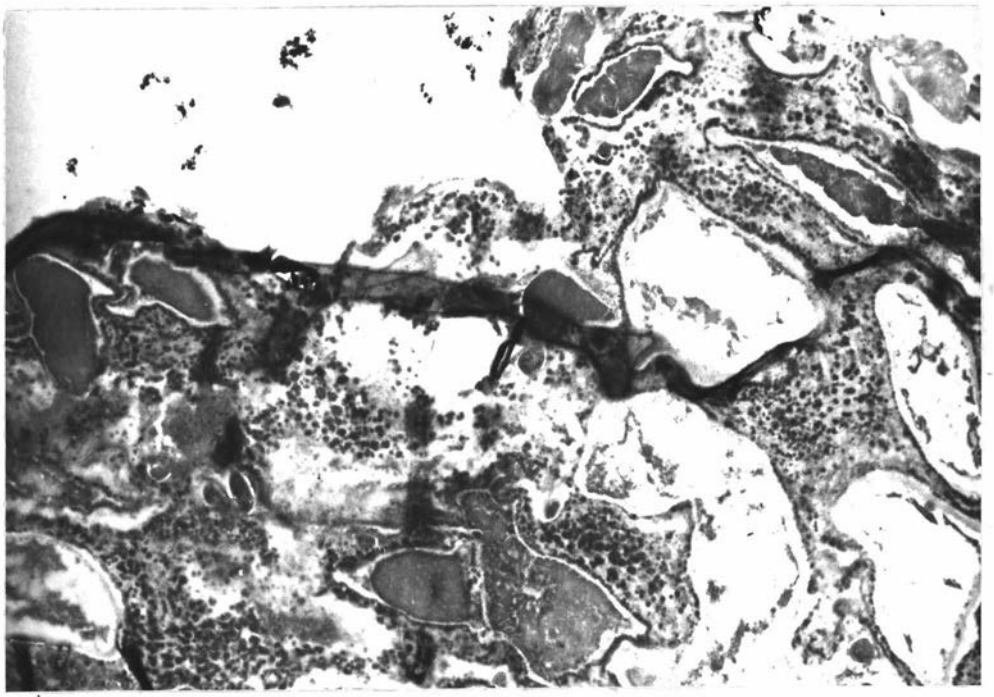

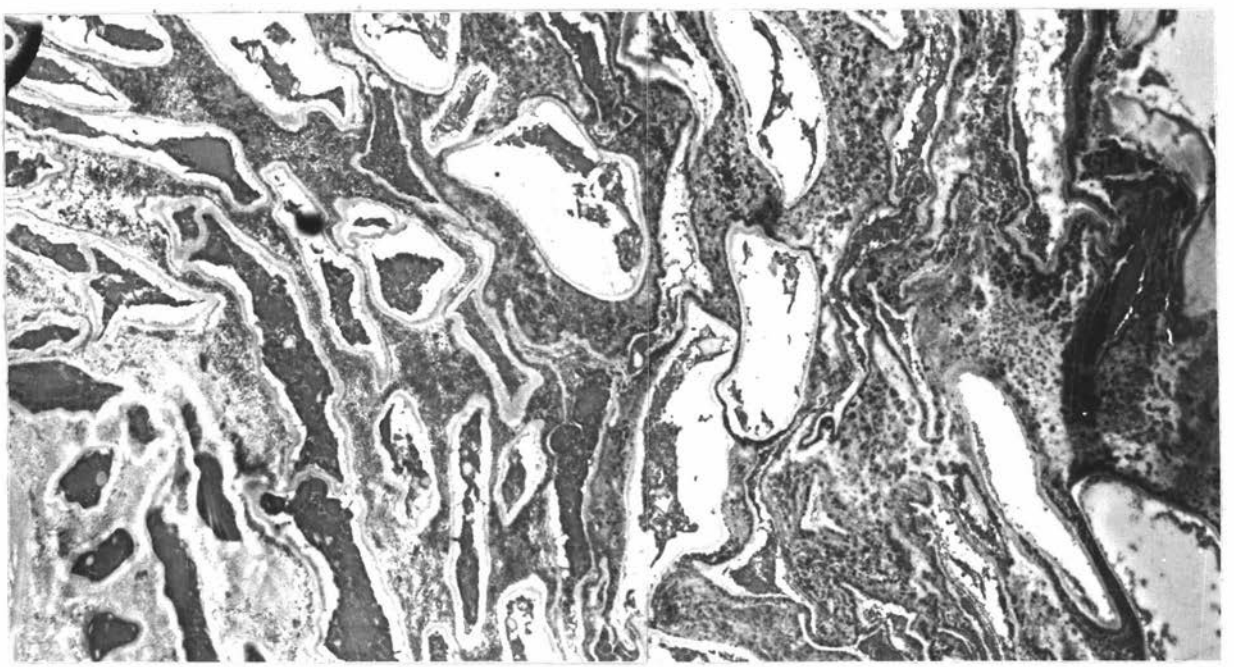

FIG. 85: Epithecium of *Drepanopeziza populorum*. *P. nigra*, Zurich Switzerland, Rimpau, 7.5.1961. X6,400.

TOP: Epithecium composed of irregular cells embedded in a dark matrix.

BOTTOM: Cells of the epithecium and paraphyses overlaying asci.

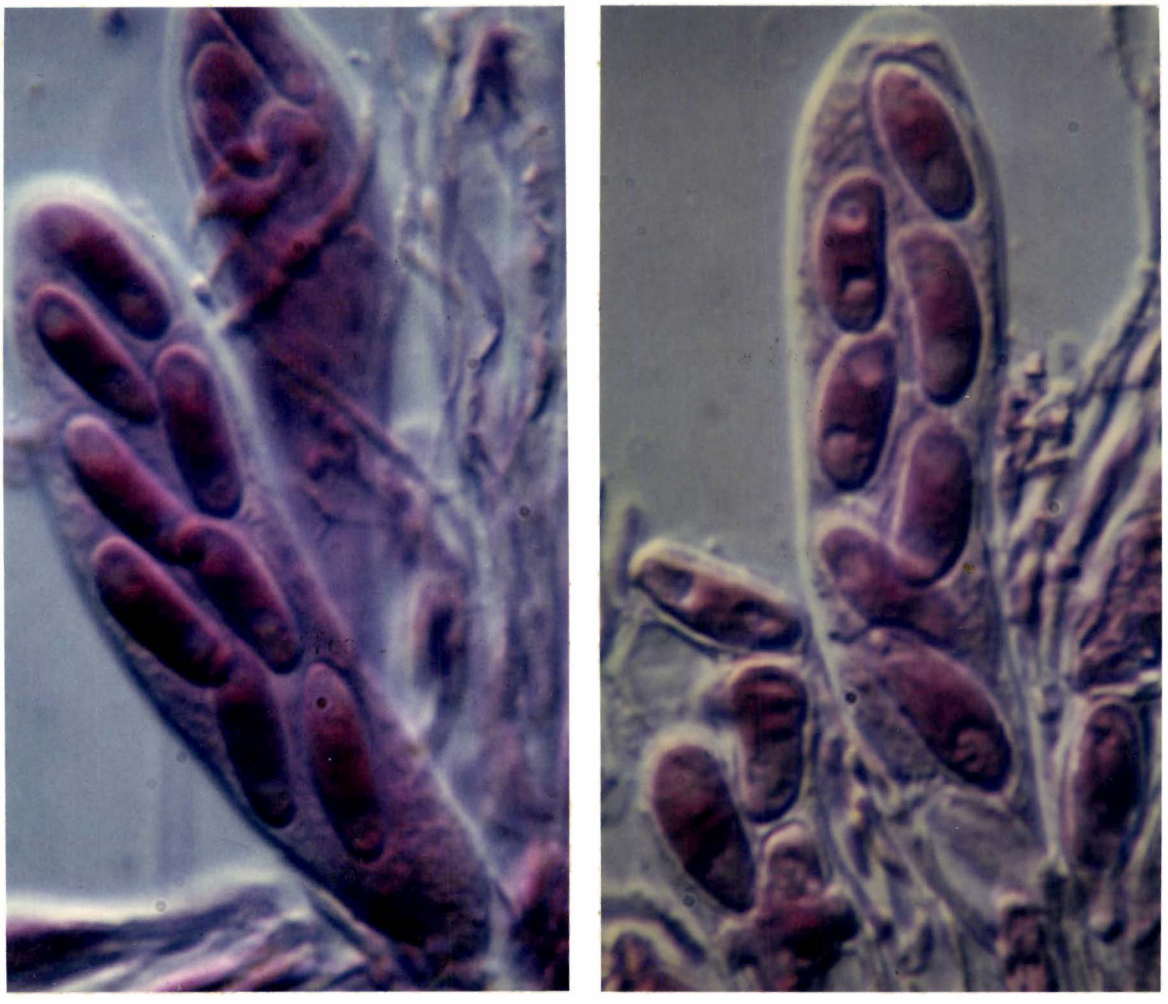

FIG. 86: Asci and ascospores of *Drepanopeziza populorum*. X1,600.

Cylindrical unitunicate asci with thickened apices. Ascospores biseriately arrayed, unicellular, ellipsoidal, smooth walled, hyaline (in this instance stained with 0.5% acid fuchsin) with two conspicuous polar bodies.

LEFT: Ex *P. nigra*, Westfalen Germany, collected by Ludwig, 1.5.1938.

RIGHT: Ex *P. nigra*, Saxonia Germany, collected by Krieger, . 4 .1899.